



# HUMAN-WILDLIFE INTERFACE IN AFRICAN SAVANNA

Quantifying landscape fragmentation for predicting wildlife  
distribution and human-wildlife conflicts

Claudia Pittiglio

Examining committee:

Prof. dr. Alfred Stein	University of Twente
Prof. dr. Anne van der Veen	University of Twente
Prof. dr. Pieter van Tienderen	University of Amsterdam
Prof. dr. Marc Naguib	Wageningen University

ITC dissertation number 220

ITC, P.O. Box 6, 7500 AA Enschede, The Netherlands

ISBN 978-90-6164-346-3

Cover designed by Henry van Burgsteden and Claudia Pittiglio

Printed by ITC Printing Department

Copyright © 2012 by Claudia Pittiglio



**UNIVERSITY OF TWENTE.**

**ITC**

FACULTY OF GEO-INFORMATION SCIENCE AND EARTH OBSERVATION

# HUMAN-WILDLIFE INTERFACE IN AFRICAN SAVANNA

QUANTIFYING LANDSCAPE FRAGMENTATION FOR PREDICTING  
WILDLIFE DISTRIBUTION AND HUMAN-WILDLIFE CONFLICTS

DISSERTATION

to obtain

the degree of doctor at the University of Twente,

on the authority of the rector magnificus,

prof. dr. H. Brinksma,

on account of the decision of the graduation committee,

to be publicly defended

on Monday 17 December 2012 at 10.30 hrs

by

Claudia Pittiglio

born on 22 June 1970

in Rome, Italy

This thesis is approved by

**Prof. dr. A. K. Skidmore**, promoter  
Faculty of Geo-Information Science and Earth Observation (ITC)  
University of Twente

**Prof. dr. H.H.T Prins**, promoter  
Resource Ecology Group  
Wageningen University

**Dr. H.A.M.J. van Gils**, assistant promoter  
Faculty of Geo-Information Science and Earth Observation (ITC)  
University of Twente

To *Henry* and *Zeno*, for their patience, love and support



# Acknowledgements

When I arrived at ITC in August 2002 as visiting scientist, I was immediately impressed by its scientific environment, inspiring and cheerful atmosphere. I left in October 2003 to work as a consultant for the Food and Agriculture Organization of the United Nations (FAO) in Rome. However I was determined to come back to ITC to undertake a PhD in Natural Resources Department. In November 2005 I started working within a Global Environment Facility (GEF) project in Tanzania as an ecologist and GIS expert of FAO. This represented the opportunity for a sandwich PhD construction between FAO and ITC. I am extremely grateful to the former head of research Prof. Martin Hale, and the chief of FAO/LEAD, Dr. Henning Steinfeld for providing the necessary conditions for this collaboration. Martin, thanks for providing effective solutions to the sandwich PhD construction, including the ITC scholarship for my study in the Netherlands. Henning, thanks for giving me the opportunity to work for an interesting project and allow the use of data for my PhD.

Special thanks go to my promoters Prof. Andrew Skidmore and Prof. Herbert Prins, who have been a source of inspiration, guidance and support throughout the study period. I really enjoyed working with you and I learnt a lot from each of you. I appreciated our scientific discussions, which often included politics, culture and life. Andrew, I still remember our first meeting in Majella National Park, where you tested my determination in undertaking such challenging and difficult experience! I confess I underestimated the complexity of this study, particularly the wavelets! I will always be grateful for your constant guidance, for always being patient and positive about my results. Herbert, you were always available to discuss my papers and results. I learnt a lot from our meetings. I would like to thank my assistant promoter and daily supervisor Dr. Hein van Gils for his availability, friendship and constant support. I really enjoyed our meetings and discussions. I could always come to your office, without notice, to discuss my doubts and findings. Thanks also for the Dutch translation of the summary. I am also grateful to Dr. Mike McCall for his contribution to my 5<sup>th</sup> chapter on crop raiding elephants. We had interesting discussions about intervening opportunities in geography, which shaped the stepping stone corridor hypothesis.

To Dr. Kees de Bie and Dr. Amon Murwira, thank you for your comments and contribution to the second chapter. Amon, I could not move my first steps into

the wavelet world without your help. Thanks a lot! I am grateful to Willem Nieuwenhuis, who wrote the wavelet algorithm in IDL. I also appreciated the support of many ITC staff, in particular Esther Hondebrink, Loes Colenbrander, Prof. Paul van Dijk, Dr. Bert Toxopeus, Dr. Tiejun Wang, Dr. Iris van Duren, Dr. Thomas Groen, Dr. Edward Westinga, Dr. Mike Weir, Gerard Reinink, Benno Masselink, Job Duim, Marga Koelen and Carla Gerritsen.

During my eight months in Arusha, I share an intense, wonderful experience with many people. I would like to thank the African Wildlife Foundation (AWF) in Arusha, and in particular Dr. James Kahurananga and Gerson Mollel for providing the logistics and facilities for my FAO consultancy and fieldwork. Our discussions on the study area, Maasai culture, and human-wildlife conflicts formed a very useful background for understanding the results of this thesis. I am grateful to the AWF canvassers for their work during the crop raiding monitoring and water source collection. Asante sana! I also thank my LEAD and ILRI colleagues, in Rome and Nairobi as partner of the GEF project, particularly Carolyn Opio and Pierre Gerber. Working and simultaneously preparing a PhD proposal during those months was not that easy. I would like to thank Prof. Guido Tosi and the OIKOS staff, Beppe and Lieve di Giulio for their friendship and advises.

Back to the Netherlands, I lived the odd experience of travelling up and down by train between Utrecht, my home, and Enschede, my office. Aiko, thank you for providing the software dongles for my analysis in the train! At ITC I was lucky to be surrounded by many friends and colleagues. First of all, I would like to thank my officemates, Tyas, Filiz, Sisi, Maitreyi, Adrie for sharing ups and downs of our PhDs, tips, jokes, dinners, and friendship. The NRS PhD tutorials were an invaluable platform for interesting and stimulating discussions. I like to thank all NRS PhD students and particularly, Nicky, Ha, Mhosisi, Shadrack, Khan, Pieter, Sabrina, Ben, Anas, Atkilt, John, Babak, Aidin, Amjad, Ullah and dearest Dan. The PhD monthly meetings, the coffee- and tea-breaks were also nice opportunities to meet the other PhD students. Thank you all. The yearly BBQ at the Skidmore farm was a pleasant happening for all NRS PhD students, including my family and I. Eva and Andrew thank you.

During the PhD period I lived the wonderful experience of becoming mother for the first time. I am so lucky to have shared the 'beauty' and the 'difficulty' of this experience with other PhD student/parents. Special thanks to Alain and Catarina, Mariela and Rafael, Laura and Anton, Carolina and Ard. We had a wonderful time together, good support and understanding of each other. I also enjoyed the weekly Italian lunch at ITC with Simona, Valentina, Guido, Gianluca, Diego, Enrico. I am also grateful to Fabio, Susan, Jamshid and Diana

for sharing a beautiful time during the first period of my PhD. Fabio, thanks for your encouragement to undertake a PhD in the Netherlands. Further I like to thank my close friend Barbara for her constant friendship and support from abroad throughout the study period. Last but not least, I am extremely grateful to my family and family-in-law, for continuous support. Mum, I really appreciated your help and constant encouragement during these years. When you could, you did not hesitate to fly to the Netherlands to help me with your grandson. In Italy you always provided a comfortable and pleasant environment for our holidays! Papa and you encouraged me to pursue my studies and ambitions. I know he would be very proud of me. The strongest support came from my partner, Henry and our son Zeno, for being always with me during these years. Henry, thank you so much. You followed me in Italy, Tanzania and the Netherlands, even sacrificing your work and career. You were supportive, positive, and helpful. Taking care of a baby and focusing on the thesis was not easy. However, you helped me in catching up with my study by taking care of our little Zeno, even bringing him to the office for breastfeeding! Thanks for reading some of my papers and improving their graphical style, including figures and book cover! And Zeno: your unconditional love compensated all the tiredness, difficulties, lack of sleep and worries! You gave me the strength to go ahead. I know you sometimes paid the prize of having a busy-student-mother. However I believe you will benefit from this multi-cultural, multi-lingual, 'multi-scale' experience in the Netherlands!



# Contents

Acknowledgements.....	i
Contents .....	v
List of Figures .....	ix
List of Tables .....	xv
List of Acronyms .....	xvii
1 Introduction .....	1
1.1 Landscape heterogeneity, fragmentation and human-wildlife conflicts: Background .....	2
1.2 The wavelet transform and the intensity-dominant scale method.....	6
1.3 Research objectives and hypotheses .....	8
1.4 The study area .....	10
1.5 Conceptual framework and thesis outline .....	11
2 A common dominant scale emerges from images of diverse satellite platforms using the wavelet transform.....	15
2.1 Introduction.....	16
2.2 Materials and Methods .....	20
2.3 Results .....	29
2.4 Discussion .....	36
2.5 Conclusions.....	41
3 Identifying transit corridors for elephant using a long time-series .....	43

3.1 Introduction.....	44
3.2 Methods.....	47
3.3 Results .....	54
3.4 Discussion .....	62
4 Elephant response to spatial heterogeneity in a savanna landscape of northern Tanzania.....	67
4.1 Introduction.....	68
4.2 Methods.....	72
4.3 Results .....	79
4.4 Discussion .....	85
5 Farms as stepping stones for crop raiding elephants in northern Tanzania ..	91
5.1 Introduction.....	92
5.2 Methods.....	94
5.3 Results .....	104
5.4 Discussion .....	110
6 Landscape heterogeneity, fragmentation and human-wildlife conflicts: a synthesis.....	113
6.1 The wavelet transform and the intensity–dominant scale method.....	115
6.2 The response of elephant to landscape heterogeneity and fragmentation using multiple resolution analysis.....	121
6.3 New approaches to identify and predict seasonal and daily corridors as well as species distribution.....	123
6.4 Fragmentation, corridors and human-elephant conflicts.....	126

6.5 Filling the gaps: What is new? What is left? Future research objectives .....	127
Appendix A .....	131
Appendix B .....	132
Appendix C .....	133
Bibliography .....	135
Summary .....	159
Samenvatting .....	161
Publications .....	165
Biography .....	167
ITC Dissertation List .....	169



# List of Figures

- Fig. 1.1: (a) Haar wavelet function, (b) Haar 2D-DWT wavelet decomposition of an image. LL, LH, HL, HH (the smooth, and the vertical, horizontal and diagonal details). The numbers indicate the level of decomposition..... 7
- Fig. 1.2: The Tarangire–Manyara ecosystem (left), its dominant vegetation (upper right) and elephant. .... 11
- Fig. 1.3: Conceptual framework of the thesis and research questions (WT, Wavelet Transform). .... 12
- Fig. 2.1: Location of the sampling units (i.e., eighteen quadrants of 8192 m × 8192 m each) in agricultural and semi-natural areas of Andalucía, Spain..... 22
- Fig. 2.2: Theoretical basis of the scale independence of landscape features from the original pixel size. (a) Spatial patterns of features in images of different pixel size ( $s_1 < s_2 < s_3$ ); (b) wavelet energy curves of images with  $s_1, s_2, s_3$  pixel size. .... 27
- Fig. 2.3: Example of the wavelet analysis of the Orthophoto for an agricultural area (quadrant 5): (a) wavelet energy curve within 64 m and 4096 m and (b) the Orthophoto showing the match between the dominant scale (256–512 m) of the curve and the fields' size. The dominant scale is highlighted by the dotted line in the graph and by the red boxes in the image. .... 30
- Fig. 2.4: Average wavelet energy curves of the Orthophoto (blue), ASTER (green) and ETM+ (orange) for agricultural areas within 64 m and 4096 m. The dominant scales (512 m) are highlighted by the dotted line. .... 32
- Fig. 2.6: Example of the wavelet energy curves of the Orthophoto for agricultural (quadrant 5 – pink line) and semi-natural areas (quadrant 5 – blue line) within 2 m and 4096 m. Dominant scales are highlighted by the dotted lines. For display reasons, the scale ( $x$  axis) is plotted as a nominal variable in order to amplify the shape of the curves. The related images are shown in Fig. 2.3 and Fig. 2.7. .... 34
- Fig. 2.7: Example of the semi-natural landscape analyzed with the wavelet transform. (a) The image represents the Orthophoto of quadrant 5. The detail on

the right (b) shows the spatial structure captured by the dominant scale (8 m) of the wavelet transform. .... 35

Fig. 2.8: Boxplot of intensity at each scale  $j$  for agricultural areas for the Orthophoto, ASTER, ETM+. (a)  $j = 64$  m; (b)  $j = 128$  m; (c)  $j = 256$  m; (d)  $j = 512$  m; (e)  $j = 1024$  m; (f)  $j = 2048$  m; (g)  $j = 4096$  m..... 37

Fig. 2.9: Boxplot of intensity at each scale  $j$  for semi-natural areas for the Orthophoto, ASTER, ETM+. (a)  $j = 64$  m; (b)  $j = 128$  m; (c)  $j = 256$  m; (d)  $j = 512$  m; (e)  $j = 1024$  m; (f)  $j = 2048$  m; (g)  $j = 4096$  m..... 37

Fig. 3.1: Study area showing boundaries of Lake Manyara National Park (LMNP), Tarangire National Park (TNP); Lolkisale Game Controlled Area (LGCA); Mkungunero Game Controlled Area (MGCA); Manyara Ranch (MR); Simanjiro Plains (SP) and wildlife migration routes described in the 1960s. Migratory species and relative references are reported for each route (1 wildebeest<sup>a</sup>, zebra<sup>a</sup>, elephant<sup>b</sup>; 2 wildebeest<sup>a</sup>, zebra<sup>a</sup>, eland<sup>a</sup>, oryx<sup>a</sup>, elephant<sup>c</sup>; 3 elephant<sup>a</sup>, buffalo<sup>a</sup>; 4 wildebeest<sup>a</sup>, zebra<sup>a</sup>, eland<sup>a</sup>, giraffe<sup>a</sup>, elephant<sup>c</sup>; 5 wildebeest<sup>a</sup>, zebra<sup>a</sup>, eland<sup>a</sup>, gazelle<sup>a</sup>, hartebeest<sup>a</sup>, elephant<sup>c</sup>; 6 elephant<sup>a</sup>, buffalo<sup>a</sup>, hartebeest<sup>a</sup>, eland<sup>a</sup>; 7 wildebeest<sup>a</sup>, buffalo<sup>a</sup>; 8 not specified<sup>a</sup>; 9 elephant<sup>a</sup>, buffalo<sup>a</sup>; 10 elephant<sup>b</sup>, wildebeest<sup>d</sup>, zebra<sup>d</sup>). <sup>a</sup>Lamprey (1964); <sup>b</sup>TCP (1998); <sup>c</sup>Galanti et al. (2006); <sup>d</sup>Mwalyosi (1991)..... 49

Fig. 3.2: Ninety-five percent of probability volume contours of the kernel density estimate of elephant and total counts elephant locations for dry (a) and wet (b) seasons. Lake Manyara National Park (LMNP); Tarangire National Park (TNP); Lolkisale Game Controlled Area (LGCA); Mukungunero Game Controlled Area (MGCA); Manyara Ranch (MR); Simanjiro Plains (SP)..... 55

Fig. 3.3: Wet (dark grey) and dry (light grey) monthly average NDVI inside (squared marker) and outside (round marker) the kernel in relation to the distance index from protected areas. The vertical dashed line marks the boundary of TNP (inside the park is on left). In the dry season the kernel areas did not include any portion of the study area between the distance indexes: 0.45–0.58, which explains the gap in the graph. .... 56

Fig. 3.4: Predicted probabilities of elephant presence and SRF elephant locations in the dry (a) and wet (b) seasons and change (c) from dry to wet season distribution models. To highlight wet season dispersal areas and transit corridors (black arrows) only probabilities > 0 are plotted in Fig. 3.4(c)..... 57

Fig. 3.5: Path diagrams showing statistically significant path coefficients (along the arrows) of the indirect and direct effects of interrelated variables on the probability of elephant occupancy in the dry (a) and wet (b) seasons. Signs indicate negative and positive relationships accordingly..... 60

Fig. 3.6: (a) Average probabilities of elephant occupancy (dark grey) and monthly average NDVI (September–October, light grey) against distance index from protected areas in the dry season. The vertical dashed line marks the boundary of TNP. Significant curvilinear functions are drawn in grey. In the dry season the kernel areas did not include any portion of the study area between the distance indexes: 0.45–0.58, which explains the gap in the graph. (b) Average probabilities of elephant occupancy (dark grey) and distance from seasonal dams (light grey) against distance index from protected areas in the wet season. Dotted vertical lines highlight the match between the local minima and maxima of the two variables..... 61

Fig. 4.1: (a) The theoretical framework showing the fragmentation of a natural savanna (in green) in relation to farming expansion (in yellow). In  $t_1$  sparse and small arable fields do not affect the dominant scale of the landscape ( $ds_1$ ), which is large; in  $t_2$  the dominant scale ( $ds_2$ ) is reduced due to the expansion of farming; in  $t_3$  the dominant scale ( $ds_3$ ) is greatest because the landscape is almost totally converted to agriculture. (b) The expected relation between the change in inverse dominant scale of landscape heterogeneity (dotted line) and the probability of elephant occurrence (solid line) over time. The dashed lines indicate the elephant population in: A) Tarangire–Manyara ecosystem, Tanzania, and B) Sebungwe region, Zimbabwe (Murwira and Skidmore, 2005). ..... 71

Fig. 4.2: Study area showing boundaries of Lake Manyara (LMNP) and Tarangire (TNP) National Parks; Lolkisale (LGCA) and Mkungunero (MGCA) Game Controlled Areas; Manyara Ranch (MR); Simanjiro Plains (SP) and quadrants (and their codes) within the Systematic Reconnaissance Flight (SRF) surveyed area. The box in the inset map shows the SRF area in Tanzania..... 73

Fig. 4.3: Wavelet energy curves, dominant scale and maximum intensity from TM 1988, ETM+ 2000, 2001, 2002, and ASTER 2006 images for each quadrant. .... 80

Fig. 4.4: The probability of elephant occurrence in 1988 (a) and 2001 (b) generated with the kernel density function. Crop fields are shown in white both in 1988 and 2000..... 81

Fig. 4.5: The quadratic relation between the probability of elephant occurrence and the dominant scale of landscape heterogeneity in 1988 (gray dash-dot line) and 2001 (black dotted line). The dominant scales of 7000 m and 8300 m sustain the highest probability of elephant occurrence in 1988 and 2001 respectively..... 83

Fig. 4.6: The logarithmic relation between the dominant scale of landscape heterogeneity and the amount of cultivated land by quadrant in 1988 (gray dashed-dot line) and 2000 (black dotted line). ..... 84

Fig. 4.7: Wavelet results for the quadrant Q002\_000: (a) Africover; (b) NDVI of ETM+ 2000; (c) wavelet coefficients at scale 240 m; the arrow shows a swampy area; the rectangular includes high wavelet coefficients, which capture the contrast between crop fields and natural vegetation (see inset (d); source: ETM+ 2000); (e) wavelet coefficients at scale 960 m; the circles show the contrast between swampy areas and open shrubs (on the right) and crop fields and closed trees (on the left); (f) wavelet coefficients at scale 7680 m (dominant scale); (g) wavelet coefficients at scale 15,360 m; (h) wavelet energy curve of Q002\_000 showing one dominant scale at 7680 m. The boundary of agricultural areas is shown in white (TNP, Tarangire National Park)..... 86

Fig. 5.1: Selected study area within the Tarangire–Manyara ecosystem in Tanzania. Elephant total counts, the boundaries of Tarangire (TNP) and Lake Manyara (LMNP) National Parks; Lolkisale (LGCA) and Mkungunero (MGCA) Game Controlled Areas; Manyara Ranch (MR), and the villages of Naitolya, Lolkisale and Loborsoit A, are shown..... 95

Fig. 5.2: Flowchart of the research approach: (a) statistical analysis of crop raiding patterns and their validation; (b) prediction of ‘daily refuge-to-crop raid’ corridors and their analysis in relation to crop raiding patterns..... 97

Fig. 5.3: (a) Crop raiding events by elephants and probability of elephant occurrence from total counts; (b) Elephant refuges (95% contour), crop raiding zones (95% contour) including high and very high vulnerable subzones (50% and 10% contours respectively), footpaths, and dry river beds. The arrow indicates the stepping stone farms (TNP, Tarangire National Park; LGCA, Lolkisale Game Controlled Area)..... 107

Fig. 5.4: Boxplot of the distance of raided farms to (a) elephant refuges and (b) dams. The dotted line represents the average elephant travel distance in TME. .... 107

Fig. 5.5: Predicted elephant corridors along: (a) footpaths, (b) dry river beds, (c) stepping stone farms, (d) control. Fig. 5(e) shows the boundary of elephant refuges, crop raiding zones, vulnerability subzones, source/destination points, outcrops, and farms potentially acting as stepping stones (in red) or barriers (light gray). TNP, Tarangire National Park; LGCA, Lolkisale Game Controlled Area. .... 109

Fig. 5.6: Boxplot of the cumulative resistance for each corridor category. The dotted line represents the average cumulative resistance among all corridors. .... 110

Fig. 6.1: The dominant scale of spatial heterogeneity in Andalucía, Spain, as measured by the intensity–dominant scale method based on the wavelet transform using Orthophoto (1 m resolution). The arrows indicate the match between the dominant scale and the landscape features both in agricultural (a) and semi-natural areas (b). .... 116

Fig. 6.2: The spatial resolution independence of the dominant landscape scale from the original pixel size of the satellite images and the ‘perception scale’ of heterogeneity by different body-sized animals. (a) Spatial patterns of features in images of different pixel size ( $s_1, s_2, s_3$ ); (b) wavelet energy curves of images with  $s_1, s_2, s_3$  pixel size and expected ‘perception scale’ by duiker, wildebeest and elephant. .... 118

Fig. 6.3: (a) Relative atmospheric correction of band 3 and 4 of a TM image acquired on 17 February 1993 using a regression analysis and a reference ETM+ image acquired on 21 February 2000. (b) Wavelet energy curves of NDVI-original (pink line) and atmospherically corrected (blue line) spatial heterogeneity of TM in three quadrants. .... 119

Fig. 6.4: The theoretical framework showing the fragmentation of a natural savanna (in green) in relation to farming expansion (in yellow). In  $t_1$  sparse and small arable fields do not affect the dominant scale of the landscape, which is relatively large; in  $t_2$  the dominant scale is reduced due to the expansion of farming; in  $t_3$  the dominant scale increases with cultivation; in  $t_4$  the dominant scale is greatest because the landscape is almost totally converted to agriculture. .... 120

Fig. 6.5: The theoretical framework showing the response of elephant to changes in heterogeneity due to farming expansion. Point A and B indicate the case studies in Tanzania and Zimbabwe (TME, Tarangire–Manyara ecosystem). .... 123

Fig. 6.6: From left to right, 50, 90 and 95% probability of volume contour for dry (in red) and wet (in blue) season. The points represent the elephant locations in the dry (up) and wet (bottom) season..... 125

Fig. 6.7: An overview of the main results in the Tarangire–Manyara ecosystem (TME). See Fig. 3.4, Fig. 4.4, Fig. 5.3 and Fig. 5.5 for reference. .... 128

Fig. C.1 Number of farms by class of damaged area per farm in the three villages in 2006 (a) and 2008 (b). Results obtained from the household survey data ..... 133

# List of Tables

Table 2.1: Date of acquisition of the Orthophoto, ASTER and ETM+ for each quadrant ( <i>n</i> ). .....	21
Table 2.2: Results of the Mann–Whitney test of the median dominant scale for agricultural and semi-natural areas. ....	31
Table 3.1: Wildlife Surveys in the Tarangire–Manyara Ecosystem (TME), 1994–2004 (LMNP, Lake Manyara National Park; SRF, systematic reconnaissance flight; TC, total count). ....	50
Table 3.2: Source, data type and unit of the independent variables. ....	52
Table 4.1: Comparison between the dominant scale of NDVI-derived landscape heterogeneity from ETM+ 2000, 2001, 2002 and ASTER 2006 images for each quadrant and the assigned dominant scale for the analysis. ....	79
Table 4.2: Regression coefficients, standard errors (s.e.), <i>t</i> and <i>p</i> values of the quadratic relations between the probability of elephant occurrence and the dominant scale of landscape heterogeneity in 1988 and 2001. ....	83
Table 4.3: Regression coefficients, standard errors (s.e.), <i>t</i> and <i>p</i> values of the logarithmic relations between the dominant scale of landscape heterogeneity and cultivation in 1988 and 2000. ....	84
Table 5.1: Predictor, evidence and conditional probability of elephant occurrence used in the Bayesian expert system. ....	102
Table 5.2: Predictors used to generate the resistance maps to elephant movement for each corridor category. ....	104
Table 5.3: Number of elephant crop raiding events ( <i>n</i> ), size (ha), damage (ha), damage per farm (%), and total amount of damaged land (ha) by village per year. Standard deviations are in square brackets [ ]. Village name abbreviation: Lolk., Lolkisale; Lob. A, Loborsoit A; Nait., Naitolya. ....	105

Table 5.4: Households (HHs) surveyed in 2006 and 2008, HHs practicing agriculture, HHs reporting damage by elephants, and their average farm size (ha) in 2006 and 2008. Village name abbreviation as in Table 5.3. .... 106

Table A.1: Statistical tests (B, logistic coefficient; s.e., standard error; Wald statistic and significance) for individual normalized predictors for dry and wet season distribution of elephant: 1 distance from dams; 2 distance from rivers; 3 distance from settlements; 4 distance index from protected areas; 5 distance index from semi-protected areas; 6 slope; 7 topographic position index (TPI); 8 distance from lakes; 9 distance from tarmac roads; 10 distance from minor roads; 11 monthly average NDVI; 12 closed trees; 13 closed shrubs; 14 cultivated areas; 15 herbaceous vegetation on flooded areas; 16 herbaceous vegetation or savanna; 17 open to very open shrubs; 18 open to very open trees; 19 river banks and bare areas; 20 trees or shrubs on flooded areas; 21 woody vegetation; 22 elevation; con, constant..... 131

Table B.1: Two-way ANOVA results of the crop raiding events obtained from the monitoring data. (VLG, village; Yr, year; VLG × Yr, interaction; Resid., residuals). .... 132

# List of Acronyms

ASTER	Advanced Spaceborne Thermal Emission and Reflection Radiometer
AVHRR	Advanced Very High Resolution Radiometer
CVh	Likelihood Cross Validation
CWT	Continuous Wavelet Transform
DWT	Discrete Wavelet Transform
ETM+	Landsat Enhanced Thematic Mapper Plus
FAO	Food and Agriculture Organization of the United Nations
GPS	Global Positioning System
HEC	Human-elephant conflict
LGCA	Lolkisale Game Controlled Area
LMNP	Lake Manyara National Park
MGCA	Mkungunero Game Controlled Area
MR	Manyara Ranch
NDVI	Normalized Difference Vegetation Index
RMSE	Root Mean Square Error
SRF	Systematic Reconnaissance Flight
TAWIRI	Tanzania Wildlife Research Institute
TC	Total counts
TME	Tarangire–Manyara ecosystem

TNP	Tarangire National Park
TPI	Topographic Position Index
UNICOR	UNiversal CORridor network simulator
UTM	Universal Transverse Mercator
VIF	Variance Inflation Factor
WMA	Wildlife Management Area

# 1

## **Introduction**

## **1.1 Landscape heterogeneity, fragmentation and human-wildlife conflicts: Background**

Landscape heterogeneity is defined as the complexity and variability of a landscape property such as vegetation cover over space and time (Li and Reynolds, 1995). Spatial and temporal heterogeneity influences biodiversity (Baldi, 2008; Cromsigt et al., 2009; Pianka, 1966) including herbivore distribution (Fryxell et al., 2005; Murwira and Skidmore, 2005) and abundance (Oliver et al., 2010; Wang et al., 2006). The more heterogeneous the environment, the higher the numbers of wildlife species, as greater heterogeneity implies greater availability of resources and habitats (Fischer and Lindenmayer, 2007; Ritchie and Olff, 1999). This is the case of the African savanna, a heterogeneous mixture of grass and trees (Sankaran et al., 2004), which sustains a wide diversity of coexisting grazing herbivores (Prins and Olff, 1998). Landscape heterogeneity, including vegetation quality and density, may occur along gradients, discrete patches or graded patches (Rogers, 2003). The way animals perceive and access heterogeneous dispersed resources differs at different scales (Fischer et al., 2004; Prins and Olff, 1998), and critically depends on body size (Ritchie and Olff, 1999). Because the metabolic requirements scale with body mass to the power of 0.75 (Kleiber, 1932), a large animal like the elephant can tolerate high quantity of low quality forage, whereas a small animal like the impala needs low quantity but high quality and concentrated food (Prins and Olff, 1998; Ritchie and Olff, 1999). As a result, heterogeneous landscapes characterized by large vegetation patches with dispersed and less concentrated food resources provide a wider selection of forage options for large body-sized herbivores (Laca, 2008), but are less suitable for small specialized herbivores, which are not able to fulfill their dietary needs across large distances (Prins and van Langevelde, 2008).

Landscape heterogeneity is often modified by natural (landslide, flooding, earthquake, animals' activity, etc.) as well as anthropogenic factors (fire, logging, farming, etc.) (Franklin et al., 2002). Fragmentation is the breaking up of a continuous natural habitat or land type into smaller patches (Forman, 1995), and often implies habitat loss (Franklin et al., 2002). A patch is an area having relatively homogeneous conditions relative to other patches (Forman, 1995). Fragmentation is a major threat to global biodiversity and species distribution (Fahrig, 2003; Fischer and Lindenmayer, 2007; Hanski, 1998; Sala et al., 2000). It affects the dispersal capacity of a species (and its distribution) by disrupting connectivity and increasing the level of isolation among suitable habitat patches (Hanski, 1998). Habitat isolation may also affect daily movements between

nesting and foraging sites (Luck and Daily, 2003). Smaller patches may lead to population decline because of the limited availability of resources (Fischer and Lindenmayer, 2007). Other negative effects on wildlife distribution and diversity include reduction of habitat and interior area, and increase of edges (Davidson, 1998). Fragmentation analysis, which is based on the island biogeography theory (MacArthur and Wilson, 1967), measures the level of patchiness and connectivity of a landscape using the geometry (e.g. size, perimeter, degree of isolation, etc.) of these homogeneous units (Bogaert, 2003). Expansion of farming and growth of permanent settlements are key drivers of fragmentation worldwide (Fischer and Lindenmayer, 2007). This is particularly severe in the tropical savanna, which suffers a change rate higher than tropical forest (Lehmann, 2010). In the savanna, farming expansion into wildlife corridors, migration routes and dispersal areas increases the isolation of protected areas, threatening species persistence and diversity (Ottichilo et al., 2000; Reid et al., 2000; Serneels and Lambin, 2001).

Corridors promote movement of taxa (Haddad et al., 2003), including seed dispersal (Damschen et al., 2006; Levey et al., 2005) and continuity of natural processes (Bennett, 1999; Gilbert-Norton et al., 2010) also in response to climate change (Channell and Lomolino, 2000). Corridors are therefore expected to mitigate the effect of fragmentation by providing habitat connectivity (Beier and Noss, 1998). Since the last decade, international conventions seek to minimize changes in biodiversity by protecting and restoring wildlife corridors as well as establishing ecological networks (e.g., Natura 2000 and the Pan-European Ecological Network of the European Union). Yet the role of corridors is controversial (Beier and Noss, 1998; Mann and Plummer, 1995; Simberloff et al., 1992) and highly debated (Boitani et al., 2007). Corridors may reduce the species survival in the connected habitat patches by facilitating disease transmission, alien species invasion, predation, hunting and poaching (Simberloff and Cox, 1987). As corridors are species-specific (Boitani et al., 2007), they may not benefit all species (Hobbs, 1992). Consequently assessing their effectiveness for keystone species at broad spatial and temporal scales may have important implications for wildlife conservation and management.

Associated with fragmented habitats are an increase in human-wildlife interfaces (Hoare and Toit, 1999; Nelson et al., 2003) and consequently an increase in human-wildlife competition for space and resources. Where such competition affects people's livelihoods, wildlife is persecuted (Sitati et al., 2005) and its conservation is at risk. In the African savanna, significant proportions of large mammals reside outside of protected areas (Hoare, 1999b; Ottichilo et al., 2000), where they are exposed to the effects of farming, legal and illegal

## Introduction

hunting and other human pressures. Conflicts result from damage to farms including livestock depredation, destruction of crops and food storage. In the savanna human-wildlife conflicts often occur over access to drinking water and competition for forage and space. The analysis of environmental and anthropogenic factors and wildlife behaviour has not clarified yet the spatial occurrence of human-wildlife conflicts (Hoare, 1999b; Sitati et al., 2005; Sitati et al., 2003). Fragmentation may represent a good indicator of human-wildlife conflicts patterns. Degrees or types of fragmentation are expected to have different effects on wildlife distribution and biodiversity (Bogaert, 2003). In savanna, small and large scale farming may drive different degrees of landscape fragmentation and conflicts. Farm size is an index of wealth and represents an important indicator for coping with crop raiding (Naughton et al., 1999). Small farms (typically less than 3 ha) are mostly related to labour-intensive, subsistence farming, while large farms (more than 100-200 hectares) are mainly related to capital-intensive, market-oriented farming on large continuous areas (Sillero-Zubiri and Switzer, 2001).

Effective protection methods against crop raiding, such as electric fencing are costly therefore can hardly be adopted by peasant farmers (Naughton et al., 1999; Osborn and Parker, 2003b). The use of traditional protection methods aiming at chasing the animals away, such as the flashlight, drums, shouts, firecrackers, stones thrown by catapults and guards, may also be successful (Osborn and Parker, 2002). However, early surveillance becomes only an effective protection method when it is reciprocally and simultaneously adopted by several smallholders (Naughton et al., 1999). Consequently, small farms are particularly vulnerable to crop raiding (Dublin and Hoare, 2004). The way farm size and distribution modifies landscape heterogeneity is poorly understood as well as the effect on wildlife density, occurrence, behaviour and the resulting crop raiding.

In synthesis, as fragmentation modifies the patchiness of the environment, wildlife numbers and diversity decline, whereas human-wildlife interface increases with potential negative effects for people and wildlife. Currently, neither the level of fragmentation that affects a species-environment relationship, nor the level of heterogeneity that maximizes species response, are well understood (Fazey et al., 2005). In addition, the way fragmentation intensifies conflicts between humans and wildlife has not yet been explicitly analyzed. Understanding the way these factors interrelate with each other is challenging and much depends on the limitations of the methods used (Bogaert, 2003). Measuring landscape heterogeneity and fragmentation is crucial for predicting species response to landscape changes (Schooley, 2006) and for the

management of semi-natural areas (Fazey et al. 2005, Guisan and Thuiller 2005), but also difficult (Bogaert, 2003). The development of remote sensing allows monitoring of landscape properties, such as vegetation cover, and their change over time across wide geographical areas at different spatial resolutions, from a few meters (i.e., QuickBird, 2.4 m pixel size) to about a km (i.e., MODIS, 1 km). However, resolution and extent of the satellite image data may produce different measures of landscape heterogeneity, known as scaling issue (Baldi and McCollin, 2003; Dungan et al., 2002; Levin, 1992; Perry et al., 2002; Wiens, 1989). Scale is an ambiguous word, having various and sometimes opposite meanings across scientific disciplines (Dungan et al., 2002). In landscape ecology and in this thesis, scale refers to the spatial detail of the data (e.g., the pixel size of a raster; Goodchild and Quattrochi, 1997; Levin, 1992), whereas extent refers to the size of the study area (Gustafson, 1998). Species' ecological traits (such as large body size, wide range size and high vagility, Ko et al., 2011; McPherson and Jetz, 2007), detectability (i.e., probability of a species to be detected; Mackenzie et al., 2002) as well as the environmental context (i.e., the characteristic of the environment surrounding a recorded presence of a species at a given site; de Knegt et al., 2011) may affect the accuracy of species distribution models (Guisan and Thuiller, 2005). Consequently, studies quantifying changes in landscape heterogeneity over time and its relation to species distribution require analysis across multiple spatial scales, over a long period of time, and species distribution models that explicitly account for the above factors (Guisan et al., 2006). Yet, studies on species-environment relationships are often conducted at a single and subjectively selected spatial scale (Fazey et al., 2005; Holland et al., 2004; Wheatley and Johnson, 2009) and over short time (in median 2 years; Fazey et al., 2005). This may be related to the methods used to characterize landscape heterogeneity from remotely sensed data (Keitt and Urban, 2005; Wheatley and Johnson, 2009) and the limited availability of long-term datasets on species occurrence (Fazey et al., 2005; Magurran et al., 2010).

Landscape heterogeneity and habitat fragmentation are traditionally analyzed using the patch mosaic approach. This method characterizes the heterogeneity of the landscape in discrete units (patches) based on categorical maps, such as land cover maps (Gustafson, 1998). The geometry of these patches is used to calculate several landscape metrics (Pearson, 2002). These measures are often redundant and correlated to each other (Li and Wu, 2004). The lack of agreement on using a few selected suitable metrics, makes quantification, prediction and comparison of fragmented patterns difficult (Bogaert, 2003). Furthermore, the method is strongly influenced by the initial definition of mapping units (Turner, 1989) and scaling issues (see Wu, 2004). Although the

patch mosaic approach has proven to perform well in agricultural landscapes, it does not accurately quantify gradient landscapes (McGarigal and Cushman, 2005), such as low human impacted savanna (Pearson, 2002). Methods based on continuous environmental variation such as the direct image approach (Goodchild and Quattrochi, 1997), measure the reflectance variance of the image at multiple spatial scales. These methods are relatively new and include: autocorrelation, correlograms, semi-variograms, quadrat variance methods, Fourier spectral analysis, fractals, and wavelets (see Couteron et al., 2006; Dale and Mah, 1998; Perry et al., 2002; Torrence and Compo, 1998). The wavelet transform does not require the stationarity of data and is therefore appropriate for characterizing natural phenomena, which are likely to be aperiodic and non uniform in pattern (Bradshaw and Spies, 1992; Saunders et al., 2005). Being able to synthesize the heterogeneity (and complexity) of a landscape using a few parameters represents an important achievement in landscape ecology (Bogaert, 2003). Murwira and Skidmore (2006) developed the intensity–dominant scale method based on the wavelet transform to simultaneously measure change in variability (previously captured by the direct image approach) and in patch size (previously captured by the patch mosaic approach) of vegetation cover from the Normalized Difference Vegetation Index – NDVI (Murwira et al., 2010). For the intensity–dominant scale method, the intensity refers to the maximum contrast or variance in vegetation cover (e.g., in NDVI) measured at successively increasing window sizes or scales. The dominant scale represents the window size or scale at which this maximum variance occurs (Murwira and Skidmore, 2005). This method explained 80% of the variance in elephant occurrence in an agriculture-dominated savanna landscape in Zimbabwe (see Murwira, 2003; Murwira and Skidmore, 2005) and outperformed two NDVI-based direct image methods of landscape heterogeneity (Murwira and Skidmore, 2010). The intensity–dominant scale method appears a useful tool for monitoring environmental heterogeneity. However, its applicability in semi-natural, gradient environments such as low human impacted savanna as well as its robustness against scaling issues has not yet been explored.

## **1.2 The wavelet transform and the intensity-dominant scale method**

The wavelet transform is a convolution of the wavelet function (little and localized waveform) with the signal, such as the satellite image data. The wavelet is squeezed and stretched (dilation), and moved along the image (translation), to quantify the local match between the wavelet and the image data at different locations and scales. The transform decomposes the image in

its separate components and identifies coherent structures and features at specific scales (Addison, 2002). The transform is performed in a smooth way by the Continuous Wavelet Transform (CWT), and in a discrete steps by the Discrete Wavelet Transform (DWT)(Addison, 2002). DWT allows faster computation and is suitable to handle large dataset. The Haar wavelet (Fig. 1.1(a)) detects edges, boundary and abrupt discontinuity in the data, such as changes and gaps in the canopy cover (Bradshaw and Spies, 1992). The Haar two-dimension Discrete Wavelet Transform (2D DWT) and multiresolution analysis were therefore used in this thesis to quantify the intensity and the dominant scale of landscape heterogeneity from remotely sensed data (Murwira and Skidmore, 2006). The DWT decomposes the image with orthogonal wavelets (the smooth and the detail function), which act like low- and high-pass filters at successive bases in the vertical (north to south), diagonal (north-east to south-west and south-east to north-west), and horizontal (east to west) direction. At each level of decomposition (which follows a sequence of the power of 2), the transform produces 4 outputs: the 'smooth' (which is an averaged version of the original image), the 'vertical', the 'diagonal', and the 'horizontal' details (Bruce and Gao, 1996)(see Fig. 1.1(b)). The details express the deviances from the average value of the image at each direction and scale (Bruce and Gao, 1996). Each output contains a set of coefficients (Bruce and Gao, 1996): high absolute values represent a good match between the shape of wavelet and the data (which indicates an abrupt change in vegetation cover); small or zero values a lack of match (Addison, 2002; Ogden, 1997).

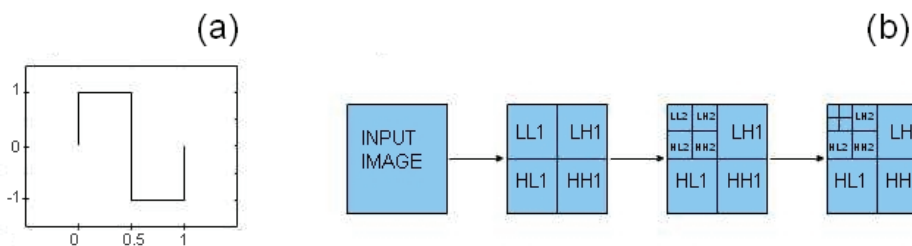


Fig. 1.1: (a) Haar wavelet function, (b) Haar 2D-DWT wavelet decomposition of an image. LL, LH, HL, HH (the smooth, and the vertical, horizontal and diagonal details). The numbers indicate the level of decomposition.

The intensity–dominant scale method based on the wavelet transform was developed by Murwira and Skidmore (2006) to quantify the level of patchiness and variability of vegetation cover and biomass as measured by the NDVI at multiple spatial scales. For this method, the intensity quantifies the maximum change in the vegetation cover across multiple spatial scales, whereas the

dominant scale quantifies the size of dominant landscape features. Consequently, the dominant scale directly relates to the level of patchiness (or fragmentation) of a landscape (Murwira and Skidmore, 2006). Algorithms and detailed descriptions of the methods are included in chapters 2 and 4.

### **1.3 Research objectives and hypotheses**

The main objective of this study was to analyze the effect of landscape heterogeneity and fragmentation on wildlife distribution across space and time and its relation with human-wildlife conflicts. Although more complex relationships exist among these factors, other feedbacks, including the landscape modifications induced by an animal, were not considered. In this thesis, heterogeneity refers to the spatial and temporal variability and patchiness in vegetation cover, as measured by NDVI. Fragmentation particularly refers to the patchiness determined by farming. NDVI is a measure of the amount of canopy "greenness" (Glenn et al., 2008), and can be considered an indicator of the vegetation cover, specifically the green vegetation cover (Roderick et al., 1999). NDVI has been successfully used to explain the distribution of herbivores (Pettorelli et al., 2005) including the elephant (Murwira and Skidmore, 2005). Understanding a species-environment relationship requires the accurate quantification of landscape heterogeneity as well as of species distribution over time and space. Quantifying heterogeneity and fragmentation in semi-natural environments at multiple spatial scales formed the backbone of this study and was performed using the intensity-dominant scale method based on the wavelet transform (Murwira and Skidmore, 2006). There is a growing demand for new approaches in corridor design (Chetkiewicz et al., 2006) based on long-term dataset on biodiversity (Magurran et al., 2010) as well as new distribution models that account for species ecological traits, detectability and environmental context (Ko et al., 2011; McPherson and Jetz, 2007; Rota et al., 2011). However, models based on expert knowledge have also shown to successfully predict species distributions in absence of direct field observations (Murray et al., 2009; Niamir et al., 2011; Skidmore, 1989). An important objective of this study was therefore the development of new approaches for predicting the distribution of animals, corridors and crop raiding patterns by integrating long-term dataset as well as expert and local knowledge.

The research focused on a single herbivore species, the African elephant (*Loxodonta africana* Blumenbach). The elephant is a vulnerable (IUCN, 2010) keystone and umbrella species of the savanna ecosystem (Hoare and Toit, 1999), which migrates seasonally over large distances (Douglas-Hamilton et al.,

2005; Galanti et al., 2006; Ngene et al., 2009a). The elephant is also a crop raider (Dublin and Hoare, 2004; Nelson et al., 2003; Sitati et al., 2005). Crop raiding is the most common form of human-elephant conflict (Hoare, 2000). Spatial patterns of crop raiding are poorly understood, making prediction and protection difficult (Hoare, 1999b; Sitati et al., 2005; Sitati et al., 2003). Habitat fragmentation combined with human disturbance (Hoare and Toit, 1999), ivory poaching (Burn et al., 2011; Wasser et al., 2010) and persecution responding to crop raiding (Nelson et al., 2003), may drastically reduce elephant populations (Murwira and Skidmore, 2005; Prins et al., 1994). Therefore, the elephant represents an ideal species to investigate the effects of habitat fragmentation on distribution and corridors as well as on crop raiding patterns. Although the study focused on elephants, it is assumed that the pattern and processes discussed in this thesis may be translated to other mammal herbivores, and other taxa.

This research tested the following hypothesis:

- 1 ) The intensity–dominant scale method based on the wavelet transform is resolution-robust, accurate and effective in characterizing both agricultural and semi-natural environments, including low human impacted savanna (chapter 2 and 4);
- 2) The intensity–dominant scale method based on the wavelet transform is seasonally-robust, i.e., it can quantify the same dominant scale using images of different date (i.e., acquired in different seasons and years). In other words, the method does not require the atmospheric correction of the images (chapter 2).
- 3) Seasonal distributions of elephant and its migration corridors can be detected by using a new method based on long-term datasets, such as total counts and Systematic Reconnaissance Flight (SRF)(Norton-Griffiths, 1978), which are broadly available, but hardly used in species distribution modelling (chapter 3);
- 4) The species distribution model presented in this study can produce accurate seasonal predictions, by accounting for species ecological traits, detectability and environmental context (chapter 3);
- 5) The seasonal migration corridors identified by the method match the historical migration routes, providing connectivity for elephant over the years (chapter 3);
- 6) In semi-natural savanna, elephant occurrence in the wet season is higher at intermediate dominant scale of heterogeneity, and lower at very small and very large dominant scales (chapter 4);

- 7) Change in the dominant scale of landscape heterogeneity due to farming expansion controls the wet season distribution and density of elephant in semi-natural savanna (chapter 4);
- 8) During the maturation of food crops, crop raiding elephants move daily along 'refuge-to-crop raid' corridors, following linear as well as stepping stone landscape features (chapter 5);
- 9) Size and distribution of scattered farms in the savanna influence elephant movements and therefore crop raiding patterns (chapter 5).

## 1.4 The study area

The research was conducted in the Tarangire–Manyara ecosystem (TME)(between 3°36'S and 4°7'S, and 35°82'E and 36°74'E), northern Tanzania. The TME is part of the Maasai Steppe (Prins, 1987) and hosts the largest population of elephant (about 3000 animals) in northern Tanzania. The study area includes protected (Tarangire and Lake Manyara National Parks), semi-protected (Manyara Ranch, Lolkisale and Mkungunero Game Controlled Areas) and unprotected areas (Fig. 1.2), and covers an area of above 15,000 km<sup>2</sup>. Elephant and other large mammals (such as zebra, wildebeest and buffalo) migrate seasonally from the National Parks to the dispersal areas outside the Parks at the onset of the rains and backwards at the end (Lamprey, 1964). This thesis analyzes a long time-series of elephant total counts and SRF, from 1988 to 2004. During this period, farming expansion into wildlife dispersal areas and migration corridors driven by high human population growth and immigration rates are increasingly threatening the viability of these protected areas (Borner, 1985). In an agriculture-dominated savanna landscape in Zimbabwe, Murwira and Skidmore (2005) showed that elephant population declined as the dominant scale of landscape heterogeneity became smaller (i.e., more fragmented), up to a certain threshold where the elephant disappeared from the ecosystem. A further study also showed that the elephant decline was related to an increase in farming expansion (Murwira et al., 2010). Compared to the Zimbabwean study area, TME appears relatively less cultivated and characterized by large portions of natural vegetation. However, the way heterogeneity and farming expansion influence elephant distribution has not yet been analyzed in the TME, neither its effect on crop raiding. Conflicts between farmers, pastoralists, policy-makers and conservationists have increased in the TME because of the lack of land use plans (Kaswamila, 2009). In 1998, the Government of Tanzania established another category of protected area, the Wildlife Management Area, with the purpose of enhancing conservation and poverty alleviation through

direct involvement of local communities in sustainable utilization of natural resources (MNRT, 1998). In order to accomplish this, scientific information is required on key wildlife species distribution, habitat fragmentation patterns and human-wildlife conflicts.

Detailed topographic, climatic and vegetation descriptions of the study area are given in chapters 3, 4 and 5.

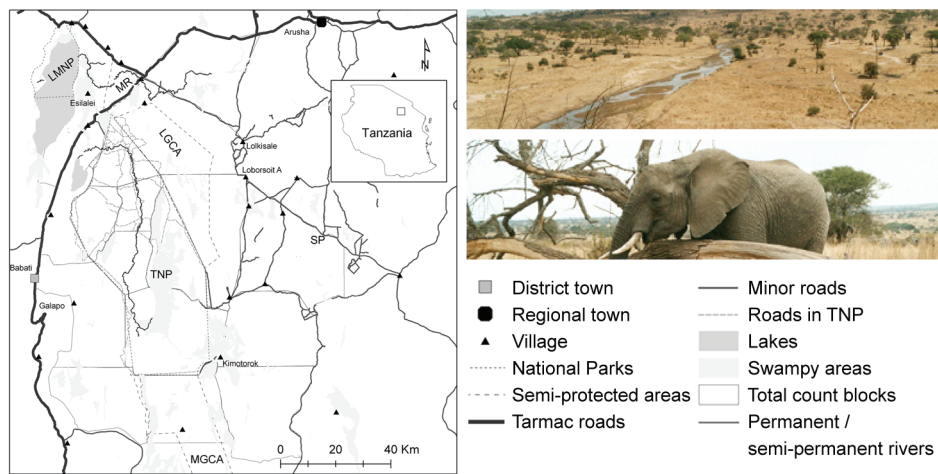


Fig. 1.2: The Tarangire–Manyara ecosystem (left), its dominant vegetation (upper right) and elephant.

## 1.5 Conceptual framework and thesis outline

This thesis includes six chapters. Besides the introduction and synthesis, the remaining chapters have been published in or submitted to peer reviewed journals. Their structure and content is largely retained in the thesis. The conceptual framework and the research questions are depicted in Fig. 1.3.

**Chapter 1** provides a synthetic review of the way environmental heterogeneity and fragmentation interact, influencing species distribution, biodiversity and the human-wildlife interface. This chapter introduces the method applied to characterize heterogeneity and fragmentation patterns, as well as objectives, hypotheses and outline of the thesis.

**Chapter 2** tests the robustness and accuracy of the intensity–dominant scale method based on the wavelet transform in characterizing landscape heterogeneity. This method is applied both in agricultural and semi-natural

areas of Andalucía (Spain) using a wide range of images of different resolution, sensors and date of acquisition.

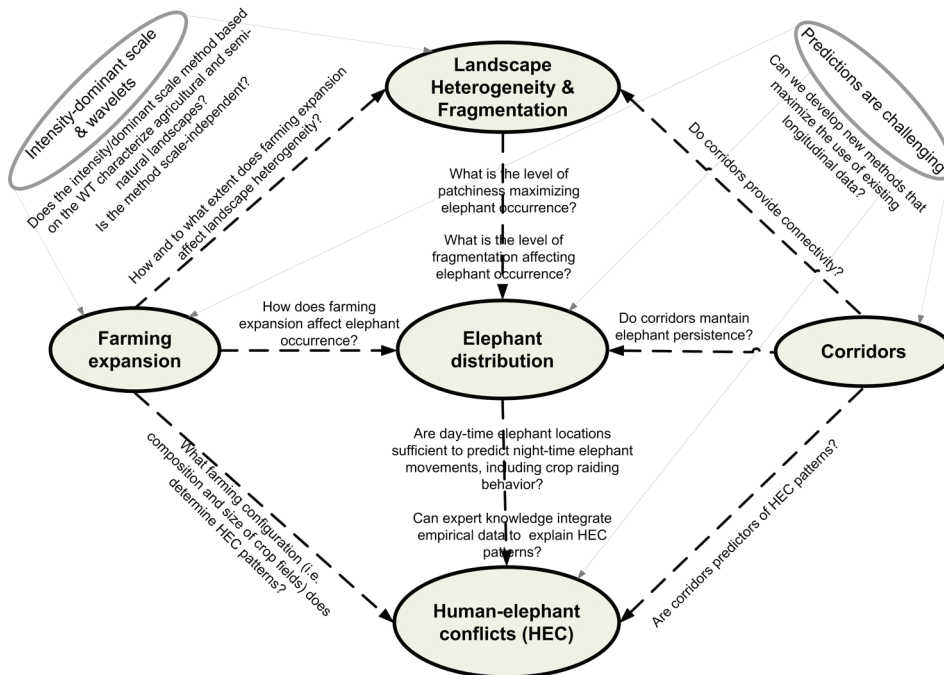


Fig. 1.3: Conceptual framework of the thesis and research questions (WT, Wavelet Transform).

**Chapter 3** tests and validates a new approach to predict species distributions and identify seasonal corridors for elephant in the TME using long-term aerial survey (total counts and SRF). The approach accounts for species ecological traits, detectability and environmental context.

**Chapter 4** focuses on identifying the level of patchiness (dominant scale) that maximizes the wet season occurrence of elephant and its change in relation to farming expansion in the TME. The landscape analysis is based on the intensity–dominant scale method developed by Murwira and Skidmore (2006). The findings are compared with the results obtained from a similar study by Murwira and Skidmore (2005) in an agriculture-dominated savanna, in Zimbabwe.

**Chapter 5** tests the hypothesis that the distribution and size of scattered farms in the savanna influence elephant movements along ‘daily refuge-to-crop raid’

corridors, determining crop raiding patterns. The daily corridors are predicted using a new approach based on the integration of an expert system with a corridor network simulator. The study presented here hypothesizes that in the TME elephant move along stepping stone corridors made by scattered small farms.

**Chapter 6** synthesized the finding of the thesis in relation to the conceptual framework illustrated in Fig. 1.3. This chapter discusses the implication of these findings to the monitoring and prediction of ecological patterns as well as the management and conservation of large mammal species in increasingly fragmented environments.



# 2

## **A common dominant scale emerges from images of diverse satellite platforms using the wavelet transform**

This chapter is based on:

Pittiglio, C., Skidmore, A.K., de Bie, C.A.J.M., Murwira, A., 2011. A common dominant scale emerges from images of diverse satellite platforms using the wavelet transform. *International Journal of Remote Sensing*. 32, 3665-3687

## Abstract

In this paper we investigate the scale dependence of spatial heterogeneity in multiresolution and multisensor data using the wavelet transform. The landscape analyzed with the wavelets retains the same dominant pattern irrespective of the original pixel size of the image. In agricultural areas, typically characterized by a mosaic of cultivated fields, the wavelet transform quantified consistently a median dominant scale of 512 m in the Orthophoto, Advanced Spaceborne Thermal Emission and Reflection Radiometer (ASTER) and Landsat Enhanced Thematic Mapper Plus (ETM+). The dominant scale represented the dominant field size of cultivated areas. The shape of the average wavelet energy curves was also similar among the images. In semi-natural areas the wavelet transform quantified consistently a median dominant scale of 128 m in the Orthophoto and ASTER. The median dominant scale of ETM+ was slightly smaller and located at 64 m. We characterized the spatial heterogeneity of agricultural and semi-natural areas in Andalucía (Spain) using multisensor data not time coincident ranging from 1 m (Orthophoto), 15 m (ASTER) to 28.5 m (ETM+). The contrast in vegetation cover was measured using Normalized Difference Vegetation Index (NDVI) in ASTER and ETM+ and red band in Orthophoto. We performed a multiresolution analysis using a Haar two-dimension Discrete Wavelet Transform to quantify and compare the intensity (maximum degree of contrast in vegetation cover), the dominant scale (the scale at which the maximum intensity occurs) and the wavelet energy curve (intensity plotted as a function of the scale) of different images at intervals of the power of 2 within the scale range of 2 m and 4096 m.

## 2.1 Introduction

Spatial and temporal patterns of landscape heterogeneity are considered important factors determining ecological processes as well as species distribution and biodiversity (Turner, 1989). The development of remote sensing has provided an opportunity to quantify spatial and temporal patterns of landscape heterogeneity. In particular, the development of sensors of increased spatial resolution has provided imagery with high spatial details (Aplin, 2006). Yet a general lack of methods for accurately characterizing landscape heterogeneity from remotely sensed data still exists in landscape ecology (Keitt and Urban, 2005). This has been mainly due to the fact that most of the methods have not explicitly considered the effect of pixel size of satellite images on metrics of spatial heterogeneity. The pixel size is one of the most significant spatial elements of remotely sensed imagery and it is closely related, although not synonymously, with the more general term of spatial resolution (Aplin, 2006;

Atkinson, 2004; Fisher, 1997). Many definitions of spatial resolution have been proposed to delineate the spatial details of the imagery based on the geometrical properties of the sensor, the spectral properties of the target objects and the spatial resolving power of the sensor (Mather, 1999). These definitions, for instance, include instantaneous field of view (the area in the ground that in theory is viewed by the instrument from a given altitude at any given instant in time), point spread function (the ability to separate point targets), modulation transfer function (the ability to measure periodicity of repetitive targets), effective resolution element (the ability to measure spectral properties of small targets) (Forshaw et al., 1983). This paper refers to the nominal spatial resolution of the satellite images, which in satellite-based platforms is directly related to the area in the ground that represents a pixel in the sensor (Mather, 1999; Nunez et al., 2006). Although the nominal spatial resolution may be influenced by the spatial resolving power of the sensor and variations in atmospheric conditions and in satellite orbit (Nunez et al., 2006), it is considered an important specification of the satellite and is commonly related to the original pixel size of the satellite image (Atkinson, 2004). This paper specifically refers to the original pixel size of the imagery and investigates the effect that the pixel size has on characterizing spatial heterogeneity from remotely sensed imagery. Traditionally, two main approaches have been used to characterize the spatial heterogeneity from remotely sensed images: the patch mosaic approach (Gustafson, 1998; Pearson, 2002) and the direct image approach (Goodchild and Quattrochi, 1997). The first approach characterizes the heterogeneity of the landscape in discrete units (patches) based on categorical maps, such as land cover maps. The geometry of these patches such as size, shape, spatial distribution, connectivity and diversity is used to calculate several landscape metrics (Pearson 2002). The second approach quantifies the spatial heterogeneity using the reflectance variance of the image, at constant pixel size. This method assumes that only the reflectance values change in space while the pixel size is fixed and arbitrarily chosen. Both approaches are affected to different extent by the pixel size of the image. In other words, by changing the pixel size, the outputs of the landscape metrics and of the variance measures change (Dungan et al., 2002; Tarnavsky et al., 2008; Wu, 2004). Wu (2004) tested several landscape metrics by varying the pixel size of images for different landscapes. He found that many of these measures showed unpredictable behaviours and concluded that they cannot be used to extrapolate results at different scales. Recently Tarnavsky et al. (2008) obtained similar results using geostatistical analysis. As a consequence the interpretation of spatial patterns analysis performed using these two approaches can strongly be affected by the pixel size of the image, a phenomenon generally called scaling issue. Scaling issues, namely the effect of scales on patterns, processes and ecological

inferences, have been analyzed in landscape ecology in relation to conventional surveys (Baldi and McCollin, 2003; Dungan et al., 2002; Levin, 1992; Perry et al., 2002; Wiens, 1989). However scaling issues affecting the characterization of spatial patterns from remotely sensed data have not been sufficiently investigated. Scale is an ambiguous word, including different and sometimes opposite meanings in cartography, geography, landscape ecology and remote sensing (Dungan et al., 2002). In this paper, scale refers to the window or dimension through which a phenomenon may be observed and operate (Levin 1992; Goodchild and Quattrocchi 1997). In both cases scale is related to the pixel size of the satellite image. In our opinion, understanding the effect of the pixel size on the analysis of spatial patterns using remotely sensed data can solve different problems, such as: a) identifying and selecting the appropriate scale of investigation of ecological processes (Atkinson and Aplin, 2004; Lloyd et al., 2005); b) understanding processes acting at multiple scales (Murwira and Skidmore, 2005); c) integrating different remotely sensed products (Tarnavsky et al., 2008).

Although the patch mosaic and the direct image approach are both influenced by the scaling issue, the patch mosaic approach appears less effective in characterizing spatial patterns of landscape heterogeneity in remotely sensed images at multiple scales (Wu 2004). Furthermore the abrupt boundaries of the patches do not consider any variation and gradients in the landscape (Pearson 2002). On the contrary, the direct image approach is particularly useful in quantifying gradient landscapes and appears more effective in addressing multiscale issues. Several methods belonging to this approach have been proposed to characterize spatial heterogeneity at multiple scales from remotely sensed data such as autocorrelation, correlograms, semi-variograms, quadrat variance methods (e.g. two-three term local quadrat variance (TTTLQV), Paired Quadrat Variance (PQV)), Fourier spectral analysis and fractals (Couteron et al., 2006; Dale and Mah, 1998; Perry et al., 2002). A weakness of these techniques is that they are based on assumptions of the data distribution (such as the stationarity) that can hardly be met in ecological and natural system. In particular, the stationarity of the data assumes that the mean of a landscape property (like vegetation cover) does not change with the location. Indeed landscape features are often aperiodic and non-stationary (Bradshaw and Spies, 1992). The quadrat variance analysis (PQV, TTTLQV), for example, generate peak drift of the variance (not coincident with the dominant scale of spatial variation) and resonance peak not related to the data (Dale and Mah, 1998). According to Bradshaw and Spies (1992) the semivariogram has limited capability to detect local features deviating from the mean. Moreover its interpretation becomes difficult with multiscale structure in the data.

In the last decade, wavelet transform has been successfully applied in different scientific disciplines such as oceanography (Meyers et al., 1993), geophysics (Varotsos et al., 2003), image fusion (Nunez et al., 1999) and compression (Addison, 2002; Torrence and Compo, 1998). Furthermore it seems a promising tool also to characterize spatial heterogeneity in landscape ecology (Murwira and Skidmore, 2006). The main advantage of this tool is that it does not assume stationarity of the data and can therefore be used to characterize spatial heterogeneity of landscape property like vegetation, which are aperiodic and non uniform in pattern (Bradshaw and Spies, 1992; He et al., 2007; Saunders et al., 2005). Other advantages of the wavelet transform are: 1) it acts as a local filter and its dimension does not need to be defined a priori; 2) the magnitude of the signal can be directly related to position in the image; 3) the wavelet can be chosen according to the form of the data and the objective of the study. A limitation of the tool is that dominant patterns smaller than the original pixel size cannot be detected because the smallest applicable wavelet is close to the cell size of the image (Strand et al., 2006).

The use of wavelet analysis has grown considerably over the last decade. This method has been applied to explore multiscale patterns in ecological data (Saunders et al., 2002; Torrence and Compo, 1998), microclimate along transects (Redding et al., 2003), spatial patterns of plants (Strand et al., 2007; Strand et al., 2006), and grassland (He et al. 2007), canopy gap structures (Bradshaw and Spies 1992), spatial variation in land cover (Lloyd et al. 2005) and spatial variation of elephant presence in a savanna landscape (Murwira and Skidmore 2005). Nunez et al. (2006) used the wavelet analysis to compare the nominal spatial resolution of two satellite images (e.g. Landsat-5 and SPOT-3) and found a difference between the relative and nominal spatial resolution. Nevertheless the application of wavelet analysis to characterize and compare the spatial heterogeneity of a landscape from multisensor and multiresolution remotely sensed data has not been investigated, though recently geostatistical methods have been used to compare the spatial variability of different Normalized Difference Vegetation Index (NDVI) products derived from Advanced Very High Resolution Radiometer (AVHRR), SPOT-VEGETATION (SPOT-VGT), Moderate Resolution Imaging Spectroradiometer (MODIS) (Tarnawsky et al. 2008). The result of the study by Tarnawsky et al. (2008) was that the NDVI products were not spatially comparable using data regularization (i.e., spatial aggregation). However it is reasonable to believe that dominant landscape features (equal or larger than the pixel size of the image) are scale independent with respect to the original pixel size of the image and that the incorrect characterization of these features at multiple scales using multiresolution images depends on the limitation of the methods used rather

than on the intrinsic structure of the landscape. In other words, images with different pixel size will show the same dominant spatial patterns, irrespective of the original pixel size of the image, for features equal or larger than the original pixel size.

We used the wavelet transform to test whether the dominant landscape features are scale independent with respect to the original pixel size of the image. In other words, wavelets are able to retain the same dominant pattern of landscape heterogeneity in images that are not time coincident, with different bands and different pixel size. Coueron (2002) found that spectral analysis (Fourier) was able to make consistent textural comparison between photographs of heterogeneous dates. Our aim was to test whether the wavelet transform is able to characterize the dominant patterns of features in agricultural, as well as in semi-natural, landscapes irrespective of the original pixel size of the images used. Specifically, we hypothesized that the dominant scales of landscape features would not be affected by the use of images different in: pixel size, waveband and time of acquisition. In this regard, we analyzed and compared the dominant scale, intensity and the wavelet energy curve of the Orthophoto (pixel size 1 m), Advanced Spaceborne Thermal Emission and Reflection Radiometer (ASTER, pixel size 15 m) and Landsat Enhanced Thematic Mapper Plus (ETM+, pixel size 28.5 m). First, we tested if the Orthophoto, ASTER and ETM+ had equal dominant scale. Second, we tested if the shape of the wavelet energy curves of these images were similar. Third, we tested if the images had equal intensity at the same scales of decomposition.

## **2.2 Materials and Methods**

### **2.2.1 Study site and sampling units**

To test the independence of scale for landscape features using the wavelet transform, we selected the study area using three main criteria: a) large extent of the area, because we wanted to perform the analysis at landscape level; b) high environmental heterogeneity to encompass a variation of vegetation types and altitudinal ranges; c) availability of a multisensor dataset to allow the simultaneous analysis of images of different nominal spatial resolution. We selected the region of Andalucía (Spain). The area covers about 87,600 km<sup>2</sup> and it is characterized by a Mediterranean climate. The landscape is heterogeneous including different altitudinal ranges (from 0 to almost 3500 m), different vegetation types (from sclerophyll to deciduous broad-leaved forests, coniferous forests, transitional woodland, shrubs, pastures and wetlands) and

large agricultural areas. A multisensor dataset composed by the Orthophoto (1 m), ASTER (15 m) and ETM+ (28.5 m) was available for our analysis (Table 2.1).

Table 2.1: Date of acquisition of the Orthophoto, ASTER and ETM+ for each quadrant ( $n$ ).

$n$	Agricultural areas ( $n = 10$ )			Semi-natural areas ( $n = 8$ )		
	Orthophoto	ASTER	ETM+	Orthophoto	ASTER	ETM+
1	Jun–Oct 04	10-Apr-01	10-Apr-01	Jun–Oct 04	14-Jul-04	10-Apr-01
2	Jun–Oct 04	3-Jul-05	10-Apr-01	Jun–Oct 04	21-Jun-04	10-Apr-01
3	Jun–Oct 04	27-Apr-04	21-Mar-02	Jun–Oct 04	16-Sep-04	10-Apr-01
4	Jun–Oct 04	27-Apr-04	21-Mar-02	Jun–Oct 04	21-Jun-04	10-Apr-01
5	Jun–Oct 04*	14-Jul-03	10-Apr-01	Jun–Oct 04*	27-Apr-04	21-Mar-02
6	Jun–Oct 04	14-Jul-03	10-Apr-02	Jun–Oct 04	19-Jun-05	25-Apr-00
7	Jun–Oct 04	25-Apr-03	21-Mar-02	Jun–Oct 04	22-Aug-00	25-Apr-00
8	Jun–Oct 04	25-Apr-03	21-Mar-02	Jun–Oct 04	13-Sep-03	20-Aug-99
9	Jun–Oct 04	21-Jun-03	25-Apr-00			
10	Jun–Oct 04	9-Jul-04	25-Apr-00			

\* The two Orthophoto shown in Fig. 2.3, Fig. 2.6 and Fig. 2.7

Because we were interested in testing the wavelet transform on regular and patchy landscapes and on gradient landscapes, we focused our analysis on two main land cover classes: agricultural and semi-natural areas. Eighteen quadrants of 8192 m  $\times$  8192 m (67 km<sup>2</sup> each) were randomly selected in Andalucía based on two categories of the CORINE Land Cover 2000 (CLC2000)(Fig. 2.1). Ten quadrants were selected in agricultural areas (including non-irrigated arable land, permanently irrigated land and rice fields) and 8 in semi-natural areas (including broad-leaved forest, coniferous forest, mixed forest, scrub and herbaceous vegetation associations, sclerophyllous vegetation and transitional woodland-shrub). The quadrants were used to subset the Orthophoto, ASTER and ETM+. Totally 54 images were prepared and analyzed with the wavelet transform. An extent of 67 km<sup>2</sup> was chosen as a compromise between the need to analyze a large area at landscape level and the limitation of data handling and memory problems arising from the calculation of the wavelet transform. The area of 67 km<sup>2</sup> corresponding to a maximum matrix of 8192 rows  $\times$  8192 columns, was the maximum extent we could analyze at once without incurring memory problems using the discrete wavelet transform Haar. Although a larger extent may be analyzed, for instance by partitioning the images in several sub-windows and applying the DWT to these instead of to the whole images, the process may introduce edge distortions. We therefore preferred analyzing at once the whole area of 67 km<sup>2</sup> because it was reasonably large for a study at landscape level and computationally convenient.

A dominant scale emerges from diverse satellite platforms

Eighteen quadrants were considered a good balance between the sampling effort and the significant representativeness of the spatial structure of the study area, without incurring an unreasonable low  $p$ -value.

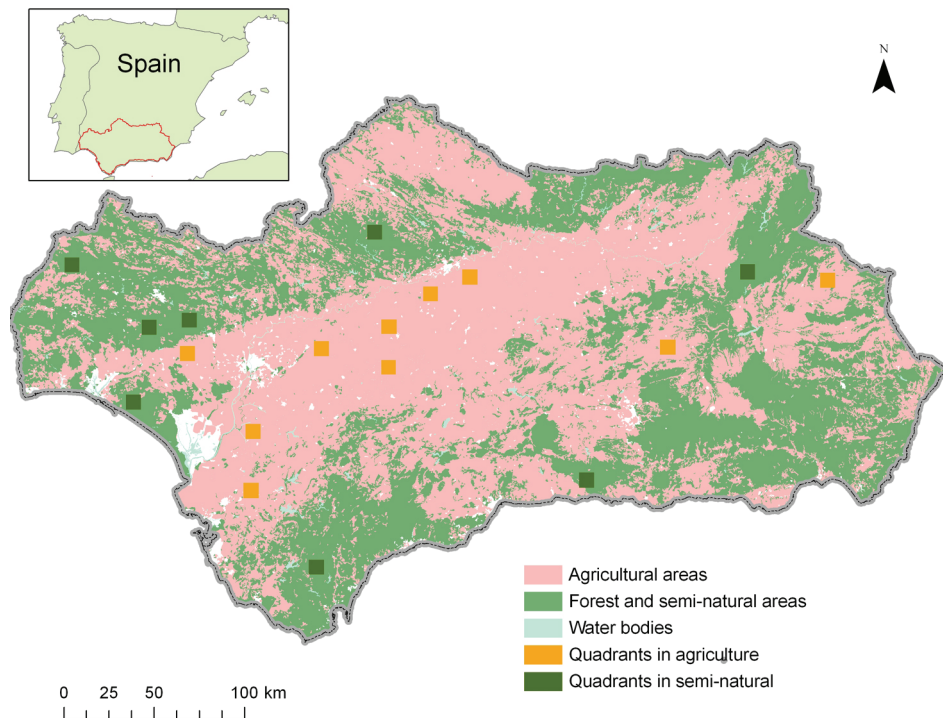


Fig. 2.1: Location of the sampling units (i.e., eighteen quadrants of 8192 m × 8192 m each) in agricultural and semi-natural areas of Andalucía, Spain.

## 2.2.2 Multisensor dataset

The Orthophoto (1 m; scale 1:10,000) were composed of aerial photos acquired between June and October 2004 and orthorectified with a Digital Elevation Model of 20 m of resolution (source: Junta de Andalucía DVD Rom). Because they have the finest resolution and highest geometric accuracy of the dataset, the Orthophoto were used as reference images to geometrically correcting ASTER and ETM+ to match at pixel level. The ASTER and ETM+ images were reprojected to UTM zone 30, datum European 1950-Spain, spheroid International 1924. The Orthophoto (four adjacent images per quadrant) were first mosaicked with the histogram matching option and then subset. ASTER 1B level (EOS, 15 m) were geometrically rectified and coregistered against the Orthophoto. The date of acquisition ranged from 2000 to 2005. The month

largely coincided with the seasonal time of the Orthophoto. Landsat 7 ETM+ (28.5 m) were geometrically rectified and coregistered against the Orthophoto. The images were acquired from August 1999 to March 2002. Therefore they did not match with the Orthophoto period.

We checked the fields' size and assumed that the spatial structure of the landscape (e.g. the pattern of the fields in agricultural areas) did not significantly change during the period of study. In other words, we assumed that, although the agricultural areas may have different crop types, the dominant spatial structure of the fields did not change. Also, we considered that the variation in phenology as well as change in land cover (due for example to deforestation) in semi-natural areas was not significant during the period of study and thus it did not affect the dominant landscape pattern of the quadrants.

The images were resampled from the original pixel size to the closest value of the power of two in order to meet the requirement of the discrete wavelet transform Haar (which decomposes the image at multiple scales based on power of 2, as we explained later). In particular, the ASTER images were resampled from 15 m to 16 m and the ETM+ from 28.5 m to 32 m. In addition, the Orthophoto and ASTER were degraded to 32 m to match the same resolution of the ETM+. We used the nearest neighbour method to resample the images.

The amount of vegetation cover was estimated in two ways depending on the image used: a) with NDVI for ASTER and ETM+ and b) with the spectral reflectance values (brightness) in the red band for the Orthophoto. We did not use the red band consistently for all the images because we wanted to test the effect of using different bands with the wavelet transform. NDVI was calculated from:

$$\text{NDVI} = \frac{(\text{NIR} - \text{R})}{(\text{NIR} + \text{R})} \quad (2.1)$$

where NIR and R are respectively spectral reflectance values in the near-infrared and in the red spectral wavebands of ASTER (NIR: 0.76 to 0.86  $\mu\text{m}$ ; R: 0.63 to 0.69  $\mu\text{m}$ ) and ETM+ (NIR: 0.75 to 0.9  $\mu\text{m}$ ; R: 0.63 to 0.69  $\mu\text{m}$ ). We used NDVI because it is an established index for estimating vegetation "greenness" (Walsh et al., 1997). It provides an effective measure of photosynthetically active biomass (Hill and Donald, 2003; Tucker and Sellers, 1986; Turner et al., 1999) and it is an index of green vegetation biomass (Goward and Dye, 1987). Murwira and Skidmore (2006) used NDVI to quantify the vegetation cover in

savanna with the wavelet transform. The NDVI data were rescaled from the range of -1 to +1 to the range of 0–255 in order to facilitate data handing in image processing software and overcome the memory problems due to the wavelet computation.

The Orthophoto had 3 bands in the visible region of the spectrum (blue, green, red - BGR) and did not include the NIR band. NDVI could not be calculated. Instead we used the spectral reflectance values in the red band (R: 0.6 to 0.7  $\mu\text{m}$ ) because it is a band designed to sense in a chlorophyll absorption region (Gorte, 1999); it is comparable with NDVI; it showed the higher visual contrast in brightness among the visual bands.

The preparation of the data was carried out using ERDAS Imagine 9.1 (Leica Geosystems) and ENVI 4.4. (ITT Visual Information Solutions).

### **2.2.3 The wavelet transform**

The wavelet transform is a convolution of the wavelet function (little and localized waveform) with the signal (Addison, 2002). The wavelet can be moved at various locations along the signal (translation) and it can be squeezed or stretched (dilation). The translation determines the location of the match between the wavelet and the signal; the dilation determines the scale of this match. The transform therefore quantifies the local match of the wavelet with the signal at different locations and scales, decomposing the signal in its separate components. When the wavelet matches the shape of the signal, the transform produces a large positive value (i.e., coefficient); when the wavelet and the signal are out of phase the transform gives a large negative value. If the wavelet does not coincide with the curve of the function, it results a small value (near zero). By moving the wavelet along the signal, coherent structures related to specific scale in the signal are therefore identified. This is done in a smooth way by the Continuous Wavelet Transform (CWT), and in a discrete steps by the Discrete Wavelet Transform (DWT)(Addison, 2002). DWT allows faster computation and are suitable to handle large dataset (limiting the computer memory problem). For this reason we used DWT for our analysis. Note that wavelets and the wavelet transform are exhaustively explained elsewhere (Addison, 2002; Mallat, 1989; Ogden, 1997).

We applied the methodology described by Murwira and Skidmore (2006), who quantified the spatial heterogeneity of a savanna landscape using the intensity–dominant scale approach. We used 2D DWT (Haar) and multiresolution analysis to quantify the intensity and the dominant scale of spatial heterogeneity from

images of different pixel size  $s$  ( $s_{\text{Orthophoto}} = 1$  m;  $s_{\text{ASTER}}=16$  m;  $s_{\text{ETM+}}=32$  m). As defined by Murwira and Skidmore (2006), the intensity is the maximum degree of contrast or variance in vegetation cover, while the dominant scale is the scale at which the maximum intensity occurs. The DWT decomposes the signal in different levels (scales), by using a series of high pass and low pass filters. The high pass filters captures the higher frequency of the signal (above the mean), while the low pass filters analyzes the low frequency (below the mean)(Addison, 2002). In other words, the DWT convolves the data with orthogonal wavelets (the smooth function and the detail function) at successive bases ( $2^j$ , with  $j = 0, 1, 2, \dots, J$ ) in the vertical (north to south), diagonal (north-east to south-west and south-east to north-west) and horizontal (east to west) directions. At each level of decomposition (which follows a sequence of the power of 2), the transform produces 4 outputs (quadrants): a smooth (which is a smooth reproduction of the original image), the vertical, diagonal and horizontal details. Each quadrant contains a set of coefficients where each coefficient is associated with a base level (scale  $j = 1, 2, \dots, J$ ), a direction and a particular location. By iteratively decomposing the image, the transform estimates the underlying smooth behaviour of the signal and the progressively finer-scale deviations from it (Bruce and Gao, 1996).

Thus, given an image  $F(x, y)$  (e.g., the Orthophoto of quadrant 1) the wavelet approximation of the original image is the sum of the smooth and detail functions at different scales:

$$\hat{F}(x, y) = S_j(x, y) + \sum_{j=1}^J \sum_{\text{dir}} D_j^{\text{dir}}(x, y) \quad (2.2)$$

$S_j$  represents the smooth coefficients and  $D_j^{\text{dir}}$  the directional details coefficients.

Each level of decomposition  $j$  (scale) corresponds to a pixel size equals  $2^j s$  where  $s$  is the size of the original pixel size of the image (in this case 1 m for the Orthophoto; 16 m for ASTER; 32 m for ETM+). In our study we totally decomposed the image from the finest to the coarsest scale. Therefore depending on the original pixel size of the image, we analyzed the following ranges of scales at intervals of the power of 2: from 2 m to 4096 m in the Orthophoto; from 32 m to 4096 m in ASTER; from 64 m to 4096 m in ETM+ . We compared the intensity, the dominant scale and the shape of the wavelet energy curves, within the range of 64 m and 4096 m.

**Wavelet energy.** Wavelet energy was calculated as a second moment of the wavelet transform defined as the sum of squares of the coefficients at base  $2^j$ , divided by the sum of squares of all the coefficients in the wavelet approximation  $\hat{F}(x, y)$  (Bruce and Gao 1996):

$$E_j^d = \frac{1}{E} \sum_{k=1}^{n/(2^j)^2} d_{j(x,y)}^2, j = 1, 2, 3, \dots, J \quad (2.3)$$

$d_{j(x,y)}$  are the detail wavelet coefficients at level  $j$  and position  $(x, y)$ ,  $E$  is the total sum of squared of  $\hat{F}(x, y)$  (all the squared coefficients); and  $n/(2^j)^2$  is the number of coefficients at level  $j$ .

To determine the dominant scale and intensity of the spatial heterogeneity of an image (e.g. the Orthophoto of quadrant 1) we used the composite wavelet energy function which is equal to the sum of the wavelet energy functions in the different directions at each level  $j$  (Murwira and Skidmore 2006). We plotted the composite wavelet energy function against scale to get the wavelet energy curve. Then we determine the maximum intensity and the dominant scale across all the levels of decomposition ( $j$ ) by selecting the highest wavelet energy value (i.e., maximum intensity) of the curve. We only used the composite wavelet energy function of the detail coefficients because detail functions are scale specific (Murwira and Skidmore 2006).

The wavelet transform was performed in IDL 6.4.1 (Interactive Data Language)(ITT Visual Information Solutions), using a revised version of the available 2D DWT Haar script which is based on Mallat's algorithm (Mallat, 1989) and Press et al. (1992).

## 2.2.4 Theoretical basis of the scale independence of dominant landscape features

The theoretical basis of the scale independence of dominant landscape features is illustrated by the diagram in Fig. 2.2(a). Given images of different pixel size such as  $s_1$ ,  $s_2$  and  $s_3$  (with  $s_1 < s_2 < s_3$ ), features equal or larger than the pixel size of the coarsest image (i.e.,  $\geq s_3$ ), determine the dominant spatial patterns and structure of the landscape and emerge from the three satellite images irrespective of the original pixel size. These dominant features analyzed using the wavelet transform also emerge from the same scale of decomposition. As shown by Fig. 2.2(b), the wavelet energy curves have the same dominant scale,

intensity as well as similar shape. The landscape features smaller than the coarsest pixel size ( $s_3$ ) are not visible at coarser scale and are not captured by the wavelet transform of coarser images. In other words, images of different pixel size such as the Orthophoto, ASTER and ETM+ show spatial patterns at the same dominant scales and have similar shape for the wavelet energy curves within the common range of scales.

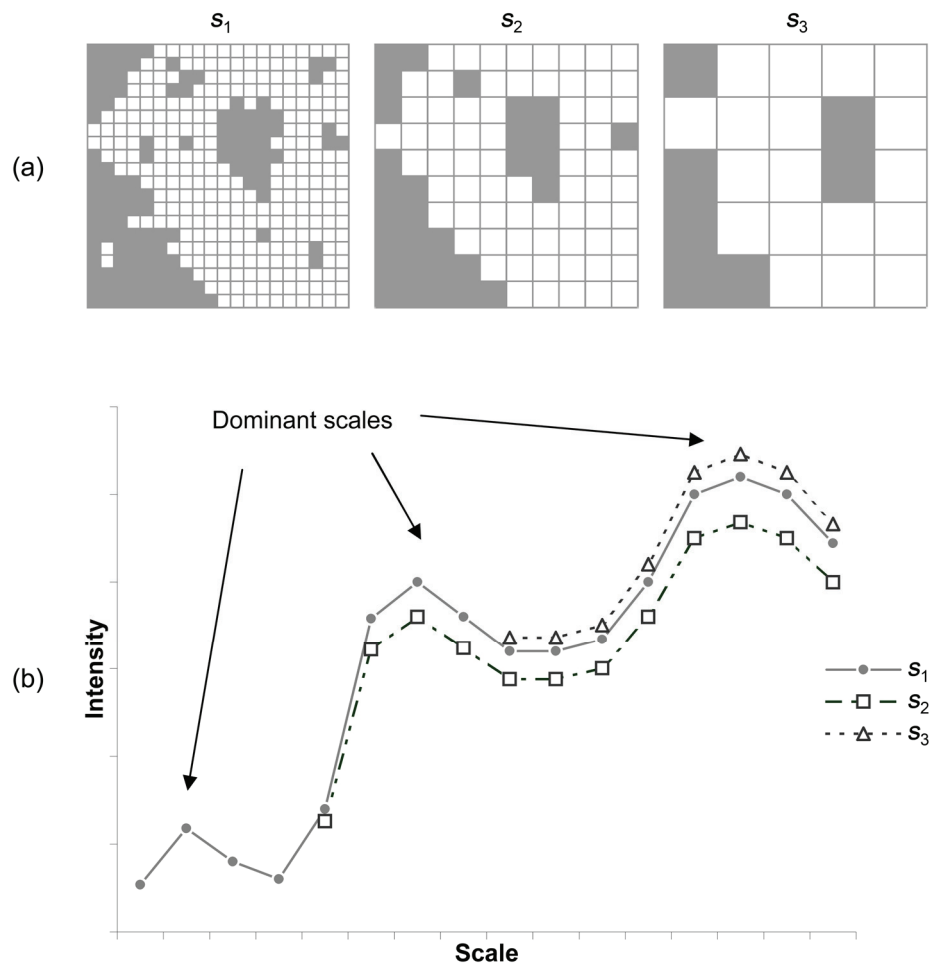


Fig. 2.2: Theoretical basis of the scale independence of landscape features from the original pixel size. (a) Spatial patterns of features in images of different pixel size ( $s_1 < s_2 < s_3$ ); (b) wavelet energy curves of images with  $s_1$ ,  $s_2$ ,  $s_3$  pixel size.

This concept may be extended to coarser images such as MODIS (250 m) and AVHRR (1 km). Comparing images within a large range of scales (for instance from the Orthophoto to AVHRR) using the wavelet transform requires a large study area and consequently a large computing capacity. This study focused on the comparison of the Orthophoto, ASTER and ETM+ within the range of 2 m and 4096 m for two reasons: 1) these images are frequently used to classify land use and land cover and their changes over time. Therefore understanding whether the spatial variability of these multiresolution images is comparable and assessing whether the pixel size is suitable to “catch” the landscape heterogeneity is important; 2) an area of circa 67 km<sup>2</sup> was the maximum extent that we could analyze at once without incurring memory problems using the wavelet Haar. This extent corresponds to a matrix of 8192×8192 for the Orthophoto; 512×512 for ASTER; 256×256 for ETM+. The same extent corresponds to a matrix of 32×32 for MODIS (250 m) and of 8×8 in AVHRR (1 km), which are insufficient for the comparison with the finer images using the wavelet transform. Although, as explained earlier, there are options for implementing DWT for large images, the analysis of images coarser than ETM+ was not within the purposes of this study.

### **2.2.5 Data analysis**

We compared the dominant scale, the intensity and the wavelet energy curves of the Orthophoto, ASTER and ETM+ in order to test whether dominant landscape features (equal or larger than the image pixel size) were scale independent from the original pixel size of the satellite images using the wavelet transform. Alternative indicators may be used to compare the detail of wavelet planes such as correlation coefficient, ERGAS index, root mean square error, etc. However, these indicators which have been used to assess the quality of fused images (Acerbi-Junior et al., 2006; Gonzalez-Audicana et al., 2005; Nunez et al., 2006; Nunez et al., 1999), were not applied in our analysis because they do not represent the intensity–dominant scale concept of landscape heterogeneity. In contrast the wavelet energy curve enables the intensity (maximum variability of vegetation cover) and the dominant scale (dominant patch size) of the landscape to be simultaneously quantified. For this reason, the wavelet energy curve combines the advantage of both the direct and patch mosaic approaches (Murwira and Skidmore 2006), resulting in a good indicator for testing the hypothesis of this study.

The dominant scale data and the intensity data were not normally distributed. A nonparametric statistical method, namely the Mann–Whitney test, was used to test whether the median dominant scale and the median intensity at each scale

$j$ , were significantly different between the Orthophoto and ASTER, the Orthophoto and ETM+, and ASTER and ETM+. In order to test similarity of the wavelet energy curves of the 3 image types, the shape of the average wavelet energy curve of the Orthophoto, ASTER and ETM+ was compared. Specifically the average wavelet energy curve of the Orthophoto was correlated and regressed against that of ASTER and of ETM+. The average wavelet energy curve of ASTER was also correlated and regressed against that of ETM+. The average wavelet energy curve of the Orthophoto, ASTER and ETM+ was calculated by taking the average intensity at each scale  $j$ . The images were compared within the common range of 64 m and 4096 m. The Orthophoto and ASTER were also examined at the finest scales (from 2 m to 4096 m for the Orthophoto and from 32 m to 4096 m for ASTER).

## 2.3 Results

### 2.3.1 Dominant scale

The dominant landscape features of agricultural areas as well as of semi-natural areas analyzed using the wavelet transform were scale independent (given that the resolution of the features within the satellite images were equal or larger than the image pixel size). In details:

In agricultural areas the median dominant scale was not significantly different among the Orthophoto, ASTER and ETM+ (median = 512 m, Mann–Whitney test,  $p > 0.05$ )(Table 2.2). Furthermore, the dominant scale of each quadrant represented the dominant size of the cultivated fields (parcels). As an example, the Orthophoto and the wavelet energy curve of quadrant 5 are shown in Fig. 2.3. Here, the wavelet energy curve indicates that the dominant scale of the Orthophoto is between 256 m and 512 m (Fig. 2.3(a)). The dominant scale represents the dominant size of the cultivated fields (between 250 m and 500 m), which was measured on the screen (Fig. 2.3(b)).

In semi-natural areas, the median dominant scale of the Orthophoto (median = 128 m) was not significantly different from the median dominant scale of ASTER (median = 128 m)(Mann–Whitney test,  $p > 0.05$ ). The median dominant scale of ETM+ (median = 64 m) was significantly smaller than the Orthophoto and ASTER (Mann–Whitney test,  $p < 0.05$ )(Table 2.2).

A dominant scale emerges from diverse satellite platforms

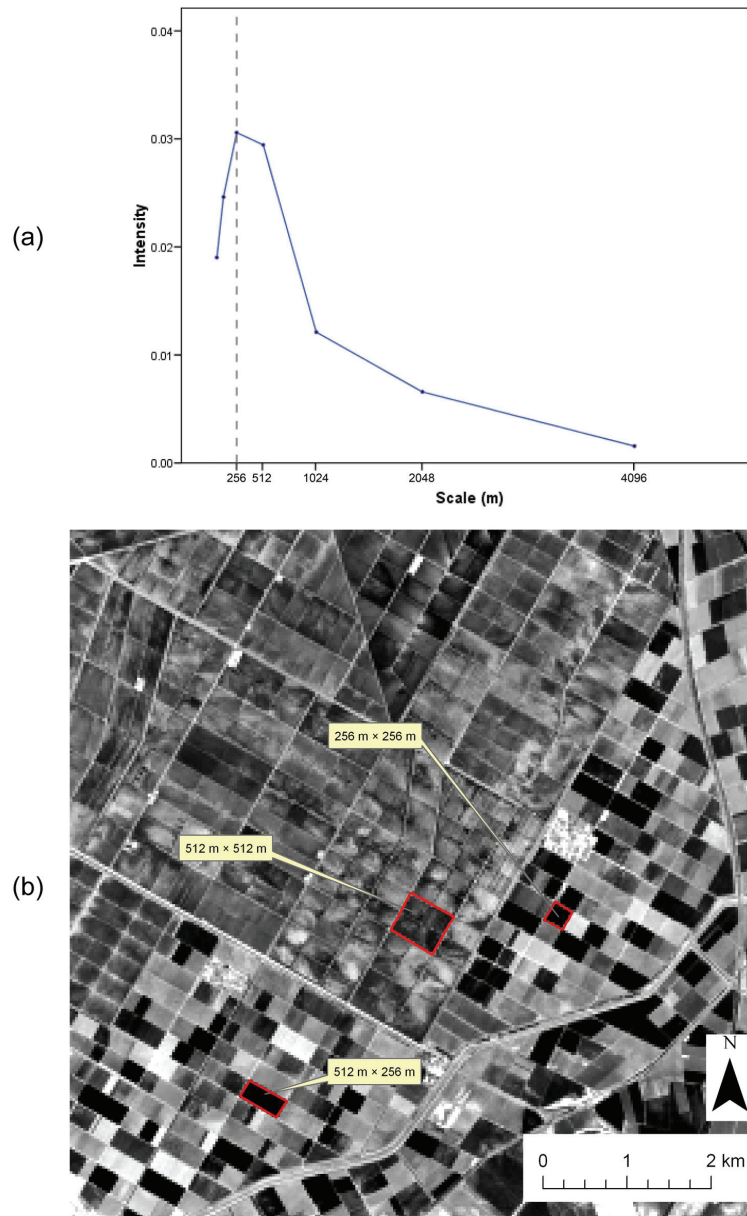


Fig. 2.3: Example of the wavelet analysis of the Orthophoto for an agricultural area (quadrant 5): (a) wavelet energy curve within 64 m and 4096 m and (b) the Orthophoto showing the match between the dominant scale (256–512 m) of the curve and the fields' size. The dominant scale is highlighted by the dotted line in the graph and by the red boxes in the image.

Table 2.2: Results of the Mann–Whitney test of the median dominant scale for agricultural and semi-natural areas.

	Agricultural areas ( $n = 10$ )			Semi-natural areas ( $n = 8$ )		
	$U$	$z$	$p$ -value	$U$	$z$	$p$ -value
Orthophoto vs ASTER	42	-0.67	0.5	25.5	-0.74	0.5
Orthophoto vs ETM+	29	-1.71	0.1	12	-2.58	0.01
ASTER vs ETM+	38	-0.97	0.3	8	-2.93	0.03

### 2.3.2 Wavelet energy curve

We tested if the average wavelet energy curves of the Orthophoto, ASTER and ETM+ had similar shape. We found that the shape of the curves was significantly correlated and that the local maximum intensity occurred at the same dominant scale.

**For agricultural areas.** The average NDVI intensity curve of ASTER was significantly correlated with the average NDVI intensity curve of ETM+ (Pearson correlation test,  $r=0.99$ ,  $p<0.001$ ; linear regression,  $b = 0.29$ ,  $t = 26.6$ ,  $p < 0.001$ , adjusted  $R^2 = 0.99$ ). The average intensity red band curve of the Orthophoto was significantly correlated with the average NDVI intensity curve of ASTER (Pearson correlation test,  $r = 0.89$ ,  $p = 0.003$ ; linear regression,  $b = 6.97$ ,  $t = 4.43$ ,  $p = 0.007$ , adjusted  $R^2 = 0.76$ ). The average intensity red band curve of the Orthophoto was significantly correlated with the average NDVI intensity of ETM+ (Pearson correlation test,  $r = 0.86$ ,  $p = 0.007$ ; linear regression,  $b = 1.92$ ,  $t = 3.75$ ,  $p = 0.01$ , adjusted  $R^2 = 0.69$ ). Fig. 2.4 shows that the shape of the average wavelet energy curves is similar and that the dominant scale of the images is the same.

A dominant scale emerges from diverse satellite platforms

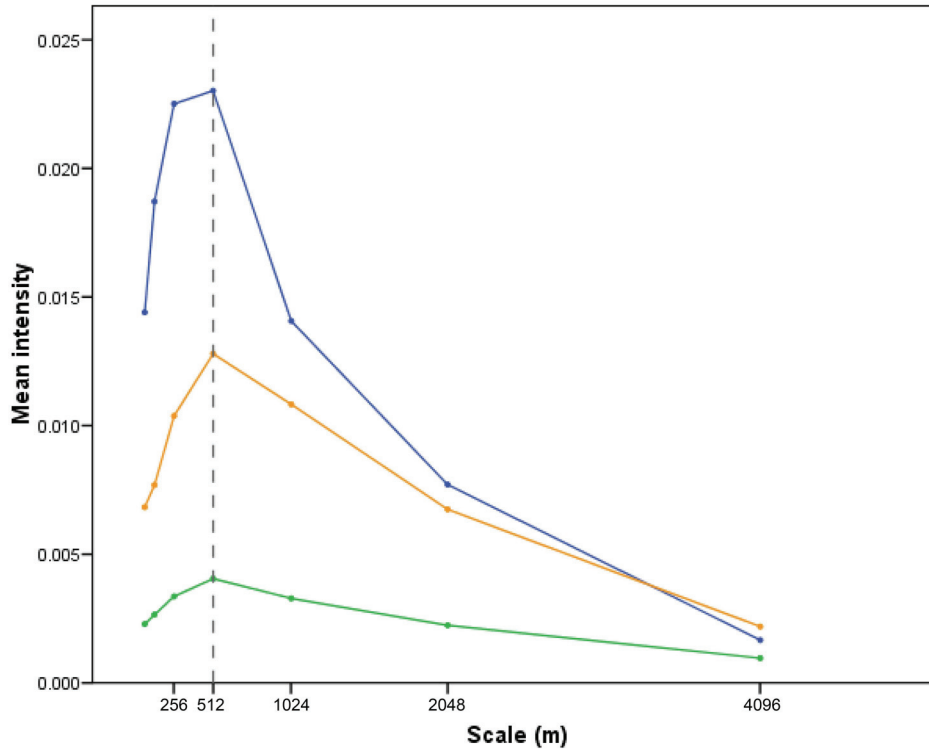


Fig. 2.4: Average wavelet energy curves of the Orthophoto (blue), ASTER (green) and ETM+ (orange) for agricultural areas within 64 m and 4096 m. The dominant scales (512 m) are highlighted by the dotted line.

**For semi-natural areas.** The average wavelet energy curves of the Orthophoto, ASTER and ETM+ were significantly correlated (Pearson correlation test, regression  $p < 0.05$ ) (Table 2.3), indicating that they had similar shapes. The amplitude of the curves was similar although the intensity values were different. Inspecting the wavelet energy curves of the Orthophoto within the range 2–4096 m, there was a highest dominant scale at 8 m and a second dominant scale at 128 m (Fig. 2.5(a) left side of the graph). ETM+ showed a descending curve from 64 m to 4096 m without any peak at 128 m (Fig. 2.5(b)).

Table 2.3: Correlation and regression statistics of the wavelet energy curves for semi-natural areas.

	Pearson test ( $n = 7$ )		Regression ( $n = 7$ )			
	$R$	$p$ -value	$R^2$	$b$	$t$	$p$ -value
Orthophoto vs. ASTER	0.99	<0.001	0.97	38.08	13.83	<0.001
Orthophoto vs. ETM+	0.88	0.004	0.73	8.98	4.18	0.009
ASTER vs. ETM+	0.81	0.013	0.59	0.21	3.11	0.027

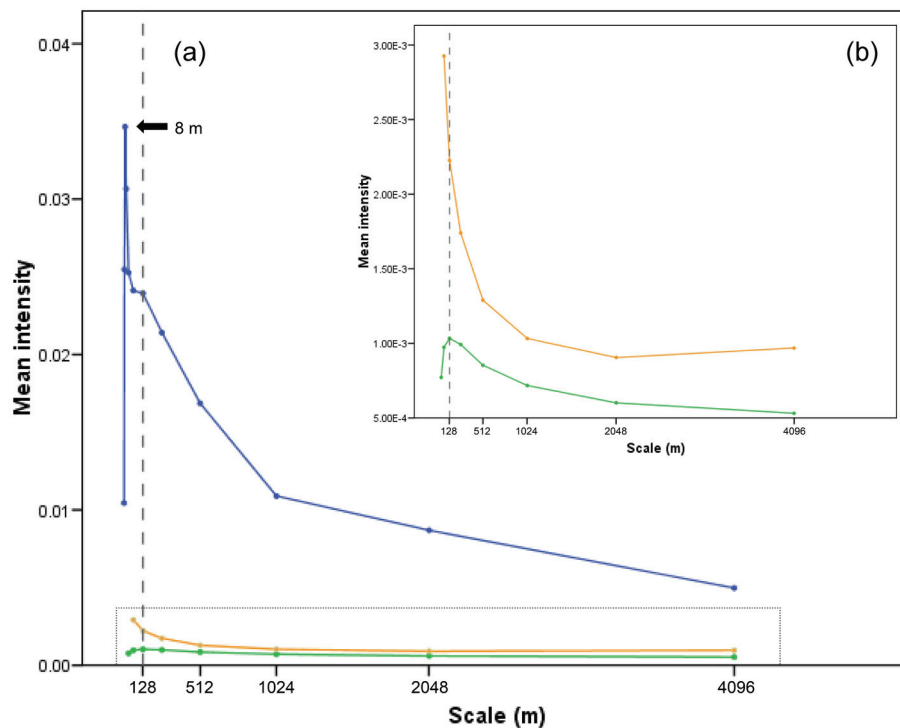


Fig. 2.5: Average wavelet energy curves of the Orthophoto (blue), ASTER (green) and ETM+ (orange) for semi-natural areas. (a) The average wavelet energy curve of the Orthophoto is plotted from 2 m to 4096 m to show the highest dominant scale at 8 m and the second dominant scale at 128 m. The average wavelet energy curves of ASTER and ETM+ show a dominant scale at 128 m (ASTER) and at 64 m (ETM+). (b) The average wavelet energy curves of ASTER and ETM+ are also displayed in the inset to better visualize their dominant scales. The dominant scales are highlighted by the dotted lines.

### 2.3.3 Comparison of dominant scale and wavelet energy curves for agricultural and semi-natural areas

Agricultural and semi-natural areas had different dominant scale and different shape of the wavelet energy curves. As an example, we plotted the wavelet energy curves of the Orthophoto of two quadrants to show the different pattern in agricultural and semi-natural areas (Fig. 2.6). The median dominant scale of agricultural areas was 32 times larger than that of the semi-natural areas. This indicates that the patchy spatial structure of agricultural areas is determined by the average size of the cultivated fields as shown by Fig. 2.3(b). In semi-natural areas the structure is determined by the dominance of small patches (8 m) as shown by Fig. 2.7(a) and (b).

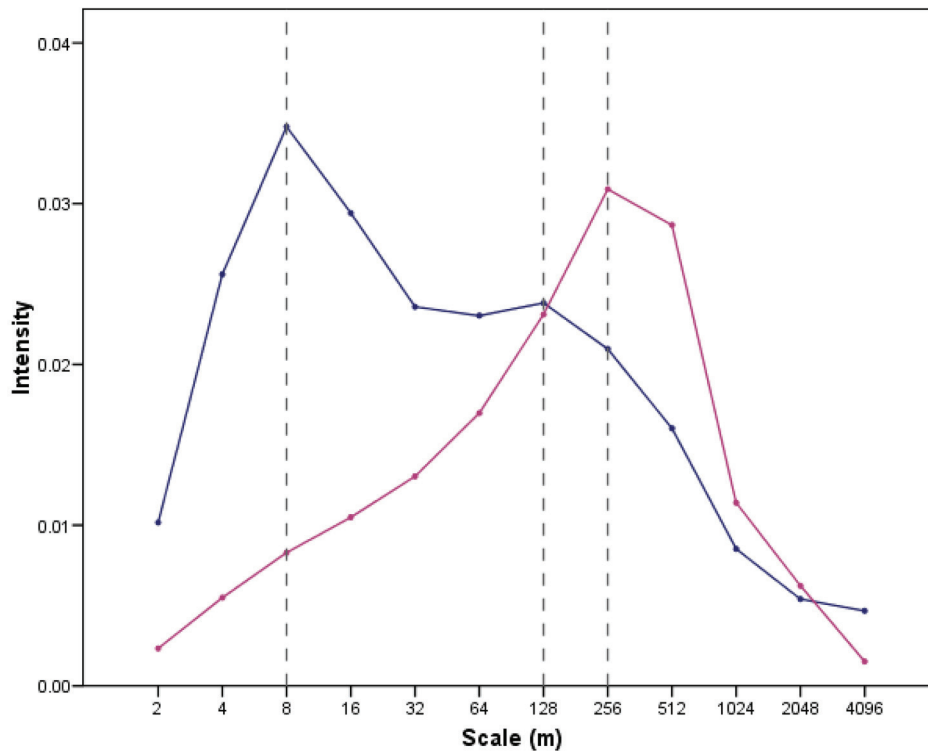


Fig. 2.6: Example of the wavelet energy curves of the Orthophoto for agricultural (quadrant 5 – pink line) and semi-natural areas (quadrant 5 – blue line) within 2 m and 4096 m. Dominant scales are highlighted by the dotted lines. For display reasons, the scale ( $x$  axis) is plotted as a nominal variable in order to amplify the shape of the curves. The related images are shown in Fig. 2.3 and Fig. 2.7.

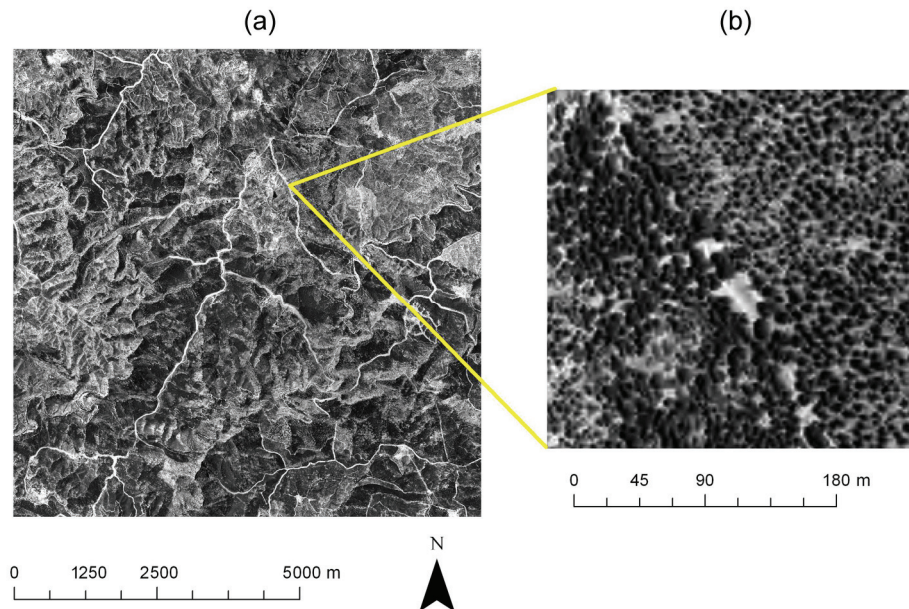


Fig. 2.7: Example of the semi-natural landscape analyzed with the wavelet transform. (a) The image represents the Orthophoto of quadrant 5. The detail on the right (b) shows the spatial structure captured by the dominant scale (8 m) of the wavelet transform.

### 2.3.4 Intensity of the Orthophoto, ASTER and ETM at each scale $j$

We tested if the median of the intensity at each scale ( $j$ ) was significantly different among the images in order to demonstrate that images of different resolution were not significantly different in intensity at given scale  $j$ . We found that the images were significantly different at almost every scale, with the exception of the coarser scales. The intensity of the Orthophoto was significantly higher than the NDVI intensity of ASTER and ETM+. ASTER had the lower intensity values. This pattern was consistent at every scale, suggesting that intensity is influenced by the use of different bands (namely red band and NDVI). In detail:

**For agricultural areas.** The median NDVI intensity of ETM+ was significantly higher than the median NDVI intensity of ASTER at every scale  $j$  (Mann–Whitney test,  $p < 0.05$ ). The median red band intensity of the Orthophoto was significantly higher than the median NDVI intensity of ASTER and ETM+ except

A dominant scale emerges from diverse satellite platforms

for the coarsest scales ( $I_{\text{Orthophoto}} = I_{\text{ASTER}}$  for scale  $j = 4096$  m;  $I_{\text{Orthophoto}} = I_{\text{ETM+}}$  for scale  $j = 1024$  m, 2048 m and 4096 m)(Fig. 2.8 (a)–(g)).

**For semi-natural areas.** The median red band intensity of the Orthophoto was significantly higher than the median NDVI intensity of ASTER and of ETM+ at each scale (Mann–Whitney test,  $p < 0.05$ ). The median NDVI intensity of ETM+ was significantly higher than that of ASTER at each scale, except at scales 2048 m and 4096 m where they were not significantly different (Fig. 2.9 (a)–(g)).

## 2.4 Discussion

### 2.4.1 Dominant scale

**Agricultural areas.** Conforming to the hypothesis that dominant landscape features are scale independent from the original pixel size of the image, the wavelet transform quantified consistently the dominant scale in agricultural areas irrespective of the original pixel size, the band used (red band or NDVI) and the date of acquisition of the Orthophoto, ASTER and ETM+. The wavelet described the patchy structure of the cultivated land. In fact the dominant scale represented the dominant patch size of the agricultural field as visually shown by Fig. 2.3. This demonstrates that the dominant scale is not an artefact of the method but represents coherent objects (patterns) in the landscape that can be localized in the map.

Our results confirm the findings of Coueron et al. (2006) who performed a multiscale analysis using aerial photos and Fourier analysis without applying atmospheric correction. They found that whatever the window size used (scale), the spatial frequencies displayed the same patterns. The present study went a step further demonstrating the independence of dominant landscape features in agricultural areas using multisensor data (thus not only aerial photos) and the wavelet transform which is robust also with non-stationary data, especially when compared with the methods based on variance analysis such as autocorrelation, PQV, TTTLQV and semivariance (Bradshaw and Spies, 1992; Dale and Mah, 1998). Contrary to PQV and TTTLQV methods, the wavelet transform did not generate peak drift and resonance drift (that is dominant scales not coincident with real data).

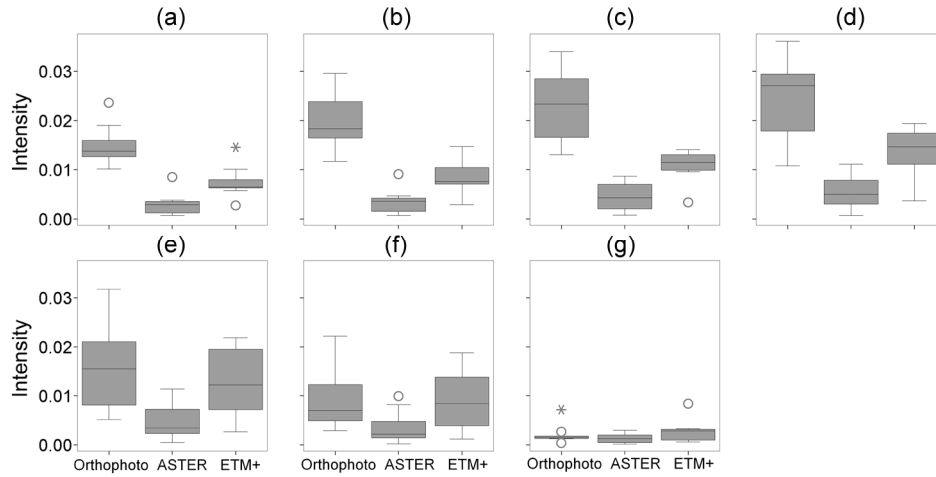


Fig. 2.8: Boxplot of intensity at each scale  $j$  for agricultural areas for the Orthophoto, ASTER, ETM+. (a)  $j = 64$  m; (b)  $j = 128$  m; (c)  $j = 256$  m; (d)  $j = 512$  m; (e)  $j = 1024$  m; (f)  $j = 2048$  m; (g)  $j = 4096$  m.

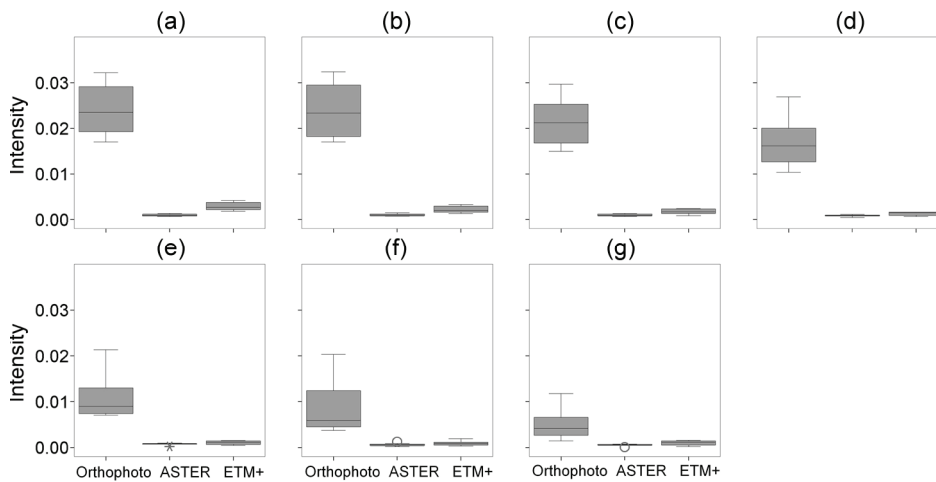


Fig. 2.9: Boxplot of intensity at each scale  $j$  for semi-natural areas for the Orthophoto, ASTER, ETM+. (a)  $j = 64$  m; (b)  $j = 128$  m; (c)  $j = 256$  m; (d)  $j = 512$  m; (e)  $j = 1024$  m; (f)  $j = 2048$  m; (g)  $j = 4096$  m.

Recently Nunez et al. (2006) compared the nominal spatial resolution of multisensor and multispectral data (i.e., Landsat-5 multispectral against SPOT-3 panchromatic) in an agricultural area using DWT. Their results showed that the relative spatial resolution of those sensors was different (though slightly) from the nominal resolution. In other words the ratio between the pixels size of the images estimated using the wavelet analysis was slightly different from the nominal one. These results may appear to disagree with our results. However the discrepancy between the findings of the two studies is mainly due to the fact that they measured different things (i.e., different bands), with different methods (different DWT such as undecimated against decimated; approximation against detail coefficients; 'a trous' filter against Haar) and indicators (correlation coefficient against intensity, dominant scale and wavelet energy curves). Moreover the two studies differed in the aim of the analysis: Nunez et al. (2006) were interested in comparing the spatial content at the level of the pixel; we were interested in identifying common dominant scale(s) which by definition are equal or larger than the coarser pixel size.

**Semi-natural areas.** Our hypothesis regarding dominant scale was partly confirmed in semi-natural areas. The Orthophoto and ASTER showed the same median dominant scale (128 m). The median dominant scale of ETM+ (64 m) was significantly lower than the other images, although the difference was not large (64 m against 128 m). Unlike the agricultural areas, the semi-natural areas were dominated by small patches of 8 m as shown by the peak in the average wavelet energy curve of the Orthophoto within the range 2 m and 4096 m (Fig. 2.5). These patches are interspersed in a gradient landscape that at coarser resolution cannot be captured. At coarser resolution the variance due to these small patches is averaged out and the landscape appears more homogeneous. This is shown for example by the ETM+ wavelet energy curve that decreases logarithmically without a peak dominant scale. It seems that for coarser resolution images (ETM+) the variance decreases logarithmically with the increase of the size of the pixel as was found by Tarnawsky et al. (2008) using semivariance.

However it may be possible that a different wavelet performs better in characterizing the spatial heterogeneity of semi-natural areas in Andalucía. For instance continuous wavelet transform and undecimated DWT with the 'a trous' filter (Nunez et al., 2006) may also be explored. We chose the Haar wavelet because of its ability to capture edges and gradients (Bradshaw and Spies, 1992) and because of its capability of handling large dataset. In addition the Haar wavelet is easy to implement, widely used in the literature and does not

produce redundancy of details such as the undecimated DWT (Amolins et al., 2007).

### 2.4.2 Wavelet energy curves

**Agricultural areas.** Our hypothesis regarding the shape of the wavelet energy curves was confirmed in agricultural areas. The wavelet energy curves of the Orthophoto, ASTER and ETM+ were statistically similar irrespective of the resolution of the images, the band (namely red band and NDVI) and the date of the image. This result also corroborates that variation in crop types or in phenology due to the different time of acquisition of the images did not influence the wavelet results.

**Semi-natural areas.** In semi-natural areas the shape of the wavelet energy curves of the Orthophoto, ASTER and ETM+ were similar and statistically correlated. The ETM+ curve however showed a logarithmically descendent shape from 64 m to 4096 m, indicating that the maximum intensity and therefore the dominant scale is smaller than 64 m. This indicates that semi-natural areas are dominated by gradients and ecotones and that the finest patterns are difficult to capture at coarser spatial resolution (like ETM+). As already explained, this is confirmed by the wavelet energy curves and the dominant scale of the Orthophoto: within the range of 2 m and 4096 m, the Orthophoto showed a dominant scale at 8 m and a second dominant scale at 128 m. This information is gradually missed at coarser resolution.

It appears that the variation in vegetation phenology (thus the use of images not time coincident but acquired in different seasons) has influenced the intensity and the dominant scale patterns of the images. This occurred mainly in the ETM+ images, which were acquired in March and April. In this period deciduous forests and shrubs do not yet have leaves; therefore the small patches (128 m) due to trees and shrubs are not captured by the image. On the contrary the Orthophoto and ASTER were mainly acquired between June and October when the vegetation cover is higher. In order to exclude the possibility that the results for semi-natural areas were influenced by the resampling process (which may cause a distortion of the spatial content of the images), we compared the shape of the wavelet energy curves of the resampled images with the wavelet energy curves of the corresponding original images for quadrant 5. Specifically we correlated the wavelet energy curves of the resampled ETM+ (32 m) and ASTER (16 m) images with the wavelet energy curves of the original ETM+ (28.5 m) and ASTER (15 m) images respectively. The result was that the shapes of the wavelet energy curves for resampled and original images were

A dominant scale emerges from diverse satellite platforms

similar and statistically correlated (Spearman correlation test,  $r_{\text{ETM}^+} = 0.96$ ,  $p < 0.001$ ,  $n = 7$ ;  $r_{\text{ASTER}} = 0.98$ ,  $p < 0.001$ ,  $n = 8$ ). Consequently the resampling process did not affect the wavelet results.

### **2.4.3 Comparison of dominant scale and wavelet energy curves of agricultural and semi-natural areas**

The different spatial structure of the landscape in agricultural and semi-natural areas are well quantified by the Haar wavelet as shown by the opposite trends of the wavelet curves in Fig. 2.6. Similar results for dominant scales were found by Atkinson and Aplin (2004) who compared the spatial variation of agricultural and semi-natural areas with geostatistical methods.

### **2.4.4 Intensity of the Orthophoto, ASTER and ETM at each scale $j$**

The results on the intensity were significantly different among the images as for agricultural areas as well as for semi-natural areas. This difference was found at each scale of decomposition from 64 m to 2048 m. The Orthophoto showed always the highest intensity, then the ETM+ and the lower was always found in ASTER images. This pattern was consistent at each scale. The higher intensity in the Orthophoto is related to the use of the red band which visually shows the higher contrast in brightness among the images. Indeed we repeated the analysis using the red band for ASTER and ETM+ (results not shown here) and we found that the differences in amplitude among the wavelet energy curves (thus difference in intensity) are highly reduced between the three images. This result confirmed the findings of Atkinson and Aplin (2004) who detected differences in local variance between the red and the NIR bands of an airborne multispectral image of 4 m resolution by using variograms.

Although Coueron et al. (2006) demonstrated that atmospheric correction did not influence the comparison of multitemporal images, we expect higher similarity in intensity amongst images once atmospheric correction is made. In fact we suspect that the use of images not time coincident has strongly affected the intensity results (therefore the amplitude of the energy curve). Nevertheless, these factors did not ultimately affect the dominant scale and the shape of the wavelet energy curves, confirming our initial hypothesis.

Contrary to the findings of Tarnawsky et al. (2008), this study suggests that dominant landscape features are scale independent from the original pixel size of the images.

## 2.5 Conclusions

The wavelet transform is a robust technique to quantify and localize the dominant pattern of spatial heterogeneity at multiple scales as in a patchy landscape such as agriculture as well as in a gradient landscape such as semi-natural areas. In agricultural areas this technique was not affected by the original pixel size of the Orthophoto, ASTER and ETM+ or by the use of different bands and images not time coincident. In fact the dominant scale was consistently quantified in all images and the wavelet energy curves were also similar. The intensity, which is directly related to the brightness of the image, was instead influenced by the bands chosen as well as by the time of acquisition. This is due mainly to two reasons: 1) the dominant features (cultivated fields) determining the dominant scale of the landscape are much larger than the pixel size of the coarser image (ETM+, resolution = 28.5 m); 2) the mosaic structure of agricultural areas does not change significantly among the seasons and years, because the fields size do not change. Therefore phenology and change in crop type do not affect the dominant scale parameter allowing comparison of images heterogeneous in time.

In semi-natural areas the results were slightly different and seemed to be affected by the heterogeneity of the images. The median dominant scale ranged between 64 m and 128 m but the analysis of the Orthophoto revealed a strong dominant scale at 8 m. In fact semi-natural landscapes are dominated by gradients and ecotones of small patches which are therefore smaller than the pixel size of the coarser image (ETM+). The small and aperiodic structure of the semi-natural areas in addition is affected by the change in phenology. These factors affected to some extent the intensity and the wavelet energy curves more than the agricultural areas. On the contrary, it is important to notice that the resampling process (which was required for the application of the Haar wavelet) did not affect the shape of the wavelet energy curves. These results suggest two main things: 1) the wavelet transform is confirmed as a robust technique to quantify spatial heterogeneity also in semi-natural areas and also at finest image resolution; 2) given the aperiodic structure and gradient of the semi-natural landscape it is advised to choose the pixel size of the image in relation to the topic of the analysis.

## Acknowledgements

This research was funded by the International Institute of Geo-Information Science and Earth Observation (ITC), the Netherlands. The authors would like

A dominant scale emerges from diverse satellite platforms

to thank Willem Nieuwenhuis who wrote a revised version of the IDL script for the wavelet decomposition of large matrices.

# 3

## **Identifying transit corridors for elephant using a long time-series**

This chapter is based on:

Pittiglio, C., Skidmore, A.K., van Gils, H.A.M.J., Prins, H.H.T., 2012. Identifying transit corridors for elephant using a long time-series. *International Journal of Applied Earth Observation and Geoinformation*. 14, 61-72.

## Abstract

The role of corridors in mitigating the effects of landscape fragmentation on biodiversity is controversial. Recent studies have highlighted the need for new approaches in corridor design using long-term datasets. We present a method to identify transit corridors for elephant at a population scale over a large area and an extended period of time using long-term aerial surveys. We investigated environmental and anthropogenic factors directly and indirectly related to the wet versus dry season distribution of elephant and its transit corridors. Four environmental variables predicted the presence of elephant at the landscape scale in both seasons: distance from permanent water, protected areas and settlements and vegetation structure. Path analysis revealed that elevation and monthly average NDVI, and distance from temporary water had a significant indirect effect on elephant distribution at local scale in dry and wet seasons respectively. Five transit corridors connecting Tarangire National Park and the northern as well as south-eastern wet season dispersal areas were identified and matched the wildlife migration routes described in the 1960s. The corridors are stable over the decades, providing landscape connectivity for elephant. Our approach yielded insights how advanced spatial analysis can be integrated with biological data available from long-term datasets to identify actual transit corridors and predictors of species distribution.

## 3.1 Introduction

Landscape fragmentation threatens biodiversity by disrupting the dispersal of organisms (Hanski, 1998). Corridors are expected to mitigate this effect by providing habitat connectivity (Beier and Noss, 1998). Yet their role is controversial (Beier and Noss, 1998; Mann and Plummer, 1995; Simberloff et al., 1992). Corridors promote seed dispersal (Damschen et al., 2006; Levey et al., 2005), movement of taxa (Haddad et al., 2003) also in response to climate change (Channell and Lomolino, 2000) and continuity of natural processes (Bennett, 1999; Gilbert-Norton et al., 2010). On the other hand, corridors may facilitate disease transmission, alien species invasion, predation, hunting and poaching, which could reduce the species survival in the connected habitat patches (Simberloff and Cox, 1987). Not all species benefit from corridors (Hobbs, 1992). Yet, corridors were often designed by monitoring a few species at local scale over short periods (see Beier and Noss, 1998; Gilbert-Norton et al., 2010). In addition corridors were mainly identified by landscape patterns (Mann and Plummer, 1995), without considering movement of target organisms (Chetkiewicz et al., 2006). Indeed corridors should be identified and assessed by determining the distribution, movement and persistence of umbrella and

keystone species at landscape scale and over long periods (Beier and Loe, 1992; Bennett, 1999; Simberloff, 1998). Recent studies have highlighted the need for new approaches in corridor design (Chetkiewicz et al., 2006) using long-term datasets in biodiversity (Magurran et al., 2010).

We present a spatiotemporal approach to identify and assess the role of transit corridors (defined as the seasonal movement of organisms) using long-term aerial surveys. Repeated aerial surveys have been widely used for monitoring large terrestrial mammals (Caughley, 1974): red kangaroo (Cairns and Grigg, 1993) and feral goat in Australia (Southwell, 1996); elk (Samuel et al., 1987), moose (Gasaway et al., 1985), caribou (Courtois et al., 2003) and white-tailed deer (Pettorelli et al., 2007; Potvin et al., 2004) in North America; saiga antelope in Asia (Singh and Milner-Gulland, 2011); elephant (Chamaillé-Jammes et al., 2008), wildebeest (Ottichilo et al., 2001), zebra (Kahurananga and Silkiluwasha, 1997), buffalo (Prins and Douglas-Hamilton, 1990) and antelopes (East, 1999; Stoner et al., 2007) in Africa. In this paper, the approach was applied to the African elephant (*Loxodonta africana*) in Tarangire–Manyara ecosystem (TME), northern Tanzania. The elephant is an umbrella and keystone species of the savanna ecosystem (Hoare and Toit, 1999), promotes seed dispersal (Gonthier, 2007), migrates seasonally over large distances (Douglas-Hamilton et al., 2005) and thus represents an ideal species for modeling transit corridors. Yet, only a few studies provide empirical description of transit corridors for elephant in Africa (Douglas-Hamilton et al., 2005; Galanti et al., 2000; Ngene et al., 2009a; Osborn and Parker, 2003a), though this information is crucial for land managers (Haddad, 2008). Moreover how current transit corridors are linked with traditional migration routes and especially population persistence in dispersal areas has not been well studied. In many Eastern and Southern African countries elephant has been monitored since the 1970s through total counts and Systematic Reconnaissance flights (SRF, see Norton-Griffiths, 1978) to determine population abundance and trends over extensive areas (Blanc et al., 2005; de Leeuw et al., 1998; Stoner et al., 2007). The studies investigating the determinants of elephant distribution from long-term aerial surveys (Chamaillé-Jammes et al., 2008; Murwira and Skidmore, 2005; Murwira et al., 2010; Prins and Douglas-Hamilton, 1990; Shrader et al., 2010; Young et al., 2009b) do not include the analysis of transit corridors. The elephant movement (Douglas-Hamilton et al., 2005; Galanti et al., 2000; Graham et al., 2009) and its interaction with the environment (Galanti et al., 2006; Harris et al., 2008; Loarie et al., 2009; Ngene et al., 2009b) were investigated by radio- and satellite-telemetry studies. These studies were based on small sample size (a few collared animals), relative short monitoring periods (on average 2-3 years) and

therefore may not represent the year round distribution and persistence of elephant distribution (Hebblewhite and Haydon, 2010).

We conducted a comprehensive analysis of the dry versus the wet season distribution of elephant at a population scale over a large area and an extended period of time. Our object was to identify environmental and anthropogenic factors directly and indirectly related to the seasonal distribution of elephant and its transit corridors using long-term aerial surveys. The Tarangire–Manyara Ecosystem (TME) hosts the largest population of savanna elephant in northern Tanzania. Here elephant moves seasonally from Tarangire National Park (TNP) and Lake Manyara National Park (LMNP) to the wet season dispersal areas outside the parks (Borner, 1985; Lamprey, 1964). The description of these movements is mostly anecdotal except for the north-east and south of TNP which were confirmed by collared elephants (Galanti et al., 2000). Since the 1980s, TNP and LMNP are at risk of isolation due to the expansion of farming particularly in dispersal areas and wildlife migration routes (Borner, 1985; Mwalyosi, 1991; Newmark, 2008; Prins, 1987). Elephant has been monitored in the TME since 1987 through total counts and SRF over an area of approximately 12,000 km<sup>2</sup> both in dry and wet seasons (TAWIRI, 2001, 2004). Although a radio–telemetry study showed a significant avoidance of human artifacts (Galanti et al., 2006), predictors of seasonal distribution of elephant and its transit corridors in TME have not been fully understood. Yet, such information is required to implement the Wildlife Policy of Tanzania (1998) which recognizes the right of villages to utilize wildlife through the zoning of Wildlife Management Areas (WMAs).

We hypothesized that transit corridors can be identified from the predicted probabilities of elephant presence generated from long-term aerial surveys. We also hypothesized that the seasonal distribution of elephant in TME is influenced by drinking water (Chamaillé-Jammes et al., 2007; de Beer and van Aarde, 2008; Western, 1975), forage (Loarie et al., 2009; Ngene et al., 2009b; Young et al., 2009a) and security (Douglas-Hamilton et al., 2005; Galanti et al., 2006; Harris et al., 2008). We expected that in the wet season, because water is not limiting (Lamprey, 1963), vegetation cover and greenness are most important, and that anthropogenic variables limit the elephant distribution in the dispersal areas, though minor roads may provide security if patrolled (Ngene et al., 2009b). Elevation and slope (only having modest variation across the study area) are expected to be poor predictors at the landscape scale, though both may influence the seasonal distribution of elephant at local scale (de Knegt, 2010; Ngene et al., 2009b). Distribution models that explicitly account for species' ecological traits, such as large body size, wide range size and high

vagility (Ko et al., 2011; McPherson and Jetz, 2007), imperfect detectability (Mackenzie et al., 2002) as well as the area surrounding a site (i.e., environmental context; de Knegt et al., 2011; Guisan and Thuiller, 2005), produce more accurate predictions than models based on point data alone, including presence-only models (de Knegt et al., 2011; Ko et al., 2011; McPherson and Jetz, 2007; Rota et al., 2011). Although in our study the probability of false absences was minimized by repeated total counts with narrow confidence limits coupled to the high detectability of elephant in the open vegetation (Prins and Douglas-Hamilton, 1990), total counts were spatially and temporally discontinuous (seasonal snapshots) and elephant is a large and highly vagile species. Employing coarse-grained predictors (Guisan and Thuiller, 2005) or a buffer around the elephant locations (de Knegt et al., 2011; Ko et al., 2011) was not considered in our study because the grain and buffer size are arbitrarily chosen and the area they include may not have the same likelihood of occupancy as the point where the elephant was observed. We therefore present a modeling approach based on the probability of elephant occupancy to account for elephant vagility, temporal discontinuity of total counts as well as environmental context.

## 3.2 Methods

### 3.2.1 Study area

The Tarangire–Manyara Ecosystem (TME) is located in Tanzania, between 3°36'S and 4°7'S and 35°82'E and 36°74'E. The research area (12,000 km<sup>2</sup>) includes protected (Tarangire and Lake Manyara National Parks), semi-protected (Manyara Ranch, Lolkisale and Mkungunero Game Controlled Areas) and unprotected areas (see Fig. 3.1). TME is predominantly a gently undulating plateau with elevations of 1000 m a.s.l. in LMNP, 900–1200 m in TNP and 1360–1600 m in Simanjiro Plains (Kahurananga and Silkiluwasha, 1997; Prins, 1988). Black cotton soil prevails in the flood plains and dark red sandy clay loam elsewhere (Kahurananga, 1979). The annual average rainfall is 450–650 mm; the higher amounts in the west (Prins and Loth, 1988) and the lower in the east (Gereta et al., 2004). The rainfall pattern is bimodal with short rains occurring from November to December and long rains from February to May. March and April are the wettest months; July and August the driest. Two types of savanna are found in TME: microphyllous savanna on riverine areas dominated by *Acacia tortilis* and broad-leaf deciduous savanna on the ridges and upper slopes dominated by *Combretum* and *Commiphora* species (Lamprey, 1963). Vegetation descriptions have been given by Lamprey (1963), Loth and Prins (1986) and Kahurananga (1979) for different parts of TME. Lake Manyara,

Tarangire river and Silale swamp are the permanent water sources in the study area for elephant (Lamprey, 1963). Ten wildlife migration routes connecting the protected areas with the dispersal areas outside the parks were described in the early 1960s (Fig. 3.1; Lamprey, 1964; Mwalyosi, 1991), before the effect of agricultural expansion (Borner, 1985). These routes were digitized using reported coordinates (Lamprey, 1964; Mwalyosi, 1991) and compared with the transit corridors generated by this study. The western routes (no. 7, 8, 9, Fig. 3.1) only partially included in the study area, were excluded from the analysis. These routes are considered blocked by farming since the 1980s (Borner, 1985).

### 3.2.2 Elephant locations data

Seven total counts of elephant from 1995 to 2004 and six SRF (Norton-Griffiths, 1978) from 1994 to 2004 were obtained from the Tanzania Wildlife Research Institute (TAWIRI) in both dry and wet seasons for a total amount of 847 and 451 locations respectively. The censuses were spatially and temporally discontinuous (Table 3.1); each census representing a snapshot of the spatial distribution of elephant by season. Each census was simultaneously flown in 2–4 days by 2 aircraft to minimize double counting due to animal movement (Norton-Griffiths, 1978). Total counts of elephant were obtained in 17 census blocks. Each block was systematically searched by flying east–west parallel transects of 1800 m interval (i.e., 900 m each side of the transect line) at approximately 500 feet. The position of elephants was recorded on a global positioning system (GPS). Whenever an animal or group of elephants was spotted, the aircraft deviated from its flight line and circled the observed animals until the exact number and the GPS location were recorded. Groups larger than 15 individuals were photographed for further confirmation (TAWIRI, 2004). Total counts were used to define presence and absence of elephants, which were used in the logistic regression for generating the seasonal predicted probabilities of elephant presence (see below). SRF (Norton-Griffiths, 1978; TAWIRI, 2001) transects ran east–west, spaced at 5 km. Each transect was divided into 30 second subunits (approximately 1.1 km). The transect width was 300 m (150 m per side). The aircrafts flew at approximately 300 feet. A detailed description of the methodology is made by Norton-Griffiths (1978). SRF data consisted of a 5 by 5 km grid of 451 GPS locations (centroids) reporting elephant density per km<sup>2</sup>. Suitable (defined as when elephant was recorded at least once during the study period) and unsuitable SRF locations for elephant (defined as otherwise) were used to validate the predicted probabilities of elephant occurrence generated by the logistic regression.

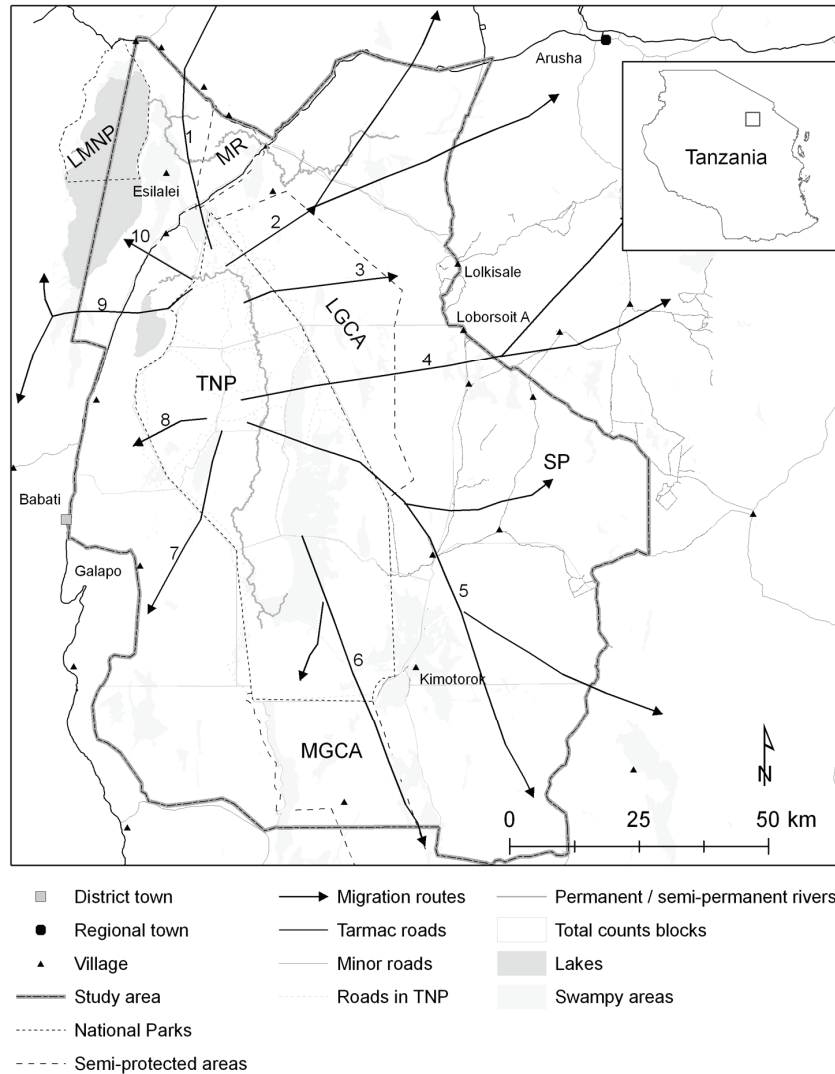


Fig. 3.1: Study area showing boundaries of Lake Manyara National Park (LMNP), Tarangire National Park (TNP); Lolikisale Game Controlled Area (LGCA); Mkungunero Game Controlled Area (MGCA); Manyara Ranch (MR); Simanjiro Plains (SP) and wildlife migration routes described in the 1960s. Migratory species and relative references are reported for each route (1 wildebeest<sup>a</sup>, zebra<sup>a</sup>, elephant<sup>b</sup>; 2 wildebeest<sup>a</sup>, zebra<sup>a</sup>, eland<sup>a</sup>, oryx<sup>a</sup>, elephant<sup>c</sup>; 3 elephant<sup>a</sup>, buffalo<sup>a</sup>; 4 wildebeest<sup>a</sup>, zebra<sup>a</sup>, eland<sup>a</sup>, giraffe<sup>a</sup>, elephant<sup>c</sup>; 5 wildebeest<sup>a</sup>, zebra<sup>a</sup>, eland<sup>a</sup>, gazelle<sup>a</sup>, hartebeest<sup>a</sup>, elephant<sup>c</sup>; 6 elephant<sup>a</sup>, buffalo<sup>a</sup>, hartebeest<sup>a</sup>, eland<sup>a</sup>; 7 wildebeest<sup>a</sup>, buffalo<sup>a</sup>; 8 not specified<sup>a</sup>; 9 elephant<sup>a</sup>, buffalo<sup>a</sup>; 10 elephant<sup>b</sup>, wildebeest<sup>d</sup>, zebra<sup>d</sup>). <sup>a</sup>Lamprey (1964); <sup>b</sup>TCP (1998); <sup>c</sup>Galanti et al. (2006); <sup>d</sup>Mwalyosi (1991).

The validation was performed with random points generated within the 5 by 5 km SRF grid with a minimum distance from adjacent points of 3.5 km. The north-western portion of the Manyara block (Fig. 3.1) was excluded from the analysis because of limited availability of SRF. The March 2000 counts were also excluded because of a prolonged dry season (TWCM, 2000).

Table 3.1: Wildlife Surveys in the Tarangire–Manyara Ecosystem (TME), 1994–2004 (LMNP, Lake Manyara National Park; SRF, systematic reconnaissance flight; TC, total count).

Year	Season	Month	Census technique	Area covered
1994	Wet	March	SRF	TME (excluding LMNP)
1994	Dry	October	SRF	TME (excluding LMNP)
1995	Dry	September	TC	TME
1996	Wet	May	TC	TME (excluding LMNP)
1997	Wet	April	SRF	TME
1998	Wet	March	TC	TME
1998	Dry	September	TC	TME
1999	Dry	October	SRF	TME (excluding LMNP)
2000	Wet <sup>a</sup>	March	TC	TME
2001	Wet	May	TC	TME
2001	Wet	May	SRF	TME
2004	Dry	October	TC	TME
2004	Dry	October	SRF	TME

<sup>a</sup> Excluded because the prolonged dry season affected the elephant distribution in March 2000

### 3.2.3 Estimate of elephant seasonal presence

Elephant distribution was studied by point pattern analysis (kernel density) of the GPS locations from the total counts ( $n = 655$ ). A kernel density function was applied to minimize the probability of false absences due to the spatial and temporal discontinuity of total counts, elephant vagility and environmental context. The standard bivariate normal kernel density function (Silverman, 1986) was used to estimate the probability of elephant occupancy for the dry ( $n = 432$ ) and wet season ( $n = 223$ ) respectively (Horne and Garton, 2006). To avoid over- or under-smoothing the data (Illian et al., 2008), the smoothing parameter  $h$  was selected through the likelihood cross validation (CVh) method (Horne and Garton, 2006). To calculate the elephant CVh per season we used Animal Space Use 1.3. beta (Horne and Garton, 2009). Kernel analysis was performed using Hawth's analysis tools 3.27 (Beyer, 2004). A threshold of 95% of the probability volume contour (Kernohan et al., 2001) defined presence and absence (inside/outside the kernel) of elephant within the total counts surveyed

area. We visually inspected the seasonal kernel estimates to confirm that the selected seasonal  $h$  and the 95% volume contour (hereafter called kernel area) included all elephant records (Illian et al., 2008). These kernel areas were also visually compared with a number of kernel estimates resulting from different  $h$  values ranging from 2 km (minimum width of transect) to 40 km (linear dimension of the largest home range of elephant in TME; Galanti et al. 2000), at 1 km increment.

### 3.2.4 Predictors

The predictors and their properties are listed in Table 3.2. Elevation, slope and topographic position index (TPI) were derived from the Shuttle Radar Topography Mission (SRTM), 3 arc-second (about 90 m) pixel, v2 (Rodríguez et al., 2006). TPI (Skidmore, 1990), identifies hilltops, ridges, bottom valley and flat areas and was calculated with the Topography tool for ArcGIS 9.3 (ESRI). Africover Tanzania Multipurpose Landcover Database full resolution (FAO-Africover, 2002) was grouped in 10 classes (Galanti et al., 2006) (see Table 3.2). A distance index from protected and semi-protected areas was developed as a proxy for the degree of risk to elephant by human activity. Increasing distance from the boundaries outside protected areas represents an increased probability of negative interaction between resident farmers and elephant and nomadic poachers and elephant. Increasing distance from the boundary inside protected areas represent increased security for elephant. The distances from the boundaries inside protected areas were multiplied by -1 to be distinguished from the distances outside. Then the index has been normalized between zero (no risk) and 1 (maximum risk) as follows:

$$I_{risk} = \frac{x - Min_{risk}}{Max_{risk} - Min_{risk}} \quad (3.1)$$

where,  $Min_{risk}$  is the minimum risk value (the largest distance from inside protected areas boundary, i.e., the safest distance);  $Max_{risk}$  is the maximum risk value (i.e., the largest distance from outside the protected areas boundary);  $Max_{risk} - Min_{risk}$  is the range. Distance rasters from settlements, tarmac and minor roads, rivers, lakes and other water sources (dams, ponds, boreholes) were generated from the related shape files using the Euclidean distance function. For the dry season analysis only permanent water sources were considered. Decadal NDVI SPOT-VEGETATION (SPOT-VTG) images at 1 km resolution from 1 April 1998 to 31 December 2004 were used as a proxy for

vegetation greenness (Walsh et al., 1997). Noise due to missing values and clouds was reduced by using the modified (Beltran-Abuanza, 2009) Adaptive Savitzky-Golay filter algorithm (Jönsson and Eklundh, 2004). Three NDVI variables were calculated: 1) monthly average NDVI; 2) monthly average NDVI (September–October); 3) monthly average NDVI (March–April).

Table 3.2: Source, data type and unit of the independent variables.

Variable	Source	Data Type	Spatial	Unit
Elevation	SRTM <sup>a</sup>	Continuous	Grid	Meter
Slope	SRTM <sup>a</sup>	Continuous	Grid	Degree
TPI	SRTM <sup>a</sup>	Continuous	Grid	Meter
Land Cover	Africover resolution full shapefile <sup>b</sup>	Categorical	Grid	10 classes
Africover-rank	Africover tree cover percentage <sup>b</sup>	Ordinal	Grid	1–10
Distance from boundaries of protected areas	National Parks boundary shapefile <sup>c</sup>	Continuous	Grid	Index: 0–1
Distance from boundaries of semi-protected areas	GCA and Manyara Ranch boundaries shapefile <sup>c</sup>	Continuous	Grid	Index: 0–1
Distance from water sources	Shapefiles of water sources <sup>c</sup>	Continuous	Grid	Meter
Distance from tarmac and minor roads	Roads shape file <sup>c</sup>	Continuous	Grid	Meter
Distance from settlements	Settlements shapefile <sup>c</sup>	Continuous	Grid	Meter
NDVI-SPOT VEGETATION	SPOT-VEGETATION (1 km) <sup>d</sup>	Continuous	Image	Index: 0–255

<sup>a</sup>USGS.

<sup>b</sup>FAO, reclassified in: closed trees, closed shrubs, cultivated areas, herbaceous vegetation on flooded area, herbaceous vegetation or savanna, open to very open shrubs, open to very open trees, river banks and bare areas, trees or shrubs on flooded area, closed woody vegetation (mixed of closed trees and shrubs).

<sup>c</sup>obtained from the Global Environment Facility project (see acknowledgments).

<sup>d</sup>obtained from <http://www.vgt.vito.be>.

All images and GIS layers were re-projected to the Universal Transverse Mercator, UTM zone 37, Spheroid Clarke 1880, Datum Arc 1960 and re-sampled (with the nearest neighbour method) to 500 x 500 m<sup>2</sup> before performing spatial analysis. Spatial analysis was performed in ArcGIS 9.3

(ESRI), ERDAS Imagine 9.3 (Leica Geosystems) and ENVI 4.7 (ITT Visual Information Solutions).

### 3.2.5 Logistic regression, model accuracy and transit corridors

Logistic regression is widely employed, robust and explicit (Barbosa et al., 2009). The results are easy to interpret for its straightforward statistical properties (standard errors, prediction intervals,  $p$  values; Wintle et al., 2005). Comparative studies have shown that, if presence and absence data are available, logistic regression provides as good, or better, predictions than more complicated methods (see Wintle et al., 2005), including presence-only methods (Brotons et al., 2004; Elith and Graham, 2009). Compared to Maximum Entropy (MaxEnt, Phillips et al., 2006), which outperforms other presence-only methods (Elith et al., 2006), logistic regression appears to generate more accurate predictions for highly detectable species (Rota et al., 2011). On the other hand, MaxEnt appears to perform better than logistic regression for small number of presence data (Wisiz et al., 2008) and low detectable/rare species (Rota et al., 2011). For these reasons, the logistic regression was used to seasonally model the probability of elephant presence in TME.

The predictors were normalized and tested for multicollinearity prior to performing the logistic regression. Predictors with Variance Inflation Factor (VIF) larger than 2.5 were excluded from the logistic regression (Allison, 1999). The variables were tested one by one. A stepwise forward logistic regression (Pearce and Ferrier, 2000) was performed using the presence (inside the kernel) and absence (outside the kernel) of elephant for both seasons. Significance thresholds of 0.05 and 0.01 were used for inclusion and exclusion of predictors respectively. The predicted probabilities of elephant presence generated by the logistic regression were then tested with the seasonal SRF locations, using the area under the receiver operating characteristic (ROC) curve (AUC). Transit corridors and dispersal areas were identified by subtracting the predicted probabilities of elephant presence in the dry season from those in the wet season as follows:

$$p_{wet} - p_{dry} > 0 \quad (3.2)$$

where,  $p_{wet}$  and  $p_{dry}$  are the probability of elephant presence in the wet and dry season, respectively. The identification of transit corridors was made by visual

pattern recognition. Transit corridors were overlaid on and compared with the digitized migration routes shown in Fig. 3.1.

Average values of the predictors were calculated in and outside the kernel and compared within seasons using *t* test for independent samples. Statistical analysis was performed in SPSS 16.0.1.

### 3.2.6 Path analysis

A path analysis (Quinn and Keough, 2002) was performed to determine the degree to which single environmental and anthropogenic variables made an independent contribution to the prediction of elephant distribution. Specifically, if the distance from protected areas, settlements and roads had an indirect effect on elephant distribution due to their association with accessibility to drinking water, vegetation structure and biomass. Africover was converted to a continuous ordinal variable (Africover-rank) by extracting the tree cover percentage from the full Africover dataset (Di Gregorio and Jansen, 2005). The kernel-based probabilities of elephant occupancy were normalized between 0 and 1 by dividing all pixels by the maximum value. Path analysis was performed in AMOS 5.0.1.

## 3.3 Results

The smoothing parameters *h* for the dry and wet season kernel density were 2992 m and 4002 m respectively. Visual inspection of the results confirmed that the CVh method did neither over-smooth nor under-smooth the data. In addition the 95% probability volume contour included all seasonal GPS locations of elephant (Fig. 3.2(a) and (b)).

During the dry season the main kernel areas were inside protected (TNP) and semi-protected areas. A few small isolated kernel areas were outside (see Fig. 3.2(a)). During the wet season the kernels expanded outside the protected and semi-protected areas to the north-east and south-east (see Fig. 3.2(b)).

In the dry season all predictors, except slope and TPI, were found to be significantly different (*t*-test,  $p < 0.01$ ) between inside and outside the kernel. In the wet season, only TPI was not significantly different. In both seasons, the areas inside the kernel were significantly closer to drinking water, more distant from human artifacts, and 'greener' than the areas outside. The difference in monthly average NDVI between inside and outside the kernel was larger in areas outside protected and semi-protected areas (Fig. 3.3) in both seasons.

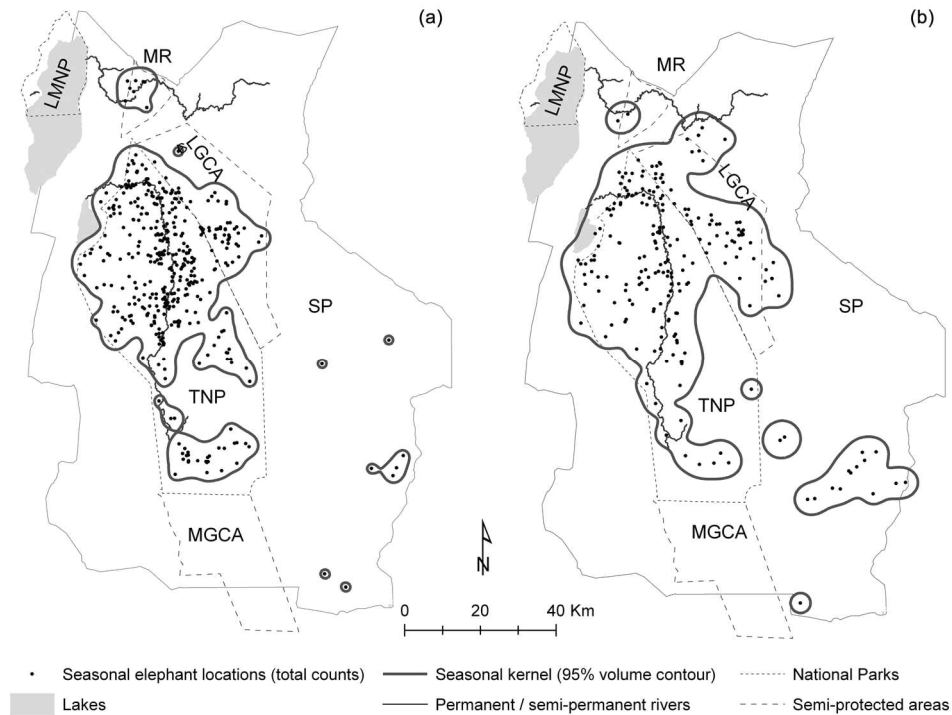


Fig. 3.2: Ninety-five percent of probability volume contours of the kernel density estimate of elephant and total counts elephant locations for dry (a) and wet (b) seasons. Lake Manyara National Park (LMNP); Tarangire National Park (TNP); Lolkisale Game Controlled Area (LGCA); Mukungunero Game Controlled Area (MGCA); Manyara Ranch (MR); Simanjiro Plains (SP).

### 3.3.1 Logistic regression and model accuracy

The predictor variables excluded from the logistic regression models due to high collinearity ( $VIF > 2.5$ ) were: a) distance from Silale swamp, monthly average NDVI (September–October) and elevation in the dry season and b) monthly average NDVI and distance from tarmac roads in wet season. The logistic regressions were statistically significant in both seasons (Wald test,  $p < 0.001$ ) accounting for 74% and 55% of the variance in elephant presence in the dry and wet season respectively (Nagelkerke  $R^2 = 0.74$  and  $0.55$ ).

Identifying transit corridors for elephant using a long time-series

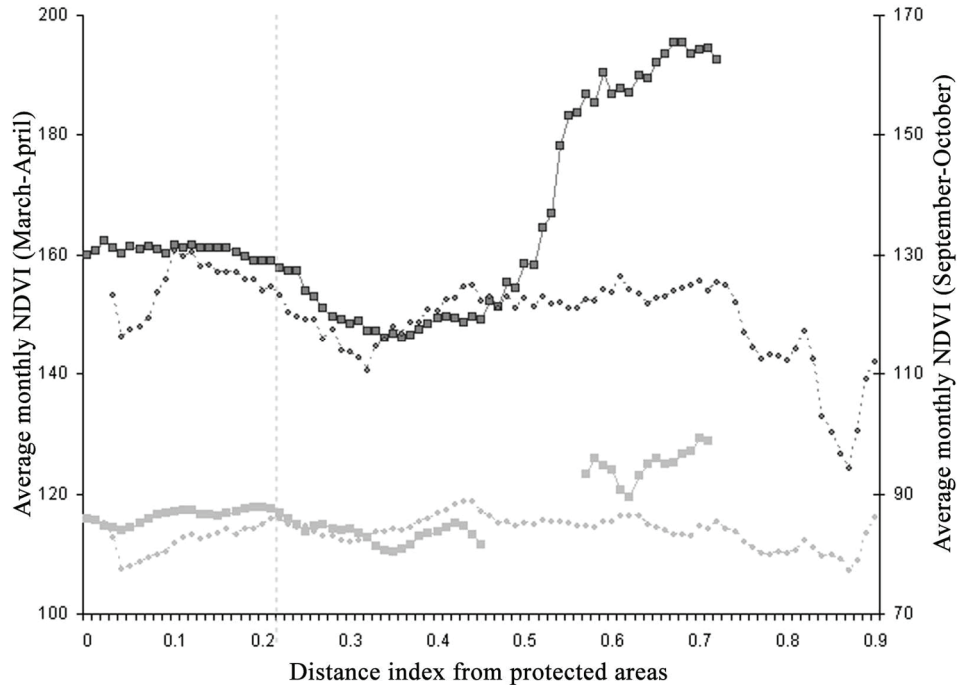


Fig. 3.3: Wet (dark grey) and dry (light grey) monthly average NDVI inside (squared marker) and outside (round marker) the kernel in relation to the distance index from protected areas. The vertical dashed line marks the boundary of TNP (inside the park is on left). In the dry season the kernel areas did not include any portion of the study area between the distance indexes: 0.45–0.58, which explains the gap in the graph.

In the dry season, distance index from protected areas was the main predictor accounting for 50% of the variance, while distance from lakes, land cover and distance from villages contributed an additional 8%, 5% and 3% respectively to the logistic regression model. Other predictors were distance index from semi-protected areas, monthly average NDVI, and distance from permanent rivers. In the wet season, distance from lakes was the most important predictor accounting for 28% of the variance, while distance index from protected areas, land cover and distance from villages contributed an additional 11%, 10% and 1% respectively to the model. Other predictors were distance from rivers, distance from dams and monthly average NDVI (March–April). The statistical tests of individual predictors are shown in Appendix A for both seasons (Table A.1).

In both seasons, elephant presence was: a) negatively associated with distance from permanent drinking water sources, distance index from protected and

semi-protected areas, slope and TPI; b) positively associated with distance from villages, minor roads, monthly average NDVI, closed woody vegetation and cultivated areas. Furthermore, in the dry season elephant was positively associated with closed shrubs, woodlands and to lesser extent savanna and open areas. In the wet season elephant was associated with herbaceous vegetation in open areas (also flooded) and negatively associated with river banks, bare soils and trees and shrubs on flooded areas.

In the dry season the area with higher predicted probabilities for elephant included northern and central TNP and portions of semi-protected areas (see Fig. 3.4(a)). Most of the unprotected areas showed low predicted probabilities for elephant, except for an area of closed woody vegetation at the eastern side of the study area. In the wet season the area with higher predicted probabilities for elephant increased outside TNP in the north, east and south-east (Fig. 3.4(b)).

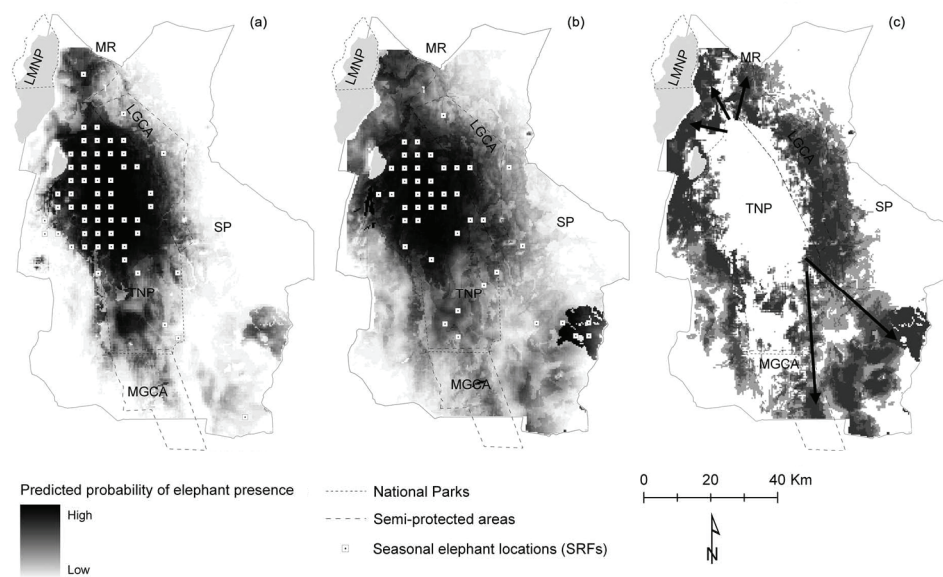


Fig. 3.4: Predicted probabilities of elephant presence and SRF elephant locations in the dry (a) and wet (b) seasons and change (c) from dry to wet season distribution models. To highlight wet season dispersal areas and transit corridors (black arrows) only probabilities  $> 0$  are plotted in Fig. 3.4(c).

In the dry season, elephant was observed in 58 out of 451 SRF locations (AUC = 0.9). In the wet season, elephant was observed in 44 out of 451 SRF locations

(AUC = 0.89). SRF locations with elephant presence are shown in Fig. 3.4(a) and (b).

### 3.3.2 Transit corridors and wet season dispersal areas

The values that define transit corridors were between 0.08 and 0.2. Values > 0.2 identified dispersal areas while values < 0.08 identified areas used by elephant in both seasons. Five main transit corridors heading to wet season dispersal areas were detected (see Fig. 3.4(c)) and matched four migration routes described in the 1960s (Borner, 1985; Lamprey, 1964). Two transit corridors connecting the southern TNP to the wet dispersal areas in the south-east of the study area matched the southern migration routes 5 and 6 (Fig. 3.1). The corridor in the south-east is approximately 40 km long. The corridor crossing MGCA is 50 km long. In the north, a small corridor of 16 km long connecting the northern TNP to Manyara Ranch on the north-eastern side was detected. This corridor was not described in the 1960s. On the western side of Manyara Ranch, a corridor 20 km long connecting northern TNP to LMNP, matches the route 1. Another one, 16 km long connecting the north-western side of TNP to LMNP, matches the route 10. Dispersal areas were detected in the north between TNP, Manyara Ranch and LMNP; in the east toward Lolkisale village and Simanjiro plains and in the south-east. In the western part of TME, dispersal areas were detected around Lake Burungi. Dispersal areas are shown in darker grey in Fig. 3.4(c).

### 3.3.3 Path analysis

Africover-rank significantly correlated with NDVI variables in both seasons (Spearman correlation test,  $r > 0.4$ ,  $p < 0.001$ ;  $n = 13,633$ ). The NDVI variables had higher correlation with the kernel-based probability of elephant occupancy than Africover-rank, and therefore the Africover-rank was not used in path analysis. Path analysis revealed a significant indirect effect of the distance from protected areas, settlements and minor roads on elephant occupancy in relation to monthly average NDVI and accessibility to water in both seasons.

In the dry season, path analysis explained 90% (square multiple correlation = 0.90) of the variance in the probability of elephant occupancy. The path diagram in Fig. 3.5(a) shows that distance from settlements had a direct positive effect (standardized coefficient = 0.63) on elephant as well as an indirect negative effect (standardized coefficient = -0.33) through permanent dams. In other words, settlements close to dams were associated with higher probabilities of elephant occupancy. Distance index from protected areas had a direct as well

as an indirect effect on elephant occupancy through permanent rivers, monthly average NDVI (September–October), elevation and TPI. Although NDVI positively influenced elephant occupancy across the study area, the overall effect of distance index from protected areas on elephant was negative (indirect and direct standardized coefficients =  $-0.47$  and  $-0.43$  respectively). In other words, elephant occupancy decreased away from protected areas and permanent rivers, but it increased at higher NDVI values, occurring at higher elevation and TPI also outside protected areas. This pattern is shown in Fig. 3.6(a): elephant occupancy decreased logarithmically ( $y = 10.95 \ln x + 51.34$ ,  $R^2 = 0.91$ ) away from protected areas whereas NDVI significantly increased ( $y = 0.002x^3 - 0.014x^2 + 0.2x + 85.28$ ,  $R^2 = 0.84$ ). Both inside and outside protected areas (index  $> 0.2$ ) local peaks of elephant occupancy matched local peaks of NDVI.

In the wet season, path analysis explained 88% (square multiple correlation = 0.88) of the variance in the probability of elephant occupancy. The path diagram in Fig. 3.5(b) shows that distance index from protected areas had a direct negative effect (standardized coefficient =  $-0.95$ ) on elephant as well as an indirect positive effect (standardized coefficient = 0.02) through its association with distance from minor roads, seasonal dams and monthly average NDVI (March–April). In other words, elephant occupancy decreased in unprotected areas but increased in proximity to seasonal dams, even close to settlements and minor roads. As shown in Fig. 3.6(b), although elephant occupancy decreased away from protected areas, local peaks of elephant occupancy in and outside protected areas locally matched the smallest distance from seasonal dams.

Identifying transit corridors for elephant using a long time-series

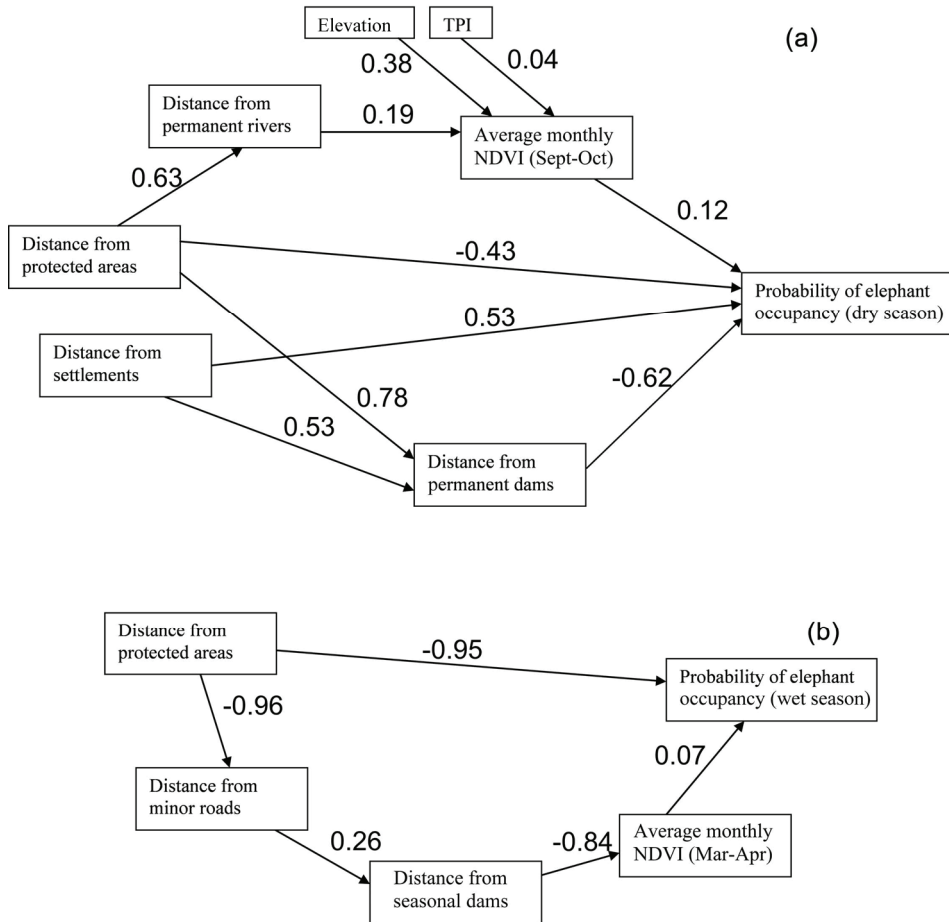


Fig. 3.5: Path diagrams showing statistically significant path coefficients (along the arrows) of the indirect and direct effects of interrelated variables on the probability of elephant occupancy in the dry (a) and wet (b) seasons. Signs indicate negative and positive relationships accordingly.

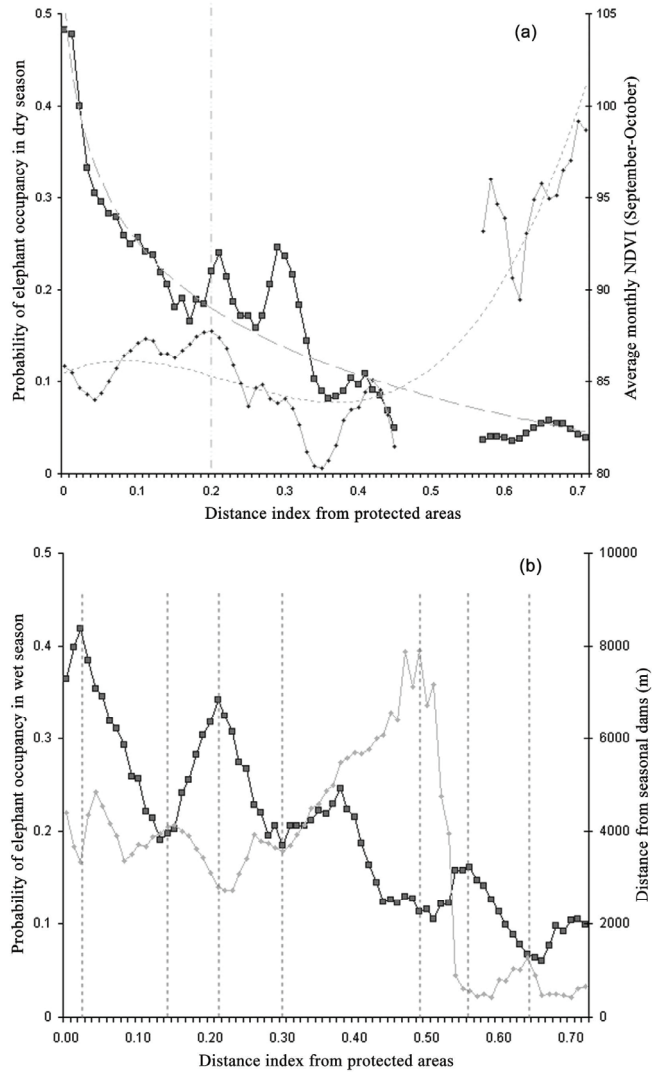


Fig. 3.6: (a) Average probabilities of elephant occupancy (dark grey) and monthly average NDVI (September–October, light grey) against distance index from protected areas in the dry season. The vertical dashed line marks the boundary of TNP. Significant curvilinear functions are drawn in grey. In the dry season the kernel areas did not include any portion of the study area between the distance indexes: 0.45–0.58, which explains the gap in the graph. (b) Average probabilities of elephant occupancy (dark grey) and distance from seasonal dams (light grey) against distance index from protected areas in the wet season. Dotted vertical lines highlight the match between the local minima and maxima of the two variables.

## 3.4 Discussion

### 3.4.1 Probability of occupancy in species distribution modeling

Recent comparative studies on high vagile animals, showed that models based on point data alone produced less accurate predictions than models explicitly accounting for vagility (e.g. daily movement distance, Ko et al., 2011), imperfect detection (Rota et al., 2011) or environmental context (de Knecht et al., 2011). In this paper we derived presence and absence locations from the kernel-based probability of elephant occupancy to account for species vagility, temporal discontinuity of total counts and environmental context. Imperfect detection was not an issue in our study because elephant is highly detectable in the open vegetation (Prins and Douglas-Hamilton, 1990). Our method (kernel-based probability of occupancy + logistic regression) produced high accurate seasonal distribution maps of elephant (AUC = 0.9). The selection of the smoothing parameter  $h$  is of great importance in this method, because large  $h$  values can over-smooth the data, affecting the regression analysis. In our study the selection of the smoothing parameters  $h$  for the dry ( $h = 3$  km) and wet ( $h = 4$  km) season was based on statistical properties of the data, through the likelihood cross validation method (Horne and Garton, 2006). The  $h$  values were largely smaller than the linear dimension of the smallest core area (7 km) and home range (11 km) of elephant in TME (kernel estimates based on 70% and 95% volume contour respectively; see Galanti et al., 2006). The  $h$  values were also smaller than the maximum straight distance travelled by radio-collared elephants in TME at the end of the dry season (about 15 km in 10 hours; Galanti et al., 2000) as well as the smallest daily movement distance estimated in the wet season (about 5 km; Galanti et al., 2000). In addition, the kernel areas (defined by the 95% volume contour) included all elephant records, without over-smoothing the data. Therefore, the kernel-based probability of occupancy appears to substantially minimize the probability of false absences, without over-smoothing the data. On the contrary, applying coarse-grained predictors (Guisan and Thuiller, 2005) or a buffer (Ko et al., 2011) to our data, for instance equal to the daily movement distance of elephant in TME, would over-smooth the data.

### 3.4.2 Seasonal distribution of elephant at landscape and local scale

Protected areas and availability of drinking water were the main predictors of elephant presence at landscape scale in both seasons. In the dry season most of the permanent water sources were inside the protected and semi-protected areas. The north-central area of the TNP, which showed higher predicted probabilities, included the main permanent water sources and high NDVI values. This area receives the highest monthly precipitation (Gereta et al., 2004) and is characterized by *A. tortilis*, which is highly nutritious in the dry season (Ludwig et al., 2008). This result is consistent with those of other studies (Chamaillé-Jammes et al., 2007; Loarie et al., 2009; Western, 1975). However, drinking water was also a major predictor in the wet season, suggesting that this factor plays an important role in the spatial and temporal distribution of elephant throughout the year (de Beer and van Aarde, 2008; Ngene et al., 2009b).

The distance from the boundary of the protected area gave a strong independent contribution to the model in both seasons and was not only related to the presence of drinking water. The elephant population of TME has recovered after the international ban on ivory trade in 1989. In Tanzania, elephant is protected but safari hunting allowed. TNP is surrounded by GCAs and hunting blocks for trophy and resident hunting. The annual hunting season lasts from the first of July to the end of December. Disturbance due to hunting and poaching (two collared elephants were poached in the most distant area from TNP) may explain the close association of elephant with boundaries of protected areas and negative association with minor roads. In contrast to the findings by Ngene et al. (2009b), in TME the roads outside the protected areas are less patrolled and do not provide security to elephant. Furthermore, because of the growing expansion of agriculture in TME (TCP, 1998), the use of unprotected areas may be hindered by farming (Murwira et al., 2010) in combination with hunting and poaching.

Land cover was a moderate predictor of elephant presence. In the dry season closed woody vegetation and closed shrubs were strongly associated with elephant. These vegetation classes significantly correlated with monthly average NDVI (September–October) suggesting a preference of the elephant for woody (Lamprey, 1963) and greener vegetation (Loarie et al., 2009) in this season. In the wet season the probability of elephant presence was strongly associated with open shrublands, open woodlands and herbaceous vegetation on flooded areas. This result agrees with the findings of other studies (Loarie et al., 2009; Prins and Douglas-Hamilton, 1990; Young et al., 2009a) indicating the

strong preference for grass over browse. According to Lamprey (1963) the elephant is a woodland species with a generalist diet ('mixed feeder') becoming strictly browser during the dry season and grazer during the wet season. This flexibility allows optimization of the seasonal intake of food by utilizing tree leaves and bark in the dry season and highly nutritious (lush) grass during the wet season. In our study area closed woody vegetation in unprotected areas might also be used by elephant as cover to avoid human disturbance (Lamprey, 1963). Our results also showed a moderate positive association of elephant with cultivated areas in both seasons, which is mostly recorded by inferential studies on crop raiding (Graham et al., 2009). Crop raiding by elephant is perceived as a major problem by the villagers around the TNP (Pittiglio, 2009).

In agreement with the findings of other studies (Harris et al., 2008; Hoare and Toit, 1999), distance from settlements had a strong positive correlation with elephant presence in both seasons. However, settlements close to permanent water sources were associated with higher local probability of elephant presence even in the dry season. Hence permanent water sources outside protected areas, but close to human infrastructure, were visited by elephant. This finding emerged from the path analysis, which explained the elephant distribution at a local scale. Specifically, although at landscape scale the probability of elephant occupancy decreased with increasing distance from the boundary of protected areas, at local scale, higher vegetation biomass (i.e., higher NDVI) and accessibility to drinking water determined local peaks of elephant occupancy also outside protected areas (see Fig. 3.6(a) and (b)). This pattern occurred also for sites close to settlements and minor roads, particularly in the wet season. This result suggests that elephant tracks water and green vegetation in both seasons (Loarie et al., 2009) even in proximity to human infrastructure. In contrast to other studies (Ngene et al., 2009b), in the TME the terrain explained little variance in elephant presence. This is explained by the small variation in elevation and slope in our research area.

### **3.4.3. Identification of transit corridors and conservation implications**

Our approach successfully identified transit corridors for elephant in the TME. These corridors matched four wildlife migration routes described in the 1960s based on field experience (Lamprey, 1964; Mwalyosi, 1991). Our results, in combination with those of Lamprey (1964), suggest that these corridors have been persistently used by elephant for more than 40 years, providing landscape connectivity in TME. The corridor connecting TNP to LGCA (matching route 2; see Galanti et al., 2006) was detected from the kernel density function (Fig.

3.2(b)) but did not clearly emerge from the wet season model. This area showed lower NDVI values than TNP in both seasons. Hence other variables rather than NDVI such as landscape heterogeneity may determine the elephant distribution in this area (Murwira and Skidmore, 2005). The corridor heading to the north along the eastern side of Manyara Ranch was not described in the 1960s. In 2001 Manyara Ranch was acquired by the Tanzania Land Conservation Trust. Our result, in combination with the observation of elephant tracks in this area (OIKOS, 2002), suggests that the protection provided by Manyara Ranch to wildlife facilitates the movement of elephant along the corridor. Empirical descriptions of transit corridors for elephant have been recently described (see Douglas-Hamilton et al., 2005; Galanti et al., 2006; Ngene et al., 2009a), though the transit corridors identified in TME were slightly shorter. This may be due to the fact that our study area excluded some wet season dispersal areas in the north (Esimingor and Marang National Forest Reserves) and in the south-east (Kiteto district). Since the 1980s TNP and LMNP are at risk of isolation due to agricultural expansion into transit corridors and dispersal areas (Borner, 1985; Mwalyosi, 1991). The predicted probability maps generated by this study may therefore be used to better delineate village land use zoning maps including WMAs. The corridors are stable over the decades. These results have conservation relevance. Land managers must frequently decide how allocating the limited resources to preserve biodiversity. Our results suggest that transit corridors are easier to protect and more cost-effective than larger and less predictable wet season dispersal areas. To our knowledge, this is the first study investigating transit corridors from the predicted probabilities of elephant presence obtained from aerial surveys and their persistence over the decades. Our approach yielded insights how advanced spatial analysis can be integrated with biological data available from long-term datasets to identify transit corridors and predictors of species distribution.

## Acknowledgments

This research was funded by the University of Twente, Faculty of Geo-Information Science and Earth Observation (ITC), the Netherlands, and the Global Environment Facility Project GCP/URT/124/WBG. The authors would like to thank Food and Agriculture Organization of the United Nations (FAO), the Livestock, Environment and Development Initiative (LEAD), Tanzania Wildlife Research Institute (TAWIRI), Istituto OIKOS, African Wildlife Foundation (AWF), International Livestock Research Institute (ILRI) and Tanzania National Parks (TANAPA) to provide the data used in this analysis.



# 4

## **Elephant response to spatial heterogeneity in a savanna landscape of northern Tanzania**

This chapter is based on:

Pittiglio, C., Skidmore, A.K., van Gils, H.A.M.J., Prins, H.H.T. Elephant response to spatial heterogeneity in a savanna landscape of northern Tanzania. In press, *Ecography*.

## Abstract

Landscape heterogeneity, namely the variation of a landscape property across space and time, can influence the distribution of a species and its abundance. Quantifying landscape heterogeneity is important for the management of semi-natural areas through predicting species response to landscape changes, such as habitat fragmentation. In this paper, we tested whether the change in spatial heterogeneity of the vegetation cover due to farming expansion affected the distribution of the African elephant in the Tarangire–Manyara ecosystem, northern Tanzania. Spatial heterogeneity (based on the Normalized Difference Vegetation Index) was characterized at multiple spatial scales using the wavelet transform and the intensity–dominant scale method. Elephant distribution was estimated from time-series aerial surveys using a kernel density function. The intensity, which relates to the contrast in vegetation cover, quantified the maximum variation in NDVI across multiple spatial scales, whereas the dominant scale, which represents the scale at which this maximum variation occurs, identified the dominant inter-patch distance, i.e., the size of dominant landscape features. We related the dominant scale of spatial heterogeneity to the probability of elephant occurrence in order to identify: 1) the scale that maximizes elephant occurrence, and 2) its change between 1988 and 2001. Neither the dominant scale and intensity of spatial heterogeneity, nor the probability of the elephant occurrence changed significantly between 1988 and 2001. The spatial scale maximizing elephant occurrence remained constant at 7000 to 8000 m during each wet season. Compared to the findings of a recent, similar study in Zimbabwe, our results suggest that the change in the dominant scale was relatively small in Tarangire–Manyara ecosystem and well within the critical threshold for elephant persistence. The method is a useful tool for monitoring ecosystems and their properties.

## 4.1 Introduction

Landscape heterogeneity, namely how a landscape property such as vegetation cover varies across space and time (Li and Reynolds, 1995), can influence wild herbivores distribution (Fryxell et al., 2005; Murwira and Skidmore, 2005), population dynamics (Oliver et al., 2010; Wang et al., 2006) and biodiversity (Baldi, 2008; Cromsigt et al., 2009; Pianka, 1966). Quantifying landscape heterogeneity is important for the management of semi-natural areas (Guisan and Thuiller, 2005) and for predicting species response to landscape changes, such as habitat fragmentation (Schooley, 2006). However, neither the level of fragmentation that affects a species dispersal, nor the level of heterogeneity that maximizes its occurrence, is well understood (Fazey et al., 2005). The ability to

predict a species–environment relationship may be hampered by methodological limitations. In particular, repeatable and quantifiable measurement of landscape heterogeneity over time and its relation to species distribution may vary with grain (i.e., detail of data; in raster the grid cell size) and extent (i.e., the size of the study area) (Baldi and McCollin, 2003; Dungan et al., 2002; Levin, 1992; Perry et al., 2002; Wiens, 1989). The accuracy of species distribution models may be affected by species' ecological traits (such as large body size, wide range size and high vagility, Ko et al., 2011; McPherson and Jetz, 2007), detectability (i.e., probability of a species to be detected; Mackenzie et al., 2002) as well as the environmental context (Guisan and Thuiller, 2005). The latter is the characteristic of the environment surrounding a recorded presence of a species at a given site (de Knecht et al., 2011). Consequently, studies quantifying changes in landscape heterogeneity over time and its relation to species distribution require analysis across multiple spatial scales, over a long period of time, and species distribution models that explicitly account for the above factors (Guisan et al., 2006).

The development of remote sensing allows monitoring of landscape properties over time, such as vegetation cover and biomass. Murwira and Skidmore (2006) developed the intensity–dominant scale method based on the wavelet transform to simultaneously measure change in variability and in patch size of vegetation cover from the Normalized Difference Vegetation Index (NDVI). For the intensity–dominant scale method, the intensity refers to the maximum contrast or variance in vegetation cover (e.g., in NDVI) measured at successively increasing window sizes (e.g., at multiple scales). The dominant scale represents the window size (e.g., scale) at which this maximum variance occurs. In other words, the intensity quantifies the maximum change in the vegetation cover across multiple spatial scales, whereas the dominant scale quantifies the size of dominant landscape features. Consequently, the dominant scale directly relates to the level of patchiness (or fragmentation) of a landscape (Murwira and Skidmore, 2006). Importantly, as shown by Pittiglio et al. (2011), this method is robust when used with different pixel sizes, such as Orthophoto (1 m pixel size), Advanced Spaceborne Thermal Emission and Reflection Radiometer (ASTER, 15 m) and Landsat Enhanced Thematic Mapper Plus (ETM+, 30 m). In other words the Murwira–Skidmore method is grain independent. Murwira and Skidmore (2005) applied the intensity–dominant scale method to quantify change in landscape heterogeneity (and fragmentation) and its relation to the distribution of the African elephant (*Loxodonta africana*, Blumenbach) in an agriculture-dominated savanna landscape in Zimbabwe. That study showed that the decline in elephant population between the early 1980s and early 1990s was correlated to a

decrease in the dominant scale of landscape heterogeneity from about 750 m to 450 m (i.e., an increase in patchiness and consequently in habitat fragmentation), caused through farm expansion (Murwira and Skidmore, 2006; Murwira et al., 2010). The same study revealed that elephant disappeared from the ecosystem when the dominant scale decreased to less than 400 m, meaning that the landscape became too fragmented for the elephant persistence (Murwira and Skidmore, 2005).

In this paper we used the intensity–dominant scale method based on wavelet transform to test whether a change in spatial heterogeneity of vegetation cover due to farming expansion affected the wet season distribution of the African elephant between 1988 and 2001 in the Tarangire–Manyara ecosystem, northern Tanzania. Our focus was on the elephant population as it recovered from severe poaching (Prins et al., 1994). Farm area increased from about 900 km<sup>2</sup> in 1988 to about 1450 km<sup>2</sup> in 2000 (OIKOS, 2002) in the Tarangire–Manyara ecosystem. However, contrary to the earlier Zimbabwean study, the elephant population remained stable (see TAWIRI, 2001). We propose a theoretical framework describing the relationship between the change in dominant scale of vegetation cover (as indicated by NDVI), and the probability of elephant occurrence (see Fig. 4.1(a) and (b)). As our study is concerned with land use change outside the park network, we focused only on the wet season, when elephants move outside the park (Drent and Prins, 1987; Lamprey, 1964) in response to available vegetation biomass and access to temporary water (Pittiglio et al., 2012).

#### 4.1.1 Theoretical framework

Fig. 4.1(a) and (b) describes how an increase in habitat fragmentation due to farm expansion (as calculated by the intensity–dominant scale method; see Murwira and Skidmore, 2005) can affect elephant occurrence, with specific reference to the Tanzanian and Zimbabwean case studies. Gradient landscapes in Fig. 4.1(a), comprising natural savanna, are characterized by a variation in vegetation cover. The dominant scale of spatial heterogeneity is large, representing (and matching) large dominant patches of relatively homogeneous vegetation (Fig. 4.1(a),  $t_1$ ). As farming expands in savanna ecosystems, the patches of natural vegetation become increasingly fragmented and smaller; consequently, the dominant scale is reduced (Fig. 4.1(a),  $t_2$ ). Eventually, the landscape becomes characterized by large blocks of farms and small patches of natural vegetation and the dominant scale is large (Fig. 4.1(a),  $t_3$ ). In savanna ecosystems the grass (including crops) is brighter than trees in the wet season.

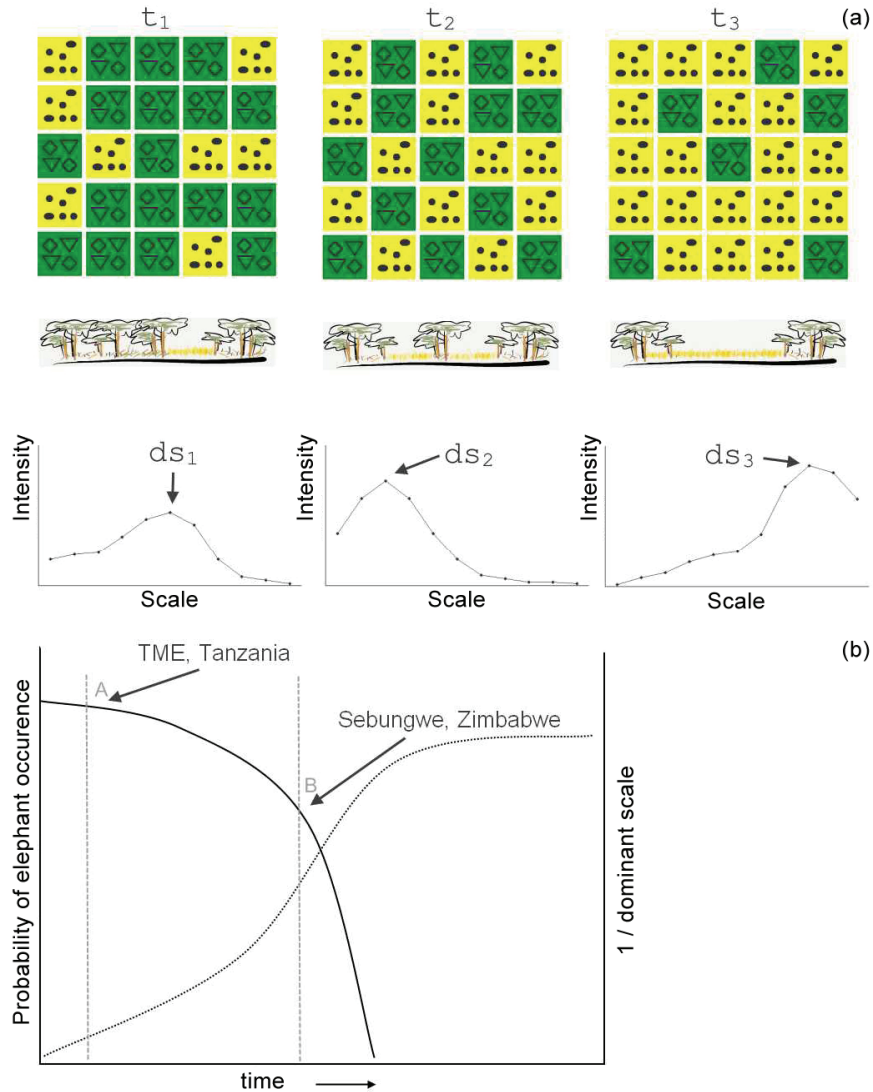


Fig. 4.1: (a) The theoretical framework showing the fragmentation of a natural savanna (in green) in relation to farming expansion (in yellow). In  $t_1$  sparse and small arable fields do not affect the dominant scale of the landscape ( $ds_1$ ), which is large; in  $t_2$  the dominant scale ( $ds_2$ ) is reduced due to the expansion of farming; in  $t_3$  the dominant scale ( $ds_3$ ) is greatest because the landscape is almost totally converted to agriculture. (b) The expected relation between the change in inverse dominant scale of landscape heterogeneity (dotted line) and the probability of elephant occurrence (solid line) over time. The dashed lines indicate the elephant population in: A) Tarangire–Manyara ecosystem, Tanzania, and B) Sebungwe region, Zimbabwe (Murwira and Skidmore, 2005).

At the beginning of the conversion process ( $t_1$ ), the intensity (which is directly related to the brightness of the satellite image and to NDVI) is low, because of the relatively homogeneous brightness of natural vegetation (Pittiglio et al., 2011). At  $t_2$ , the intensity increases because the NDVI variation (and reflectance) between crops and natural vegetation is higher and the boundary between these patches is crisp. The highest intensity occurs at  $t_3$ , because the reflectance of crops is at a maximum, and higher than grass and trees in the wet season. The probability of elephant occurrence remains high and relatively stable in semi-natural savanna, while only small changes in the dominant scale occur (determined by small and sparse arable fields, see Fig. 4.1(b), point A). Then the probability of elephant occurrence slowly decreases in response to habitat fragmentation (and consequently smaller dominant scales)(Fig. 4.1(b)). However, as observed in Zimbabwe by Murwira and Skidmore (2005), when the patches of natural vegetation become increasingly fragmented and the size of the dominant scale reaches a certain threshold, the probability of elephant occurrence drops sharply, disappearing from the ecosystem (see Fig. 4.1(b), point B). Because the elephant population of the Tarangire–Manyara ecosystem remained stable during the study period (TAWIRI, 2001), we hypothesized that: a) the dominant scale of spatial heterogeneity that maximizes elephant occurrence was large, representing large patches of natural vegetation (see point A, Fig. 4.1(b)); b) compared to the findings in Zimbabwe (Murwira and Skidmore 2005), the change in the dominant scale was expected to be relatively small in Tarangire–Manyara ecosystem and not approaching the critical threshold (point B) of elephant persistence.

## 4.2 Methods

### 4.2.1 Study area

The Tarangire–Manyara ecosystem (between 3°36'S and 4°7'S, and 35°82'E and 36°74'E) is part of the Maasai steppe (Prins, 1987) and hosts the largest population of elephant (*Loxodonta Africana*) in northern Tanzania. The research area includes protected (Tarangire and Lake Manyara National Parks), semi-protected (Manyara Ranch, Lolkisale and Mkungunero Game Controlled Areas) and unprotected areas (see Fig. 4.2). The Tarangire–Manyara ecosystem is predominantly formed by a gently undulating plateau with elevations between 1000 and 2000 m a.s.l. (Prins, 1988). The annual average rainfall is 450–650 mm (Prins and Loth, 1988). The rainfall pattern is bimodal with short rains occurring from November to December and long rains from February to May. Two types of open savanna are found in the Tarangire–Manyara ecosystem: microphyllous savanna on the riverine areas dominated by *Acacia tortilis* trees,

and broad-leaf deciduous savanna on the ridges and upper slopes dominated by *Combretum* and *Commiphora* species (Lamprey, 1963). Vegetation descriptions have been given by Lamprey (1963), Loth and Prins (1986), and Kahurananga (1979) for different parts of the Tarangire–Manyara ecosystem. Seasonal distribution of elephant and its determinants can be found in Pittiglio et al. (2012).

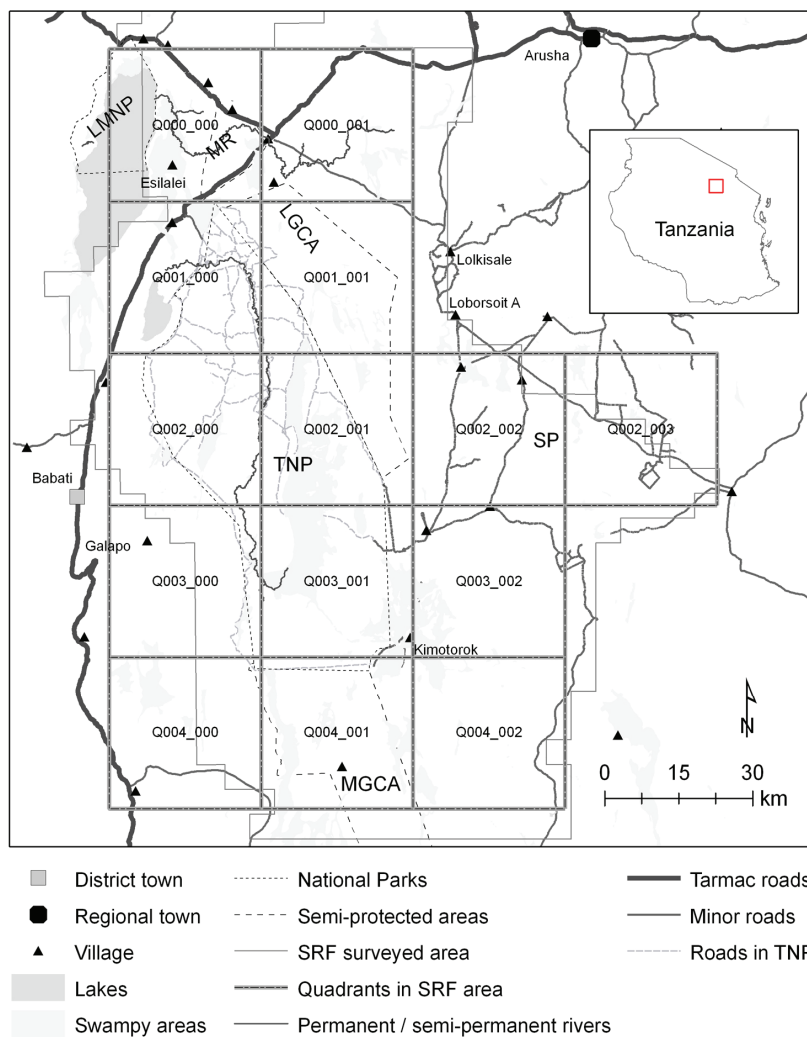


Fig. 4.2: Study area showing boundaries of Lake Manyara (LMNP) and Tarangire (TNP) National Parks; Lolkisale (LGCA) and Mkungunero (MGCA) Game Controlled Areas; Manyara Ranch (MR); Simanjiro Plains (SP) and quadrants (and their codes) within the Systematic Reconnaissance Flight (SRF) surveyed area. The box in the inset map shows the SRF area in Tanzania.

## 4.2.2 Locations and estimation of elephant occurrence

Elephant distribution was studied by point pattern analysis of the GPS locations (grid cell centroids) obtained by the Systematic Reconnaissance Flight method - SRF (Norton-Griffiths, 1978; TAWIRI, 2001) in May 1988 and May 2001, during the wet season. SRF data consisted of a 5 by 5 km grid (totally 587 cells), covering an area of 14,675 km<sup>2</sup>. For each grid cell the elephant density per km<sup>2</sup> is reported. The elephants were recorded in 458 grid cells in May 1988 and 507 grid cells in May 2001. Although the elephant is highly detectable in the open vegetation (Prins and Douglas-Hamilton, 1990), it is also vagile and inhabits heavily wooded as well as narrow riverine forest areas. Because these characteristics may affect the accuracy of distribution models based on point data (Ko et al., 2011; McPherson and Jetz, 2007) and because SRF data are seasonal population samples (Norton-Griffiths, 1978), we estimated the elephant distribution using a kernel density function, as described by Pittiglio et al. (2012). The standard bivariate normal kernel density function (Silverman, 1986) was used to estimate the probability of elephant occurrence in both years, weighted by the elephant density per location (Horne and Garton, 2006) and normalized between 0 and 1. Hence, locations with higher elephant density had a higher probability of elephant occurrence. A threshold of 95% of the probability volume contour (Kernohan et al., 2001) defined the area of occupancy by elephant. To avoid over- or under-smoothing the data (Illian et al., 2008), the smoothing parameter  $h$  was selected using the likelihood cross validation (CVh) method (Horne and Garton, 2006). In 2001 the total counts aerial survey (see Norton-Griffiths, 1978) and the SRF survey were both flown in May (the wet season), but a few days apart (TAWIRI, 2001). Because these surveys produced a different estimation of elephant occurrence in southern TME, the two datasets were integrated. In particular, the probability of the elephant occurrence generated separately for each survey were added together and normalized between 0 and 1. To calculate the elephant CVh per year, we used Animal Space Use 1.3. beta (Horne and Garton, 2009). The kernel analysis was performed using Hawth's analysis tools 3.27 (Beyer, 2004).

## 4.2.3 The wavelet transform analysis

The wavelet transform is a convolution of the wavelet function with the satellite image data. By moving the wavelet along the image, the transform quantifies the local match of the wavelet with the image at different locations and scales, thereby identifying coherent features related to a specific scale in the image (Addison, 2002; Dale and Mah, 1998). The Haar wavelet detects edges, boundary and abrupt discontinuity in the data such as, changes and gaps in the

canopy cover (Bradshaw and Spies, 1992). We used the Haar two-dimension Discrete Wavelet Transform (2D DWT) and multiresolution analysis to quantify the intensity and the dominant scale of NDVI-derived landscape heterogeneity from remotely sensed data (Murwira and Skidmore, 2006; Pittiglio et al., 2011). The DWT decomposes the image with orthogonal wavelets (the smooth and the detail function), which act like low- and high-pass filters at successive bases ( $2^j$ , with  $j = 0, 1, 2, \dots, J$ ) in the vertical (north to south), diagonal (north-east to south-west and south-east to north-west), and horizontal (east to west) direction. At each level of decomposition (which follows a sequence of the power of 2), the transform produces 4 outputs: the 'smooth' (which is a smooth reproduction of the original image), the 'vertical', the 'diagonal', and the 'horizontal' details (Bruce and Gao, 1996). The details express the deviances from the average value of the image at each direction and scale (Bruce and Gao, 1996). Each output contains a set of coefficients (Bruce and Gao, 1996): high absolute values represent a good match between the wavelet and the data (i.e., a change in vegetation cover); small or zero values a lack of match. Each coefficient is associated with a base level (scale  $j = 1, 2, \dots, J$ ), a direction and a particular location. By iteratively decomposing the image, the transform estimates the underlying smooth behaviour of the image data and its progressively finer-scale deviations (Bruce and Gao, 1996). Thus, given an image  $F(x, y)$  the wavelet approximation of the original image is the sum of the smooth and detail functions at different scales:

$$\hat{F}(x, y) = S_j(x, y) + \sum_{j=1}^J \sum_{\text{dir}} D_j^{\text{dir}}(x, y) \quad (4.1)$$

where  $S_j$  represents the smooth coefficients and  $D_j^{\text{dir}}$  the directional detail coefficients.

Each level of decomposition  $j$  (scale) corresponds to a pixel size and equals  $2^j s$  where  $s$  is the size of the original pixel size of the image. For details see Bruce and Gao (1996), Murwira and Skidmore (2006), and Pittiglio et al. (2011).

The wavelet energy was calculated as a second moment of the wavelet transform, defined as the sum of squares of the coefficients at base  $2^j$ , divided by the sum of squares of all the coefficients in the wavelet approximation  $\hat{F}(x, y)$  (Bruce and Gao, 1996):

$$E_j^d = \frac{1}{E} \sum_{k=1}^{n/(2^j)^2} d_{j(x,y)}^2, j = 1, 2, 3, \dots, J \quad (4.2)$$

where  $d_{j(x,y)}$  is the detail wavelet coefficient at level  $j$  and position  $(x, y)$ ,  $E$  is the total sum of squares of  $\hat{F}(x, y)$  (all the squared coefficients); and  $n/(2^j)^2$  is the number of coefficients at level  $j$ . Higher energy values reflect the presence of larger coefficients and therefore identify dominant patterns at a given scale (Bradshaw and Spies, 1992). The Stein's unbiased risk estimation (SURE) threshold was applied to the wavelet coefficients from the first to the fourth level of decomposition to remove white noise from the energy calculation (Donoho and Johnstone, 1995; Ogden, 1997). The wavelet energy was used to determine the intensity and dominant scale of landscape heterogeneity. The composite wavelet energy (i.e., the sum of the wavelet energy in the different directions at each level  $j$ ; Murwira and Skidmore, 2006; Pittiglio et al., 2011) was plotted against scale to obtain the wavelet energy curve. Then the maximum intensity and the dominant scale across all levels of decomposition ( $j$ ) were determined by selecting the highest wavelet energy value (i.e., maximum intensity) of the curve (Pittiglio et al., 2011). Only the composite wavelet energy function of the detail coefficients was used because detail functions are scale specific (Murwira and Skidmore, 2006).

To efficiently analyze the study area with the wavelet transform, the images were split into 20 quadrants of 30,720 m  $\times$  30,720 m (i.e., 1024  $\times$  1024 pixels in TM and ETM+, and 2048  $\times$  2048 pixels in ASTER), and each quadrant was decomposed from the finest to the coarsest scale along intervals of the power of 2. The intensity and dominant scale of each image were calculated for each quadrant and the results between years were compared within the common scale range of 60 m to 15,360 m, at intervals of the power of 2. The size of the quadrants was chosen according to the average home range extent of the elephant in this area (average linear dimension = 30 km; see Galanti et al., 2000). The quadrants represent the sampling units for the statistical analysis.

The wavelet transform was performed in IDL 6.4.1 (ITT Visual Information Solutions), using a revised version of the available Haar 2D DWT script, which is based on Mallat's algorithm (Mallat, 1989) and Press et al. (1992). The SURE thresholding was performed in R (R Development Core Team, 2010), using the Waveslim package (V.1.6.4; Whitcher, 2010).

#### 4.2.4 Satellite images

The amount of vegetation cover was estimated from the NDVI using the near-infrared and red bands of the satellite images (Walsh et al., 1997) acquired at the time of the elephant surveys. NDVI is a measure of the amount of canopy "greenness" (a composite property of leaf chlorophyll content, leaf area, canopy cover and structure; Glenn et al., 2008), and can be considered an indicator of the vegetation cover, specifically the green vegetation cover (Roderick et al., 1999). NDVI has been successfully used to explain the distribution of herbivores (Pettorelli et al., 2005) including the elephant (Murwira and Skidmore, 2005). We selected Landsat Thematic Mapper (TM, 30 m pixel size) and ETM+ (30 m) images based on 3 criteria: a) time-coincidence with the aerial surveys; b) cloud cover less than 20%; and c) availability from the GLOVIS website (<http://glovis.usgs.gov/>). Sixty-nine images acquired between 24 June 1984 and 31 May 2003 were inspected for our analysis. The ETM+ images acquired after May 2003 were affected by the Scan Line Corrector problem (SLC-off) and were not considered in this study. As most of the images acquired in the wet season were affected by high cloud cover (between 20% and 90%), only six images could be selected for our analysis: two adjacent TM images from 17 October 1988 (path/row: 168/62 and 168/63; 0% cloud cover), two ETM+ images from 21 February 2000 (path/row: 168/62 and 168/63; 0% cloud cover), one ETM+ image from 28 April 2001 (path/row: 168/63; 12% cloud cover), and one ETM+ image from 2 June 2002 (path/row: 168/63; 17% cloud cover). The images with the same date were first mosaicked using histogram matching (Richards and Jia, 2006), resized to an area of 18,874 km<sup>2</sup>, and then split into 20 squared quadrants for the wavelet analysis. Only quadrants included in the SRF survey area were considered for the analysis ( $n = 14$ ; total area = 13,212 km<sup>2</sup>; see Fig. 4.2). Drought significantly affects the green vegetation cover and consequently the dominant scale. The ETM+ 2000 image was characterized by a prolonged dry season (see TWCM, 2000). Hence only 8 quadrants of the ETM+ images (showing cultivation in 2000 or cloudless in 2001–2002) could be considered for the analysis (see Table 4.1). Because a recent study by Pittiglio et al. (2011) demonstrated that the dominant scale of spatial heterogeneity in semi-natural areas is not substantially affected by pixel size (e.g. ETM+ versus ASTER), we used the ASTER images for the remaining quadrants. Nine adjacent ASTER 1B level (EOS, 15 m) cloudless images from 27 January and 5 February 2006 were first mosaicked using histogram matching (Richards and Jia, 2006), then geometrically corrected using a first order polynomial transformation plus 14 GPS reference points collected on the ground (RMSE < 0.5 pixel size), resampled using the nearest neighbour resampling technique and split into 20 quadrants. The TM/ETM+ images were geometrically rectified and co-registered

(RMSE < 0.5 pixel size) with the mosaicked ASTER image prior to performing the wavelet analysis. The wavelet energy curves from the NDVI of the ASTER 2006 were compared with those obtained from the NDVI of the ETM+ 2000, 2001 and 2002 for each shared quadrant. The dominant scale was obtained from the ASTER images if these curves were similar, and from the ETM+ images otherwise. All images were geometrically corrected, re-projected to the Universal Transverse Mercator, UTM zone 37, Spheroid Clarke 1880, Datum Arc 1960 and re-sampled (with the nearest neighbour method) to  $15 \times 15 \text{ m}^2$  (for ASTER) or  $30 \times 30 \text{ m}^2$  (for TM and ETM+) before performing the wavelet transform. The images were not atmospherically corrected because the dominant scale, as quantified by the wavelet transform for images of different dates, is not significantly affected by different atmospheric conditions (Pittiglio et al., 2011).

To quantify farming expansion, a shapefile of crop farming in 1988 and 2000 (OIKOS, 2002) was updated for the study area by digitizing new farms from the satellite images acquired for the wavelet analysis. The amount of cultivation was calculated for each quadrant and related to the dominant scale of landscape heterogeneity for both 1988 and 2001.

#### **4.2.5 Relating the probability of elephant occurrence to landscape heterogeneity**

To test whether elephant distribution and landscape heterogeneity changed significantly between 1988 and 2000, we calculated the average probability of elephant occurrence, the dominant scale and the intensity of NDVI-derived landscape heterogeneity for each quadrant of  $30,720 \text{ m}$  by  $30,720 \text{ m}$  ( $n = 14$ ) and for each year. The variables were square root transformed to approximate a normal distribution prior to performing the statistical analysis. The difference between the average probability of elephant occurrence between 1988 and 2001 was tested using a *t* test for paired samples. This test was also applied to compare the average dominant scale of NDVI-derived landscape heterogeneity (hereafter named dominant scale of landscape heterogeneity) between the same period. The non-normality of the average intensities of NDVI-derived landscape heterogeneity (hereafter named intensity) could not be removed by any transformation. The nonparametric Wilcoxon signed-rank test was therefore applied to test for the difference in median intensity between 1988 and 2001. To quantify the spatial scale maximizing elephant occurrence, the probability of elephant occurrence was regressed for each quadrant against the dominant scale of landscape heterogeneity. A quadratic function was chosen, following the method by Murwira and Skidmore (2005). Only the quadrants within the

kernel contours (average normalized probability of elephant occurrence > 0.002) were analyzed ( $n = 9$ ). The predictors were centered (i.e., the average was subtracted from each value) to reduce collinearity (see Allison, 1999) in the quadratic regression (Quinn and Keough, 2002). To test whether the change in the dominant scale of landscape heterogeneity affected the elephant distribution, the difference in the probability of elephant occurrence was linearly regressed against the difference in dominant scale of landscape heterogeneity between 1988 and 2001. A linear regression was chosen because the elephant population was known to be relatively stable during the study period and a zero slope was expected. Statistical analysis was performed in SPSS 16.0.1.

### 4.3 Results

Fig. 4.3 shows the NDVI wavelet energy curves obtained from the TM 1988, ETM+ 2000, 2001 and 2002 and ASTER 2006 images. The comparison of these curves in 8 shared quadrants confirmed no major change in landscape heterogeneity due to farming expansion occurred between 2000 and 2006, apart from in one quadrant (Q001\_001; Fig. 4.3). Here the dominant scale of landscape heterogeneity decreased from 7680 m in 2001 to 480 m in 2006. Hence for this quadrant the dominant scale obtained from the ETM+ 2001 was used for further analysis, while for the other quadrants the dominant scales obtained from the ASTER 2006 images (which were not significantly different to the ETM+ images) were used (Table 4.1).

Table 4.1: Comparison between the dominant scale of NDVI-derived landscape heterogeneity from ETM+ 2000, 2001, 2002 and ASTER 2006 images for each quadrant and the assigned dominant scale for the analysis.

Quadrant	ETM+ 2000 dominant scale	ETM+ 2001 dominant scale	ETM+ 2002 dominant scale	ASTER 2006 dominant scale	Assigned dominant scale
000_000				7680	7680
000_001	15,360			15,360	15,360
001_000	7680			7680	7680
001_001		7680		480	7680
002_000	7680			7680	7680
002_001				7680	7680
002_002				15,360	15,360
002_003				7680	7680
003_000	15,360			15,360	15,360
003_001		7680		7680	7680
003_002		15,360	15,360	15,360	15,360
004_000	15,360			15,360	15,360
004_001				7680	7680
004_002				3840	3840

## Elephant response to landscape heterogeneity

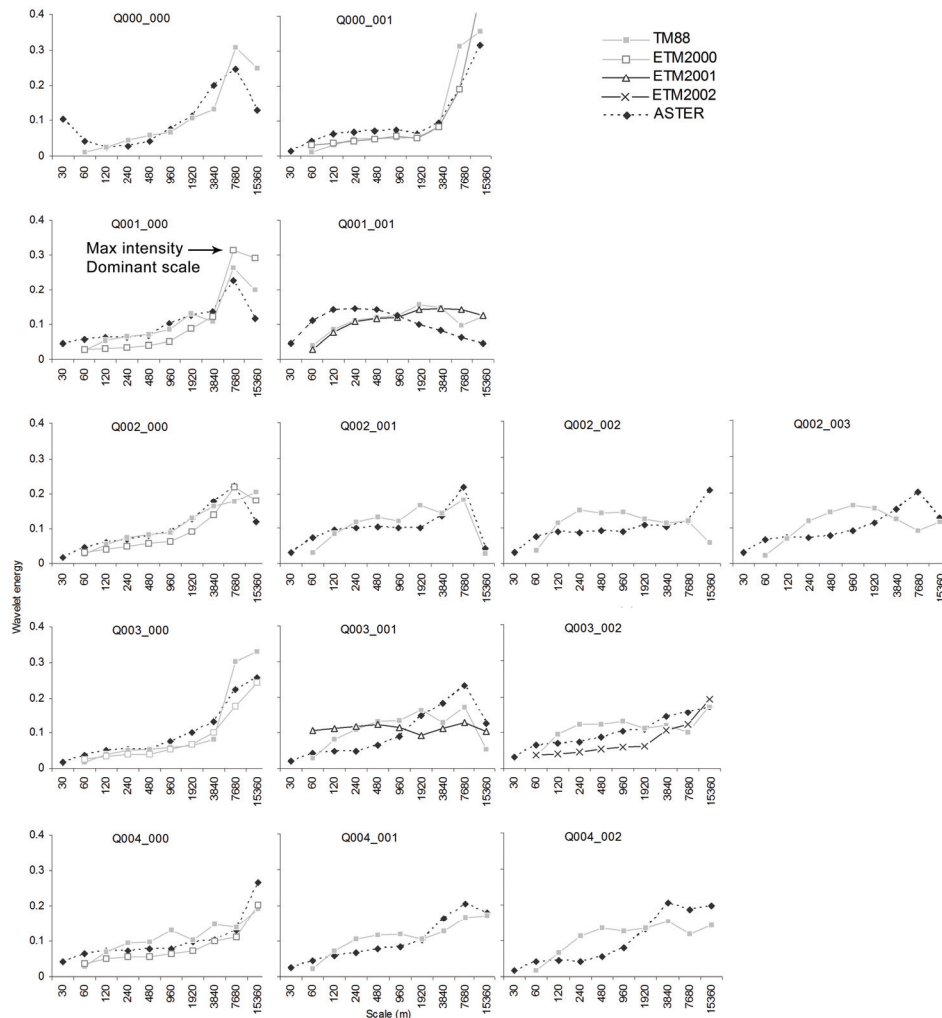


Fig. 4.3: Wavelet energy curves, dominant scale and maximum intensity from TM 1988, ETM+ 2000, 2001, 2002, and ASTER 2006 images for each quadrant.

The average dominant scale of landscape heterogeneity in 1988 (mean = 89.03; 95% CI = 67.03–111.03; back transformed mean = 7900 m) did not significantly differ from 2000 (mean = 98.76, 95% CI = 86.88–110.66; back transformed mean = 9700 m;  $t = -0.97$ ,  $p = 0.35$ ,  $df = 13$ ). The median intensity of landscape heterogeneity in 1988 (median = 0.18, range = 0.21,  $n = 14$ ) was not significantly different from 2000 (median = 0.22, range = 0.15,  $n = 14$ ;  $z = -1.1$ ,  $p = 0.27$ ,  $n = 14$ ). Minor changes in the dominant scale were observed in five quadrants (Fig. 4.3). In Q002\_000 and Q004\_001 the dominant scale

decreased from 15,360 m to 7680 m, while in Q001\_001, Q002\_002 and Q002\_003 the dominant scale increased from 1920 m to 7680 m (Fig. 4.3).

The smoothing parameters  $h$  were set at 7400 m for the SRF data and at 4708 m for the total counts. Visual inspection of the kernels confirmed that the CVh method did neither over-smooth nor under-smooth the data (Fig. 4.4(a) and (b)). The average probability of elephant occurrence in 1988 (mean = 0.15; 95% CI = 0.05–0.24) was not significantly different from the probability in 2001 (mean = 0.18; 95% CI = 0.08–0.29;  $t = -0.63$ ,  $p = 0.54$ ,  $df = 13$ ). The spatial distribution of the probability of elephant occurrence (as depicted by 95% of the probability volume contours) slightly changed from 1988 to 2001. Specifically, in 2001 the elephant distribution in northern Tarangire National Park expanded in and outside the protected area, towards the south and east (see Fig. 4.4(a) and (b)).

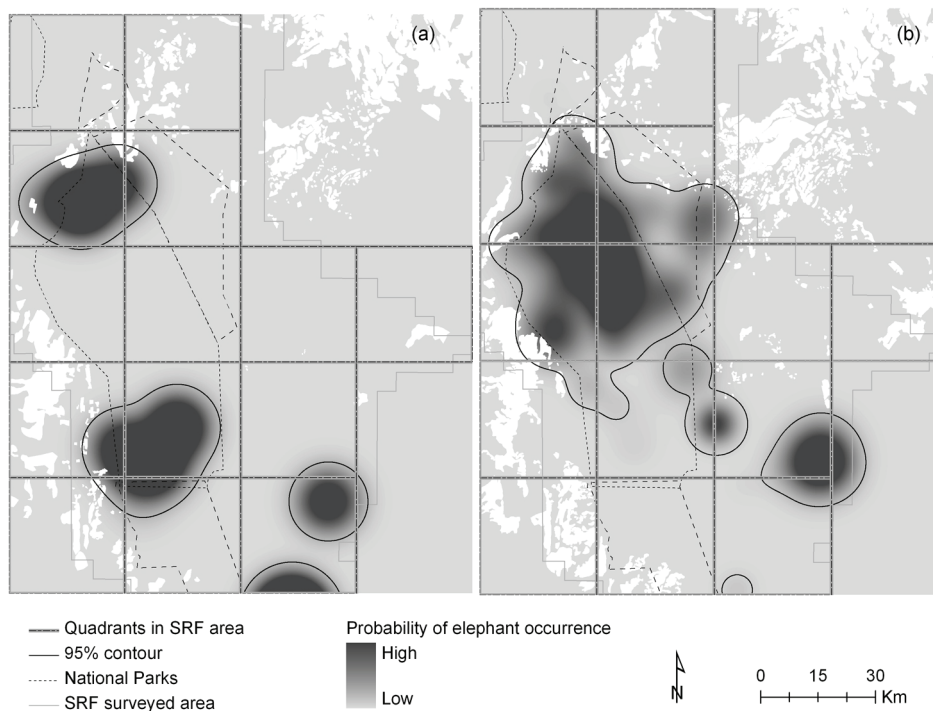


Fig. 4.4: The probability of elephant occurrence in 1988 (a) and 2001 (b) generated with the kernel density function. Crop fields are shown in white both in 1988 and 2000.

#### Elephant response to landscape heterogeneity

In 1988 the average probability of elephant occurrence was significantly related to the dominant scale of landscape heterogeneity (adjusted  $R^2 = 0.82$ ;  $p = 0.002$ ,  $n = 9$ ) by a quadratic function (Table 4.2). The highest probability of elephant occurrence was found at a dominant scale of 7000 m (this value is derived by back transforming the variable, see Fig. 4.5). In 2001 this relationship was marginally significant (adjusted  $R^2 = 0.44$ ;  $p = 0.07$ ,  $n = 9$ ) (Table 4.2) and the dominant scale occurred at 8300 m (Fig. 4.5). Lower probabilities of elephant occurrence were related to both larger and smaller dominant scales of landscape heterogeneity. The largest dominant scale captured blocks of cultivated fields (e.g., in Q003\_000 and Q004\_000) as well as substantial portions of herbaceous and wooded savanna on the eastern side of the study area (e.g., in Q003\_002). Small dominant scales represented patterns of highly heterogeneous land cover types such as the mosaic of open-trees and open-shrubs in flooded areas in Q002\_002 and closed-trees and shrubs in Q004\_002. No relation was found between the change in elephant occurrence and the change in dominant scale of landscape heterogeneity for the two periods ( $p > 0.05$ ).

The cultivated area was 750 km<sup>2</sup> in 1988 and 1140 km<sup>2</sup> in 2000. The increase in cultivation (between 50 and 150 km<sup>2</sup>) occurred in the western part of the study area (Q001\_000, Q002\_000, Q004\_000, Q004\_001; Fig. 4.4(a) and (b)). The largest amount of cultivation by quadrant of about 260 km<sup>2</sup> was recorded in Q004\_000 in 2000. We found a logarithmic relation between the dominant scale of landscape heterogeneity and the cultivated area for both years ( $p = 0.05$ , Table 4.3). No relation with heterogeneity was found for quadrants with a cultivated area of less than 25 km<sup>2</sup>. Fig. 4.6 shows that the dominant scale levels off for cultivated areas larger than 100–150 km<sup>2</sup>.

Table 4.2: Regression coefficients, standard errors (s.e.),  $t$  and  $p$  values of the quadratic relations between the probability of elephant occurrence and the dominant scale of landscape heterogeneity in 1988 and 2001.

	1988 ( $n = 9$ )				2001 ( $n = 9$ )			
	Coefficient	s.e.	$t$	$p$	Coefficient	s.e.	$t$	$p$
Dominant Scale	-0.002	0.001	-2.91	0.03	-0.003	0.002	-1.4	0.21
Dominant Scale <sup>2</sup>	-0.0002	0.000	-5.52	<0.001	-0.0003	0.000	-2.52	0.04
Constant	0.445	0.042	10.62	<0.001	0.375	0.056	6.66	<0.001

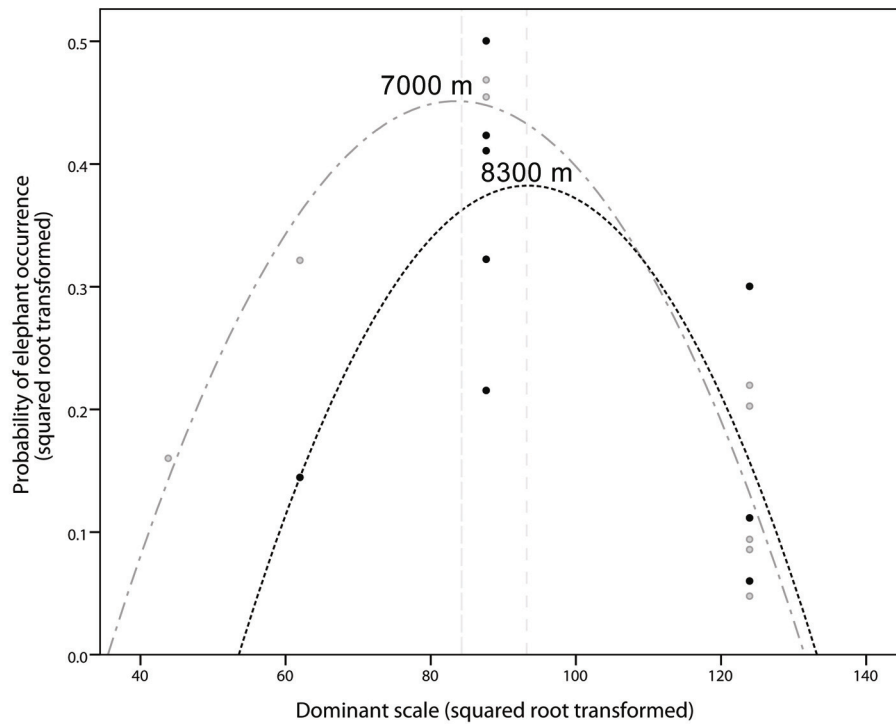


Fig. 4.5: The quadratic relation between the probability of elephant occurrence and the dominant scale of landscape heterogeneity in 1988 (gray dash-dot line) and 2001 (black dotted line). The dominant scales of 7000 m and 8300 m sustain the highest probability of elephant occurrence in 1988 and 2001 respectively.

Elephant response to landscape heterogeneity

Table 4.3: Regression coefficients, standard errors (s.e.),  $t$  and  $p$  values of the logarithmic relations between the dominant scale of landscape heterogeneity and cultivation in 1988 and 2000.

	1988 ( $n = 8$ )				2000 ( $n = 8$ )			
	Coefficient	s.e.	$t$	$p$	Coefficient	s.e.	$t$	$p$
Cultivation	6113	2488	2.5	0.05	4843	2064	2.3	0.05
Constant	-15,189	10,767	-1.4	0.2	-12,520	9898	-1.3	0.2

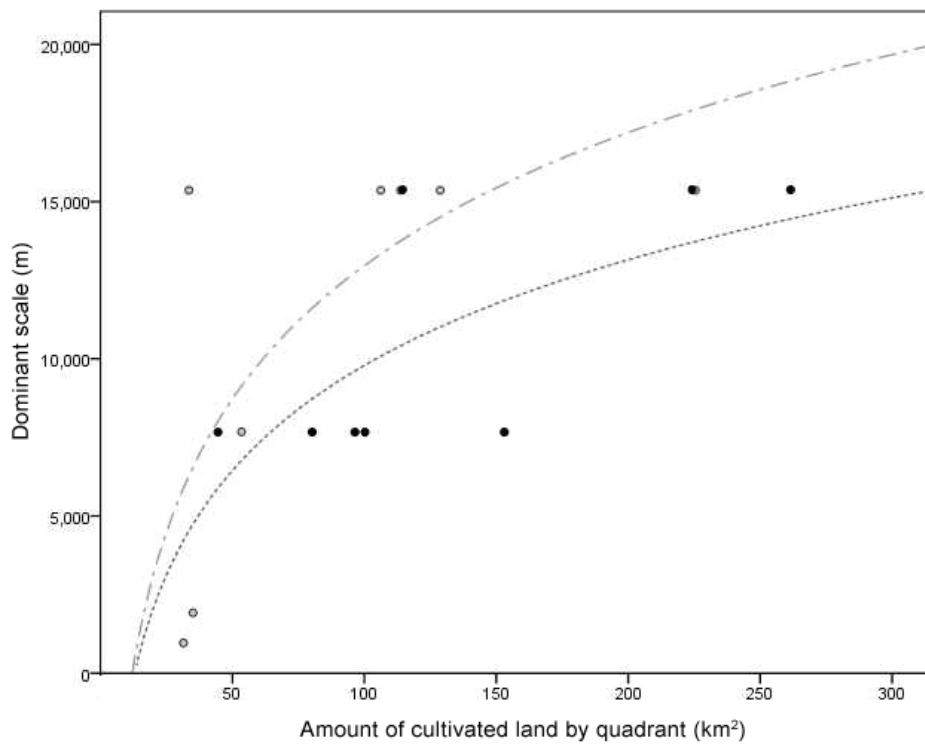


Fig. 4.6: The logarithmic relation between the dominant scale of landscape heterogeneity and the amount of cultivated land by quadrant in 1988 (gray dashed-dot line) and 2000 (black dotted line).

To further demonstrate that the dominant scale of landscape heterogeneity effectively represents dominant landscape features, the wavelet results obtained from the NDVI of ETM+ 2000 are shown for a single quadrant

(Q002\_000, see Fig. 4.2 for reference). This quadrant is characterized by extensive cultivation outside, and large patches of homogeneous vegetation inside the Tarangire National Park (see the land cover map in Fig. 4.7(a)). The wavelet energy curve showed one dominant scales of landscape heterogeneity at 7680 m (see Fig. 4.7(h)). The wavelet coefficients are shown at increasing scales of decomposition. It can be noted that at finer scales (i.e., 240 m) these coefficients identify boundaries between landscape features such as swampy areas (see the arrow in Fig. 4.7(c)), as well as the contrast between different crop fields (see the ETM+ 2000 image in the inset of Fig. 4.7(c) and (d)). At increasing scales of decomposition (hence at coarser resolutions) the method captures the inter-patch distance of dominant vegetation. For instance, at a scale of about 960 m, the patch size between open-shrubs and open-trees, as well as between agriculture and semi-natural vegetation become obvious (see the circles in Fig. 4.7(e)). The dominant scale of about 7680 m identifies the boundary between homogeneous semi-natural vegetation inside the park and the agricultural area outside the park. Moreover, it identifies the size of the forest (in the mountain) at the lowest left corner of the map (Fig. 4.7(f)). Fig. 4.7(g) shows that at a scale of 15,360 m the highest contrast in NDVI occurs between forest and agriculture at the lower left corner of the map.

#### 4.4 Discussion

This study did not find any substantial change in dominant scale and intensity of NDVI-derived landscape heterogeneity in the wet season between 1988 and 2000. On average, the dominant scale was large in both years, representing large patches of natural vegetation (e.g., in Q003\_002) as well as large blocks of farms (e.g., in Q003\_000). These findings support our first hypothesis as illustrated in Fig. 4.1(a) and (b). The results on the probability of elephant occurrence in the Tarangire–Manyara ecosystem in the wet season did not show any change between 1988 and 2001, confirming the results for elephant trends obtained by SRF in the wet season for the same period (TAWIRI, 2001).

Elephant response to landscape heterogeneity

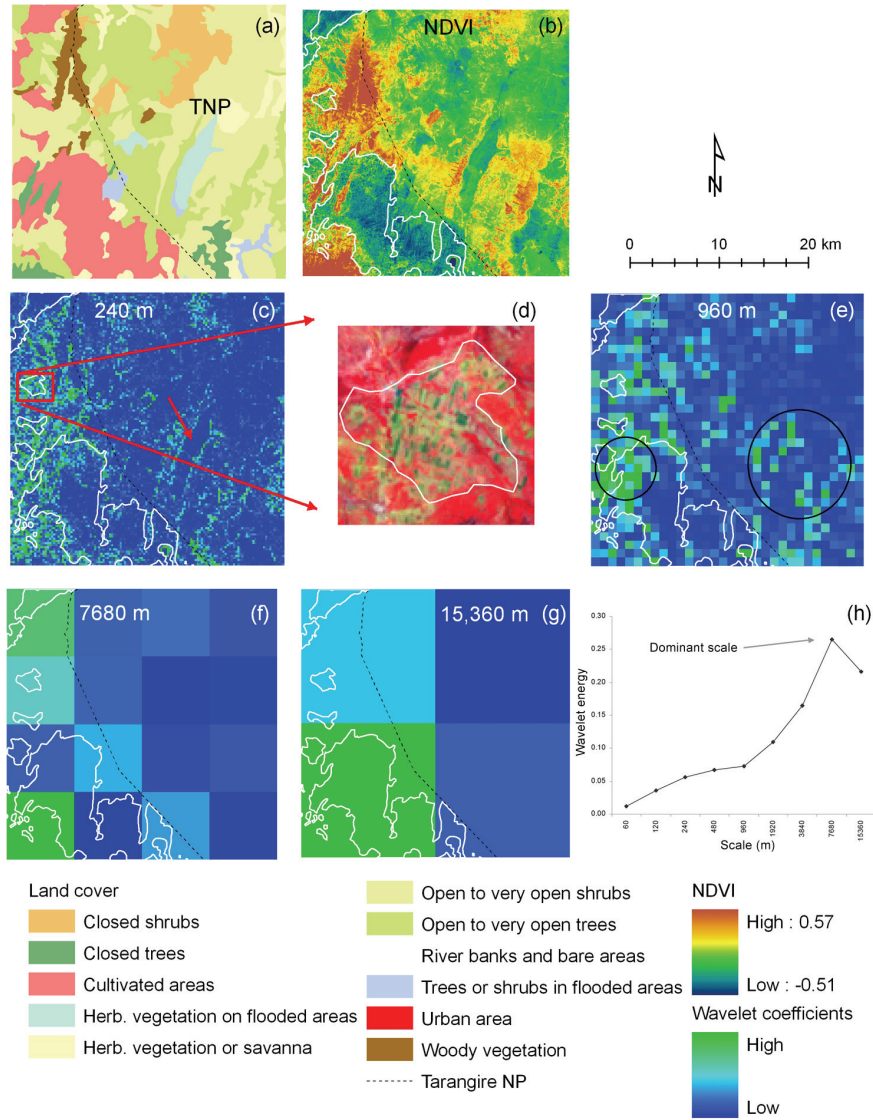


Fig. 4.7: Wavelet results for the quadrant Q002\_000: (a) Africover; (b) NDVI of ETM+ 2000; (c) wavelet coefficients at scale 240 m; the arrow shows a swampy area; the rectangular includes high wavelet coefficients, which capture the contrast between crop fields and natural vegetation (see inset (d); source: ETM+ 2000); (e) wavelet coefficients at scale 960 m; the circles show the contrast between swampy areas and open shrubs (on the right) and crop fields and closed trees (on the left); (f) wavelet coefficients at scale 7680 m (dominant scale); (g) wavelet coefficients at scale 15,360 m; (h) wavelet energy curve of Q002\_000 showing one dominant scale at 7680 m. The boundary of agricultural areas is shown in white (TNP, Tarangire National Park).

The dominant scale of landscape heterogeneity was significantly correlated with the probability of elephant occurrence, leading to the conclusion that elephants respond to an inter-patch distance of 7000–8000 m in the Tarangire–Manyara ecosystem during the wet season. These patches are about 10 times larger than those observed by Murwira and Skidmore (2005) in a heavily human impacted savanna landscape in Zimbabwe. In that study, the dominant scale maximizing elephant occurrence was about 750 m in early 1980s, and reduced to 450 m in early 1990s, due to agricultural expansion. The Zimbabwean study further showed that elephant numbers not only declined between the 1980s and the 1990s, but disappeared from the ecosystem if the dominant scale decreased to less than 400 m (Murwira and Skidmore, 2005). A highly fragmented landscape, with a threshold of 30–40% of land being converted to agriculture, was earlier identified in Zimbabwe as the tipping point for elephant persistence (Hoare and Toit, 1999). Our results suggest that the vegetation structure and cover of the Tarangire–Manyara ecosystem has not been modified by human activity (including agriculture) to the extent that it causes a decrease in the density of large body sized generalist herbivores, such as the elephant. Indeed, large vegetation patches and thus different forage options over large units may provide a wider selection for elephant (see Laca, 2008). These findings further support our hypothesis that in Tarangire–Manyara ecosystem the dominant scale of NDVI-derived landscape heterogeneity does not approach the critical threshold of elephant persistence (see point A in Fig. 4.1(b)).

The results of this study revealed that the spatial distribution of elephant has slightly changed in the Tarangire–Manyara ecosystem between 1988 and 2001 during the wet season. The ranging patterns of elephant was severely affected by illegal hunting, human disturbance and harassment (Osborn, 2004). In the 1980s a poachers' campsite was located in both the Lolkisale and the Mkungunero Game Controlled Area (H.H.T. Prins, personal observation), thus limiting elephant distribution to the Tarangire National Park. As the risk of poaching outside Tarangire National Park decreased after the international ban on ivory trade in 1989, elephants roamed over larger unprotected areas. As shown in Fig. 4.4(a) and (b), the elephant range expanded in semi-protected (Lolkisale Game Controlled Area) and unprotected areas at the north-eastern and south-eastern side of the study area. Because of the existence of large blocks of cultivated land in the western part of the study area (20–30% of the quadrants), the elephants may have utilized the less cultivated areas in the north-eastern and south-eastern part of the study area. Therefore, we believe that agriculture may have contributed to reshaping the spatial distribution of elephants in the Tarangire–Manyara ecosystem during the wet season, without

affecting the total population. This further corroborates the initial hypotheses illustrated in Fig. 4.1(b).

Farming covered 6% of the total study area in 1988 (about 750 km<sup>2</sup>) and 9% in 2000 (1140 km<sup>2</sup>), indicating that only a small portion of land was converted to agriculture (about 33 km<sup>2</sup> yr<sup>-1</sup> or a 5% annual increase). On the contrary, in the Zimbabwean study, cultivation increased from 8% of the total study area in 1984 (about 294 km<sup>2</sup>) to 44% in 1992 (1651 km<sup>2</sup>; Murwira et al., 2010), determining a significant change in the landscape structure (about 170 km<sup>2</sup> yr<sup>-1</sup> or a 58% annual increase). As shown in Fig. 4.6, the dominant scale of landscape heterogeneity was significantly related to the area of cultivation by quadrant for both years. The relationship was not significant if we included quadrants with arable land less than 25 km<sup>2</sup>. The results suggest that these patches did not substantially modify the landscape structure, as they are not clustered in large cultivated blocks. The quadrants with largest cultivated areas were located in the western and north-eastern part of our study area (see quadrants Q000\_001, Q002\_000, Q003\_000, Q004\_000 in Fig. 4.4(a)) and predate 1988 (OIKOS, 2002). We found that the dominant scale reaches an asymptote for areas of cultivation larger than 100-150 km<sup>2</sup> by quadrant. This is related to the size of the quadrants (about 30 km × 30 km), which determine the number of the wavelet decompositions and therefore the largest dominant scale of 15,360 m. In our study, the largest cultivated area by quadrant was about 260 km<sup>2</sup> (see Q004\_000 in 2000 in Fig. 4.4(b)), which relates to a linear dimension of about 16,000 m. Hence, the largest dominant scale of 15,360 m (and therefore the size of the quadrant) was effective in capturing the largest linear dimension of cultivated land (about 16,000 m) in our study area. In other words, our method was able to pick up large changes that may pose a risk to the elephant persistence.

A challenge for elephant persistence may be the expansion of agriculture on their migration routes (Bolger et al., 2008; Borner, 1985; Prins, 1987). The elephant routes from Tarangire National Park to the dispersal areas on the western side of the park were seriously threatened by agriculture in the 1980s (see Borner, 1985). Current migration routes for elephant connect Tarangire National Park to the northern, north-eastern, southern and south-eastern dispersal areas outside the park (Galanti et al., 2006; Pittiglio et al., 2012). According to our analysis, no substantial changes occurred in the dominant scale of landscape heterogeneity along these migration routes between 1988 and 2006, except for two quadrants. In quadrant Q001\_001 (including Lolkisale Game Controlled Area and Lolkisale village, see Fig. 4.2), the dominant scale increased from 1920 m in 1988 to 7680 m in 2001, but then decreased to 480 m

in 2006 (after the period of the SRF surveys). In quadrant Q004\_001 (including the Mkungunero Game Controlled Area) the dominant scale decreased from about 15,360 m in 1988 to 7680 m in 2006. In both quadrants agriculture has increased over the past 30 years (OIKOS, 2002); continued agricultural expansion may obstruct the migration routes of elephant towards the dispersal areas outside the park.

Our study reveals a few shortcomings of the intensity–dominant scale method proposed by Murwira and Skidmore (2005) that require further clarification. The size of the quadrant is an important parameter and should be chosen in relation to the environmental conditions, area of cultivation, and species home range. Therefore quadrants of 30 km × 30 km may not be large enough for agriculture-dominated savanna landscapes. The pixel size of the image determines the smallest applicable wavelet. In other words, the Haar 2D DWT cannot detect dominant patterns smaller than 30 m from the ETM+ images. Therefore we advise to use images of finer pixel size (e.g., 1 m IKONOS-2 or Orthophoto) to capture fine landscape features that might be relevant to the distribution of small body-sized and sedentary species (e.g., the impala). Furthermore, NDVI is known to saturate for high vegetation biomass values (Hobbs, 1995). This may prevent the wavelet transform from capturing the variation in areas with high vegetation biomass. In our study this problem was limited by deriving the NDVI from images acquired at the beginning of the short and long wet seasons (late October and early February), when the vegetation has not yet reached the maximum productivity and biomass. However, more robust vegetation indices, such as the Enhanced Vegetation Index (EVI), may be needed for quantifying landscape heterogeneity under different climatic and environmental conditions.

## Acknowledgments

This research was funded by the University of Twente, Faculty of Geo-Information Science and Earth Observation (ITC), the Netherlands, and the Global Environment Facility Project GCP/URT/124/WBG. The authors would like to thank the Food and Agriculture Organization of the United Nations (FAO), the Livestock, Environment and Development Initiative (LEAD), the African Wildlife Foundation (AWF), the Tanzania Wildlife Research Institute (TAWIRI), and the Instituto OIKOS for providing the data used in this analysis. Willem Nieuwenhuis is thanked for writing a revised version of the IDL script for the wavelet decomposition of large matrices.



# 5

## **Farms as stepping stones for crop raiding elephants in northern Tanzania**

This chapter is based on:

Pittiglio, C., Skidmore, A.K., van Gils, H.A.M.J., McCall, M.K., Prins, H.H.T.,  
Farms as stepping stones for crop raiding elephants in northern Tanzania.  
Under review.

## Abstract

Crop raiding is a major cause of human-elephant conflict. However, spatial patterns of crop raiding are poorly understood, making prediction and protection difficult. Anecdotal evidence suggests that elephants use corridors between daytime refuges and nighttime crop raiding. Corridors may follow footpaths for ease of movement, dry river beds for cover and safety, as well as the shortest distance to refuges. We hypothesized that crop raiding elephants follow stepping stone corridors along scattered unprotected, small farms, which represent 'snack points', and avoid protected large farms, which act as barriers. We used crop raiding and elephant location data, household surveys and expert knowledge to predict four alternative categories of daily corridors in northern Tanzania: 1) footpaths, 2) dry river beds, 3) stepping stone farms, and 4) trajectories of shortest distance to refuges. The corridor alignments were compared by their minimum cumulative resistance to elephant movement and the impact of crop raiding per village related to corridor resistance. The corridors along the stepping stone farms provided the best prediction of the crop raiding patterns. The resistance along these corridors was significantly higher, whereas the resistance along dry river beds was significantly lower, than the alternatives. These results suggest that the stepping stone farms modify elephant movement behavior away from dry river beds. Our study demonstrates that the spatial configuration of small farms between elephant refuges and farming blocks increase habitat connectivity for elephant with potential negative consequences for both farmers and elephants.

## 5.1 Introduction

The African elephant (*Loxodonta africana* Blumenbach), is a vulnerable keystone species of the savanna ecosystem (Hoare and Toit, 1999) as well as a crop raider (Dublin and Hoare, 2004; Nelson et al., 2003). Crop raiding is the most common form of human-elephant conflict (Hoare, 2000) and occurs mainly at night (Graham et al., 2009; Sitati et al., 2005) when food crops are ripe (Chiyo et al., 2005). Mostly small farms are affected (Dublin and Hoare, 2004; Graham et al., 2010b) due to insufficient protection (Sitati et al., 2005). Spatial patterns of elephant crop raiding have been associated with human population density (Hoare and Toit, 1999; Newmark et al., 1994), amount of cultivated land (Sitati et al., 2003), elevation (Smith and Kasiki, 2000), slope (Graham et al., 2010b; Wall et al., 2006), and proximities to settlements (Hoare, 1999b), roads (Sitati et al., 2003), water sources (Smith and Kasiki, 2000), protected areas (Hoare, 1999b) and daytime elephant refuges (Graham et al., 2010b; Naughton-Treves, 1998). Yet, the uneven distribution of crop raiding amongst farms

remains poorly understood (Sitati et al., 2005). The poor spatial predictions of crop raiding has been attributed to insufficient analysis of the sexual composition of raiding herds (Hoare, 1999b), palatability of cultivated crops (Chiyo et al., 2005), farm protection methods (Sitati et al., 2005), and farm size (Graham et al., 2010b; Sitati et al., 2005), as well as to the spatial resolution of the data and of the analysis (Graham et al., 2010b; Sitati et al., 2003).

Anecdotal evidence suggests that proximity to elephant corridors influence crop raiding patterns (Smith and Kasiki, 2000). Studies on elephant movement show that corridors may follow linear environmental features such as footpaths (Ngene et al., 2009a), dry river beds with dense riverine vegetation (Kikoti, 2009; Osborn and Parker, 2003a), and least relief resistance, such as flatter terrain and lower elevations (Ngene et al., 2009a; Smith and Kasiki, 2000; Wall et al., 2006). Resistance refers to the degree of impedance of a landscape to animal movements (Ricketts, 2001). However, we suggest here that elephants may also move along stepping stone corridors. Stepping stones are an array of small habitat patches offering shelter, food and/or rest during movement and dispersal (Bennett and Mulongoy, 2006). The effectiveness of these corridors depends on patch size and inter-patch distance, as well as the resistance of the landscape around these patches (Uezu et al., 2008). Birds (Fischer and Lindenmayer, 2002; Uezu et al., 2008), frogs (Vos, 1999), insects (Haddad, 2000) and mammals (Kramer-Schadt et al., 2011) have been found to successfully move and disperse along 'stepping-stone corridors'. Outside protected areas, and particularly within small-scale farming land, elephants move between refuges and feeding grounds at night and at high speed to avoid people (Galanti et al., 2006; Ngene et al., 2009a). Because elephants are attracted to ripe food crops (Chiyo et al., 2005), small farms that are surrounded by savanna are particularly vulnerable to crop raiding (Graham et al., 2010a). Therefore in this study, we hypothesized that the spatial distribution of scattered small farms surrounded by savanna enhances landscape connectivity for elephants, thus connecting elephant refuges with crop raiding zones. In other words, scattered small farms act as 'stepping stone corridors', increasing the vulnerability of farms along and at the termini of these corridors. Large farms on the other hand, which employ effective protection methods (Sillero-Zubiri and Switzer, 2001) and often cultivate less palatable cash crops such as coffee and tea, may hamper elephant movement by acting as barriers, and may thereby further amplify the vulnerability of neighboring small farms.

We propose a 'daily refuge-to-crop raid' corridor hypothesis to predict patterns of crop raiding by elephant. We tested this hypothesis in the Tarangire–Manyara ecosystem, northern Tanzania, using elephant movement data obtained from

totals counts and expert knowledge and crop raiding events. Total counts have been successfully used to predict elephant migration routes and dispersal areas (Pittiglio et al., 2012), and expert systems (Skidmore, 1989) have been shown to successfully predict wildlife distribution in the absence of direct field observations (Murray et al., 2009; Niamir et al., 2011). We used the UNiversal CORridor network simulator (UNICOR; Landguth et al., 2012) to predict four alternative categories of 'daily refuge-to-crop raid' corridors along: 1) footpaths, 2) dry river beds, 3) stepping stone farms, and 4) 'control corridors', with the control corridors being based on proximity to refuges and following trajectories of low relief. We believe that this is the first study demonstrating the corridor hypothesis with crop raiding, and in particular the effect of stepping stone farms on elephant movement behavior.

## 5.2 Methods

### 5.2.1 Study area selection

The Tarangire–Manyara ecosystem (TME) (between 3°36'S and 4°7'S, and 35°82'E and 36°74'E) is part of the Maasai Steppe (Prins, 1987) and hosts the largest population of elephant (*Loxodonta africana*) in northern Tanzania. The TME includes protected (Tarangire and Lake Manyara National Parks), semi-protected (Manyara Ranch, Lolkisale and Mkungunero Game Controlled Areas) and unprotected areas (Fig. 5.1). The area is a gently undulating plateau with an elevation between 1000 and 2000 m a.s.l. (Prins, 1988). The landscape is dotted with steep rocky outcrops and carved by temporary rivers with dense riverine vegetation. Steep rocky outcrops act as barriers to elephant movement (Edkins et al., 2008), whereas dry river beds with dense riverine vegetation provide cover and connectivity for elephants outside the protected areas (Kikoti, 2009). In TME, the elephants move seasonally from the National Parks to the dispersal areas outside the Parks in response to seasonal vegetation biomass and drinking water (Pittiglio et al., 2012). Elephant seasonal migration corridors are predicted in the TME (Galanti et al., 2006; Pittiglio et al., 2012), but 'daily refuge-to-crop raid' corridors are not.

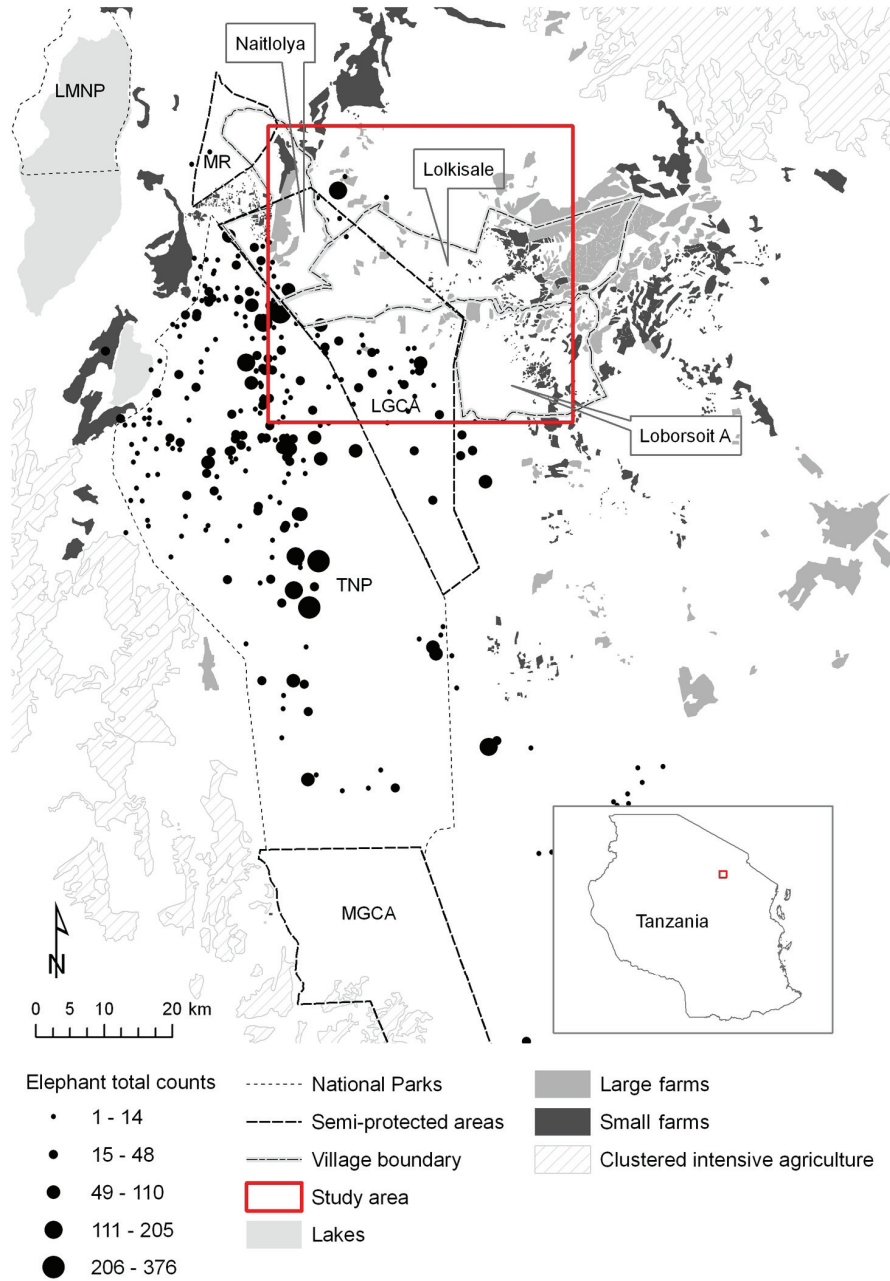


Fig. 5.1: Selected study area within the Tarangire–Manyara ecosystem in Tanzania. Elephant total counts, the boundaries of Tarangire (TNP) and Lake Manyara (LMNP) National Parks; Lolkisale (LGCA) and Mkungunero (MGCA) Game Controlled Areas; Manyara Ranch (MR), and the villages of Naitlolya, Lolkisale and Loborsoit A, are shown.

Recent household surveys revealed a low tolerance for elephants by villagers living in the dispersal areas due to crop raiding (Kaswamila, 2009; Pittiglio, 2009). Crop farming expanded in the TME over the past 30 years (OIKOS, 2002), whilst the elephant population remained stable over the same period, and even crashed during the 1990s (Prins et al., 1994; TAWIRI, 2001). The research area (1940 km<sup>2</sup>) was selected in the north-eastern TME, to include an important elephant dispersal area located inside the administrative boundary of three adjacent villages, namely Loborsoit A (Simanjiro District), Naitolya and Lolkisale (Monduli District) (Galanti et al., 2006). These villages have similar land use (i.e., small and large crop farms), cultivated crops (mostly maize and beans), and human population density (< 17 inhabitants km<sup>2</sup>) (Castel, 2009; National Bureau of Statistics Tanzania, 2006). Open savanna is the dominant vegetation type (Kahurananga, 1979).

### **5.2.2 Research approach**

A flowchart illustrates the research approach (Fig. 5.2). First, we tested whether the impact of crop raiding was different between years and villages as well as related to proximity to water and elephant refuges. The results of this statistical analysis were validated using household survey data. Second, we integrated a Bayesian expert system with a corridor network simulator to predict four alternative corridor categories between the daytime refuges and nighttime crop raided zones. The corridors were compared based on their resistance to elephant movement. Then, we tested whether the impact of crop raiding at a given destination point was related to the resistance of the corridors heading to that point for each corridor category. Lastly, the predicted pattern of crop raiding was compared with the pattern obtained from the statistical analysis.

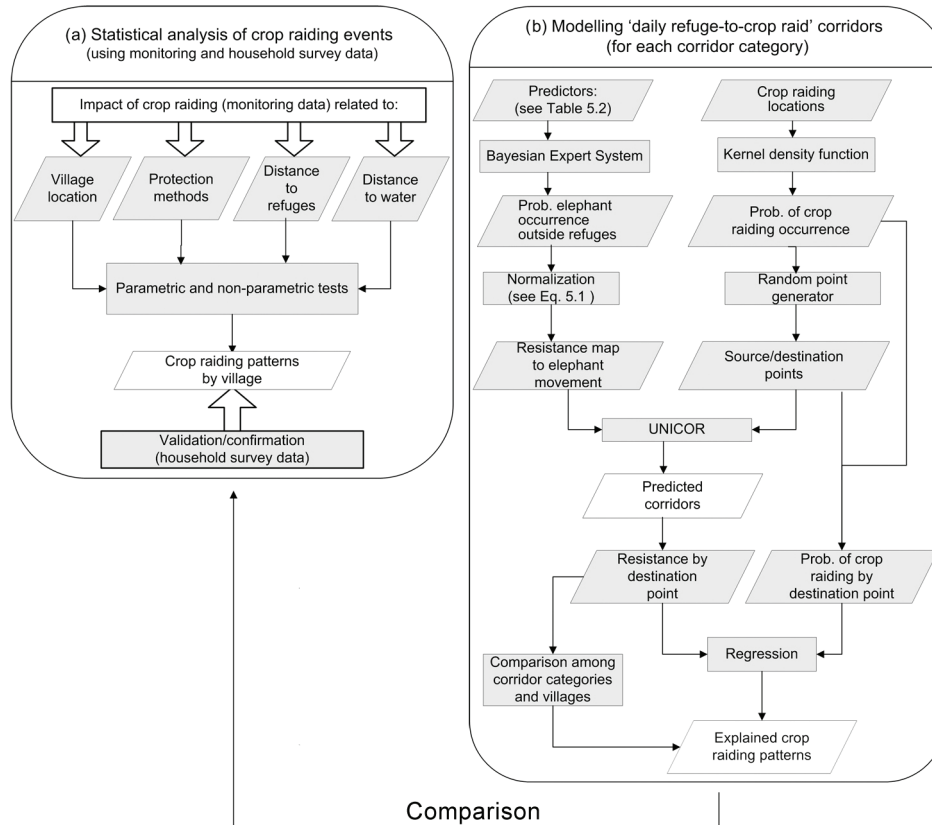


Fig. 5.2: Flowchart of the research approach: (a) statistical analysis of crop raiding patterns and their validation; (b) prediction of 'daily refuge-to-crop raid' corridors and their analysis in relation to crop raiding patterns.

### 5.2.3 Statistical analysis of crop raiding events

Wildlife crop raiding events were recorded by a local canvasser for each village using a standardized form (Hoare, 1999a), immediately before and during the crop ripening period (Chiyo et al., 2005; Sitati and Walpole, 2006) from May 2006 to September 2008. Farmers were encouraged to report the raiding events to the canvasser who then visited the farms for verification and quantification (Hoare, 1999a). The recorded information was: name of the farmer; date of raiding event; GPS location of the raid; type of damaged crop(s); farm size; extent of spatial damage; species responsible for crop damage; protection methods. The protection methods employed by the farmers were surveyed following the approach of Sitati et al. (2005) and Osborn and Parker (2002), and included: a) active deterrents - presence of a watchman, fires on the property

boundary, shouting, torches, tins and drums, smoke from burning hot chillies or from burning livestock or elephant dung; b) passive deterrents - home-made barriers/fences of vegetation, wire, rope; or c) a combination of the two (mixed methods). Because large farms (> 40 ha) were only occasionally damaged by elephants, the statistical analysis focused on crop raiding events for small farms (< 40 hectares) in 2006 and 2008. This farm class boundary was based on expert knowledge (Kibebe, 2005). The damaged area and the proportion of the damaged area per farm were calculated to reflect actual and relative loss (Sitati et al. 2005). The statistical analysis of crop raiding included: 1) a two-way ANOVA to test whether the average damaged area per farm and the average proportion of damage, as well as the average farm size, were related to the specific village locations (Naitolya, Lolkisale and Loborsoit A) for both years (2006 and 2008), and tested for their interaction. Because the data were not normally distributed, we applied a rank transformation (Conover and Iman, 1981). Subsequently, the ranks were analyzed with ANOVA (Conover and Iman, 1981). The Tamhane T2 post hoc multiple comparison test was used to test differences among the three villages; 2) a non-parametric Kruskal–Wallis test to analyze differences in median damaged area as well as the proportion of damaged area per farm between the types of protection methods (active, passive and mixed) at village level; 3) a one-way ANOVA to compare the average distance of raided farms to the boundary of elephant refuges (described below) and to water sources (dams) among the three villages. These distances were  $\log_{10}$ -transformed to approximate a normal distribution. We took into account the average elephant daily travel distance i.e., 5 km, as extrapolated by the average speed of 7 radio-collared elephants in TME (Galanti et al., 2006), as an explanatory factor of the pattern of crop raiding observed in the villages. In other words, villages with average distance of crop raided farms less than 5 km from refuges and water were excluded from further analysis.

The crop-raiding patterns were validated with the household survey data. Four canvassers conducted two socio-economic surveys in 2006 and 2008 for a total of 363 and 359 surveyed households respectively (Castel, 2009). The recorded information on crop raiding was: farm size and percentage of farm area damaged (5 classes: no damage; < 25%; 25-50%; 50-75%; > 75%), frequency and time of crop raiding, type of damaged crops, and wildlife species involved.

#### **5.2.4 Mapping small and large-scale farms**

A shapefile of crop farming in 2000 (OIKOS, 2002) was updated to 2006 by digitizing new farms and deleting abandoned farms using three adjacent ASTER

1B level (EOS, 15 m) cloudless images from 21 January and 5 February 2006 and 14 IKONOS-2 images (GeoEye, 1 m) acquired between 12 September and 28 November 2005. The ASTER images were mosaicked with the histogram matching option (Richards and Jia, 2006), then geometrically corrected using a first order polynomial transformation plus 14 GPS reference points (RMSE < 0.5 pixel size), resampled with a nearest neighbour resampling technique and clipped to the extent of the study area. The IKONOS-2 images were geometrically rectified and co-registered (RMSE < 0.5 pixel size) with the mosaicked ASTER image prior to update the crop farming shapefile. The farms were classified as small farms (< 40 ha), or large farms (> 40 ha) by using village land use maps (Castel, 2009) and by visual image interpretation.

### **5.2.5 Daytime refuges, nighttime crop raiding zones, and connecting corridors**

A standard bivariate normal kernel density function (Silverman, 1986) was used for estimating the daytime wet season elephant refuges, the nighttime crop raiding zones as well as vulnerability subzones within the crop raiding zones. The probabilities of elephant occurrence were estimated from 223 GPS locations of the total counts aerial surveys in the wet season (May 1996, March 1998, May 2001; see Pittiglio et al., 2012). The probabilities of crop raiding were estimated from 259 GPS locations of crop raiding events recorded in 2006, 2007 and 2008. The kernel smoothing parameter  $h$  was selected through the likelihood cross validation method (Horne and Garton, 2006) using Animal Space Use 1.3. beta (Horne and Garton, 2009). A threshold of 95% of the probability volume contour (Kernohan et al., 2001) defined the boundaries of the elephant refuges and of the crop raiding zones. 'High' and 'very high' vulnerable subzones were defined as the probabilities of crop raiding included by the 50% and 10% volume contours.

We generated two input data: 1) source/destination points, and 2) a 'resistance raster' for each corridor category. Each pixel in this resistance raster has a value representing the resistance to an elephant movement across the pixel in any direction (Landguth et al. 2012). We used the UNiversal CORridor network simulator (UNICOR; Landguth et al., 2012) to estimate daily corridors for elephants between the refuges and the crop raiding zones. UNICOR avoids the assumption of the Dijkstra's algorithm (Pinto and Keitt, 2009) that all individuals move along a single optimal path (Landguth et al., 2012). UNICOR estimates all least-resistance movement paths (i.e., optimal paths) between each combination of source/destination pairs of points, given a number of source and destination points, and a raster of 'landscape resistance' to animal movement.

Then, a kernel density function is applied on these paths to generate a corridor density map (Landguth et al., 2012): the higher the density, the higher the probability of animal movement along the predicted corridor.

The kernel probabilities of elephant occurrence and of crop raiding were used as weights to randomly generate 10 source points within refuges and 10 destination points in crop raiding zones. That is, points with higher probability of elephant occurrence (or of crop raiding) had a higher chance of being selected as starting (or ending) nodes of the corridors. Points were placed at least 5 km apart in the elephant refuges, and 3 km apart in the conflict zones, using Hawth's analysis tools 3.27 (Beyer, 2004). Because these two distances approximate the average elephant travel distance by day and by night (Galanti et al., 2006), source and destination points were considered to be spatially and temporally independent within the elephant refuges and crop raiding zones.

A Bayesian expert system (Murray et al., 2009; Niamir et al., 2011; Skidmore, 1989) was used to generate a map of resistance to elephant movement between refuges and crop raiding zones for each corridor category. Bayesian inference estimates the probability that a hypothesis (H) is true given evidence (E). A forward chaining expert system was used to infer the posterior probability that an elephant occurs at location ( $X_{ij}$ ) given a set of expert rules based on items of evidence ( $E_b$ ; for  $b = 1, \dots, k$  explanatory variables; i.e., GIS layers) known at location ( $X_{ij}$ ) for each of the four corridor categories. In setting up a hypothesis (H) that an elephant occurs at location ( $X_{ij}$ ), a rule was defined as: given a piece of evidence ( $E_b$ ), then infer (H), e.g., given the evidence that location ( $X_{ij}$ ) is 100 m away from the boundary of elephant refuges, then the conditional probability of the evidence given the hypothesis that elephant occurs at ( $X_{ij}$ ) is 0.9 (see Table 5.1). Predictors and conditional probabilities (i.e.,  $P(E|H)$ ) (see Table 5.1) were subjectively defined by combining knowledge acquired from researchers, villagers, literature, as well as field observations. Because data on elephant occurrence outside the refuges was unavailable, we initially assigned equal prior probabilities. Predictors are reported for each corridor category in Table 5.2. The 'control' corridor is based on predictors that are shared with the other corridors (Table 5.2). Rocky outcrops (Edkins et al., 2008) and large farms were considered to be barriers in all corridors and were classified as 'no data'. Three predictors were based on the direction of elephant movements from refuges to raiding zones. We assigned higher probabilities to angular directions close to 0 degrees and to 180 degrees (Fischer and Lindenmayer, 2002) (see Table 5.1). The predictors were tested for

multicollinearity. Predictors with a Variance Inflation Factor (VIF) larger than 2.5 were excluded from the analysis (Allison, 1999).

The probabilities of elephant occurrence generated by the expert system were normalized between 0 (low resistance) and 100 (high resistance), such that low probabilities reflect higher movement resistance (Chetkiewicz et al., 2006). Specifically, the movement resistance for an elephant to cross a pixel at location ( $X_{i,j}$ ) was:

$$Resistance_{(X_{i,j})} = \frac{(x_{max} - x_{i,j})}{(x_{max} - x_{min})} \times 100 \quad (5.1)$$

where  $x_{max}$  and  $x_{min}$  are the maximum and minimum predicted probabilities of elephant occurrence and  $x_{i,j}$  is the predicted probability at pixel ( $X_{i,j}$ ). The resistance raster map was imported into the UNICOR software and the corridors were predicted for each combination of source/destination pairs of points based on their minimum cumulative resistance to elephant movement. The (minimum) cumulative resistance for a corridor is the Euclidean distance weighted by the cumulative resistance of all cells traversed (Pinto and Keitt, 2009). The average cumulative resistance of the predicted corridors heading to the same destination point was calculated for each corridor category and  $\log_{10}$ -transformed to approximate a normal distribution. This measure, hereafter named 'cumulative resistance' reflects the resistance for an elephant to move from any source point in the refuges to any given destination point in the crop raiding zones following the predicted corridors. A one-way ANOVA was performed to test differences in average cumulative resistances among the four corridor categories, and a  $t$ -test to compare differences between the villages. Furthermore the cumulative resistance was linearly regressed against the probability of crop raiding at each destination point. Crop raiding probabilities were  $\log_{10}$ -transformed to approximate a normal distribution prior to regression analysis. We applied the Gaussian kernel density function on the predicted corridors to generate the corridor density maps (Landguth et al., 2012).

Farms as stepping stones for crop raiding elephants

Table 5.1: Predictor, evidence and conditional probability of elephant occurrence used in the Bayesian expert system.

Predictors	Evidence	P(E H)*
Distance to boundary of elephant refuges (m)	< 200	0.9
	200–5000	0.6
	5000–10,000	0.3
	10,000–15,000	0.2
	15,000–20,000	0.1
	20,000–30,000	0.001
Direction from refuges to conflict zones (degree)	< 1	0.9
	1–100	0.1
	100–160	0.9
	160–180	0.6
	180–200	0.9
	200–206	0.5
	206–208	0.8
	208–216	0.6
	216–256	0.9
	256–270	0.6
	270–290	0.9
	290–360	0.2
Inside/outside elephant refuges	Inside	0.8
	Outside	0.3
Distance to footpaths (m)	< 300	0.9
	300–500	0.7
	500–1000	0.5
	1000–2000	0.4
	2000–5000	0.2
	5000–12,000	0.0001
Distance to dry river beds (m)	< 50	0.9
	50–200	0.7
	200–500	0.5
	500–1000	0.3
	1000–2000	0.1

	2000–5000	0.00001
Distance to small farms (m)	< 500	0.99
	500–1000	0.8
	1000–2000	0.7
	2000–5000	0.6
	5000–10,000	0.5
	10,000–15,000	0.3
	> 50,000	0.00001
Direction from small farms to conflict zones (degree)	< 1	0.9
	1–29	0.4
	29–91	0.7
	91–199	0.4
	199–291	0.7
	291–326	0.6
	326–360	0.4
Distance to large scale farms (m)	< 500	0.0001
	500–1000	0.3
	1000–50,000	0.5
Direction from large farms to conflict zones (degree)	< 1	0.0001
	1–80	0.2
	80–100	0.0001
	100–259	0.5
	259–285	0.0001
	285–360	0.2
Slope (degree)	< 2	0.9
	2–3	0.6
	3–4	0.5
	4–6	0.3
	6–10	0.1
	10–34	0.05
Elevation (m)	< 1600	0.8
	1600–3000	0.1

\* Conditional probability, i.e. probability that there is evidence that an elephant occurs.

Table 5.2: Predictors used to generate the resistance maps to elephant movement for each corridor category.

Corridor category	N predictors	Description of predictors
Footpaths	6	Distance and direction from boundary of elephant refuges; inside/outside elephant refuges; slope, elevation and distance from footpaths
Dry river beds	6	Distance and direction from boundary of elephant refuges, inside/outside elephant refuges, slope, elevation and distance from the dry river beds
Stepping stone farms	9	Distance and direction from small farms, large farms, and boundary of elephant refuges; inside/outside elephant refuges, slope and elevation
Control	4	Distance and direction from boundary of elephant refuges, slope and elevation

The GIS layers were obtained from a Global Environment Facility project (Pittiglio et al., 2012), re-projected to the UTM zone 37, Spheroid Clarke 1880, Datum Arc 1960 and re-sampled (with the nearest neighbour method) to 30 × 30 m before performing spatial analysis. Spatial analysis was performed in ArcGIS 9.3 (ESRI) and statistical analysis in SPSS 16.0.1. The Bayesian expert system algorithm was programmed in ENVI 4.7 (ITT Visual Information Solutions).

UNICOR was downloaded from <http://cel.dbs.umt.edu/software/UNICOR/>

## 5.3 Results

### 5.3.1 Statistical analysis of crop raiding

A total of 406 crop raiding events were recorded. About 300 ha were damaged by wildlife, affecting 27% of the monitored farms, that is 3% of all small farms. The most frequently damaged crops were: maize (55%), lablab beans (22%), beans (9%) and green gram (7%). Crop raiding was mostly at night (92%), mainly caused by elephant (65%), warthog (37%), zebra (31%) wild pig (27%) and antelope (17%), though often by more than one species per night. Elephant crop raiding statistics are reported in Table 5.3. The damaged area per farm, as well as farm size, were significantly smaller in Loborsoit A than in Lolkisale and Naitolya, while the proportion of damage was significantly higher in Naitolya

than in Loborsoit A and Lolkisale (see Appendix B, Table B.1). No differences were found between 2006 and 2008. However, in Lolkisale the extent of the damage, as well as the proportion of the damaged area per farm, increased between 2006 and 2008 ( $p = 0.06$  and  $p < 0.001$ ), whereas they remained unchanged in Naitolya and Loborsoit A. The median damaged area per farm was not significantly different when comparing between protection methods ( $p > 0.05$ ).

Table 5.3: Number of elephant crop raiding events ( $n$ ), size (ha), damage (ha), damage per farm (%), and total amount of damaged land (ha) by village per year. Standard deviations are in square brackets [ ]. Village name abbreviation: Lolk., Lolkisale; Lob. A, Loborsoit A; Nait., Naitolya.

Village name	2006					2008				
	$n$	Farm size	Damage	%	Total damage	$n$	Farm size	Damage	%	Total damage
Lolk.	62	5 [7.3]	0.5 [0.5]	10 [10]	31	79	3 [3]	1 [1]	20 [10]	84
Lob. A	11	1.5 [2.3]	0.3 [0.3]	20 [10]	4	14	1.3 [0.8]	0.4 [0.8]	10 [10]	6
Nait.	22	4 [6.3]	2 [6]	20 [10]	53	21	3 [2]	1 [1]	20 [10]	23
Total	95				88	114				113

The results of the household survey are shown in Table 5.4. Agriculture was the main land use in Lolkisale and Naitolya in both years. In Loborsoit A, half of the respondents were mixed crop-livestock farmers, though the number of farmers decreased by 25% by 2008. Crop raiding mostly occurred at night (for 85% of the farmers), mainly caused by elephant (75%), warthog (29%) and zebra (19%). The highest percentage of farmers reporting crop raiding by elephant was found in Naitolya and the lowest in Loborsoit A during both years (Table 5.4). In Lolkisale the number of raided farms more than doubled between 2006 and 2008. Average farm size per village (Table 5.4) and damage extent (Appendix C, Fig. C.1) were similar to those obtained from the monitoring data (Table 5.3).

Table 5.4: Households (HHs) surveyed in 2006 and 2008, HHs practicing agriculture, HHs reporting damage by elephants, and their average farm size (ha) in 2006 and 2008. Village name abbreviation as in Table 5.3.

Village name	Pop 2002	<i>n</i> HHs	HHs 2006	HHs 2008	HHs farm 2006	HHs farm 2008	Raided HHs 2006	Raided HHs 2008	Farm size 2006*	Farm size 2008*
Lolk.	7599	844	149	140	134	125	45 (34%)	102 (82%)	4 [3] (45)	4 [3] (98)
Lob. A	5443	825	143	135	80	35	24 (30%)	7 (20%)	1 [1] (24)	3 [2] (7)
Nait.	1295	429	71	70	69	64	51 (93%)	61 (95%)	2 [1] (51)	2 [1] (60)
Missing				14		2		1		
Total			363	359	283	226	120	171	120	165

\*standard deviation in square brackets [ ] and number of farms in round brackets ( ).

### 5.3.2 Daily refuges, nighttime crop raiding zones and connecting corridors

The kernel smoothing parameter  $h$  for the refuges was 4000 m, and for the crop raiding zones 594 m. The distribution of crop raiding events did not overlap with the elephant occurrence predicted by the total counts (Fig. 5.3(a)). The vulnerability to crop raiding was low in Loborsoit A and high in Naitolya and Lolkisale (Fig. 5.3(b)).

Fig. 5.4(a) and (b) shows a boxplot of the distances from raided farms to elephant refuges and dams. The average distance to refuges was significantly shorter in Naitolya than in Loborsoit A and Lolkisale, whereas the longest distance was in Lolkisale ( $F(2, 256) = 432.5, p < 0.001$ ; post hoc test,  $p < 0.05$  for all pairs). The average distance to dams was significantly shorter in Loborsoit A than in Lolkisale and Naitolya; and the longest distance was in Naitolya ( $F(2, 256) = 22.4, p < 0.001$ ; post hoc test,  $p < 0.05$  for all pairs). Because in Naitolya both distances were less than 5 km, this village was excluded from the corridor analysis.

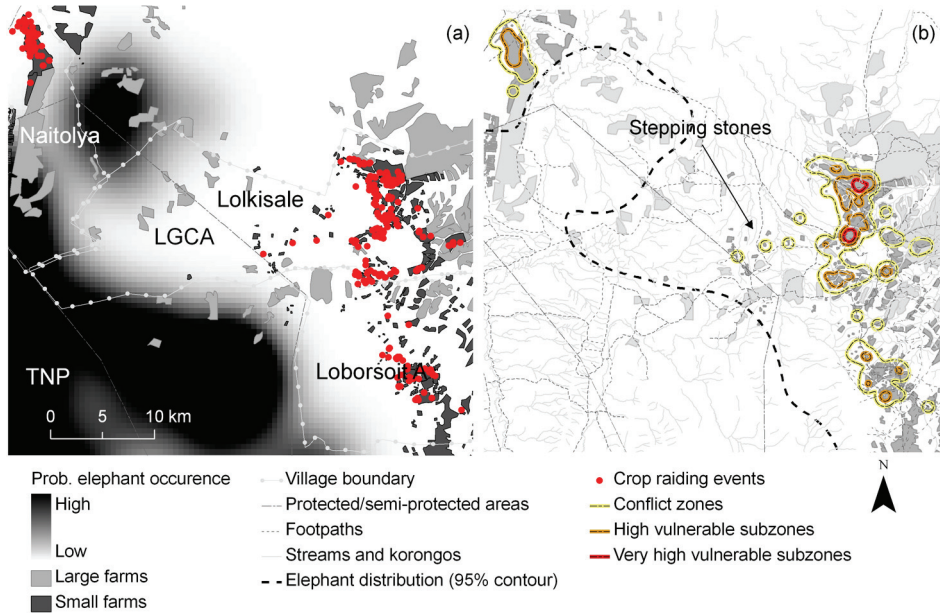


Fig. 5.3: (a) Crop raiding events by elephants and probability of elephant occurrence from total counts; (b) Elephant refuges (95% contour), crop raiding zones (95% contour) including high and very high vulnerable subzones (50% and 10% contours respectively), footpaths, and dry river beds. The arrow indicates the stepping stone farms (TNP, Tarangire National Park; LGCA, Lolkisale Game Controlled Area).

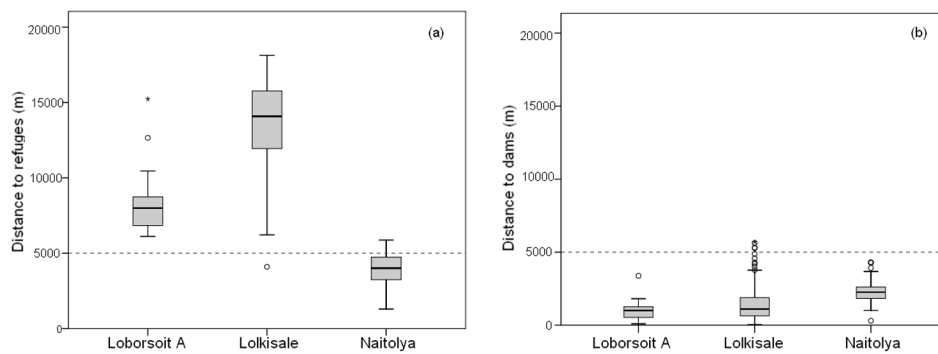


Fig. 5.4: Boxplot of the distance of raided farms to (a) elephant refuges and (b) dams. The dotted line represents the average elephant travel distance in TME.

The Variance Inflation Factor (VIF) was lower than 1.2 for each environmental predictor. Fig. 5.5(a)–(e) shows the corridor density maps of each corridor category in Lolkisale and Loborsoit A. Elephant refuges were directly connected with the crop raiding zones of Lolkisale through two high density footpath corridors, two high density dry river bed corridors, two high density stepping stone farm corridors and one high density control corridor. In contrast, in Loborsoit A the crop raiding zones were only indirectly connected with the refuges, except for one high density control corridor and one low density dry river bed corridor (Fig. 5.5(a)–(e)). The average size of the stepping stone farms was 8 ha (sd = 7.5,  $n = 36$ ) and the average distance to the next closest stepping stone farm (as calculated using polygon's centroid) was 1000 m (sd = 1420,  $n = 36$ ).

The average cumulative resistance was significantly different among the corridor categories ( $F(3,36) = 79.9$ ,  $P < 0.001$ ). The resistance was significantly higher for the stepping stone farm corridors, and lower for the dry river bed corridors than for the other corridors (post hoc test,  $P < 0.001$ ) (Fig. 5.6). No difference was found between the resistance for the footpath and for the control corridors (Fig. 5.6). The cumulative resistance was significantly and negatively related to the probability of crop raiding at each destination point for the stepping stone corridors ( $b = -3.8$ ,  $t(8) = -2.3$ ,  $p = 0.05$ ;  $R^2_{adj} = 0.32$ ,  $F(1, 8) = 5.3$ ,  $p = 0.05$ ), but was not significant for the footpath, dry river bed and control corridors ( $p > 0.05$ ). The average cumulative resistance was significantly higher in Loborsoit A than in Lolkisale for both the stepping stone ( $t(8) = -3.9$ ,  $p < 0.001$ ) and the dry river bed corridors ( $t(8) = -2.3$ ,  $p = 0.05$ ). No significant difference was found between the two villages for the footpath and control corridors ( $p > 0.05$ ).

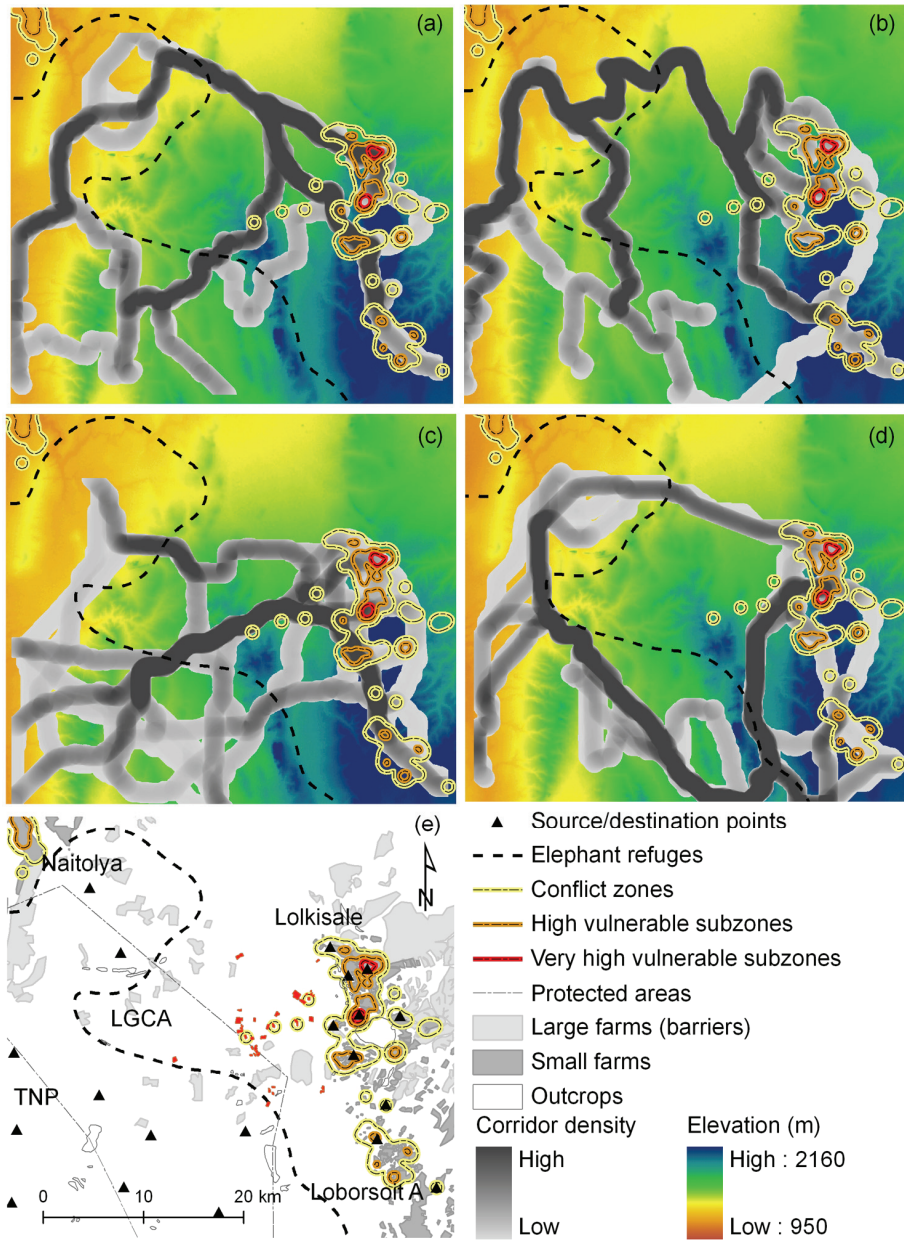


Fig. 5.5: Predicted elephant corridors along: (a) footpaths, (b) dry river beds, (c) stepping stone farms, (d) control. Fig. 5(e) shows the boundary of elephant refuges, crop raiding zones, vulnerability subzones, source/destination points, outcrops, and farms potentially acting as stepping stones (in red) or barriers (light gray). TNP, Tarangire National Park; LGCA, Lolkisale Game Controlled Area.

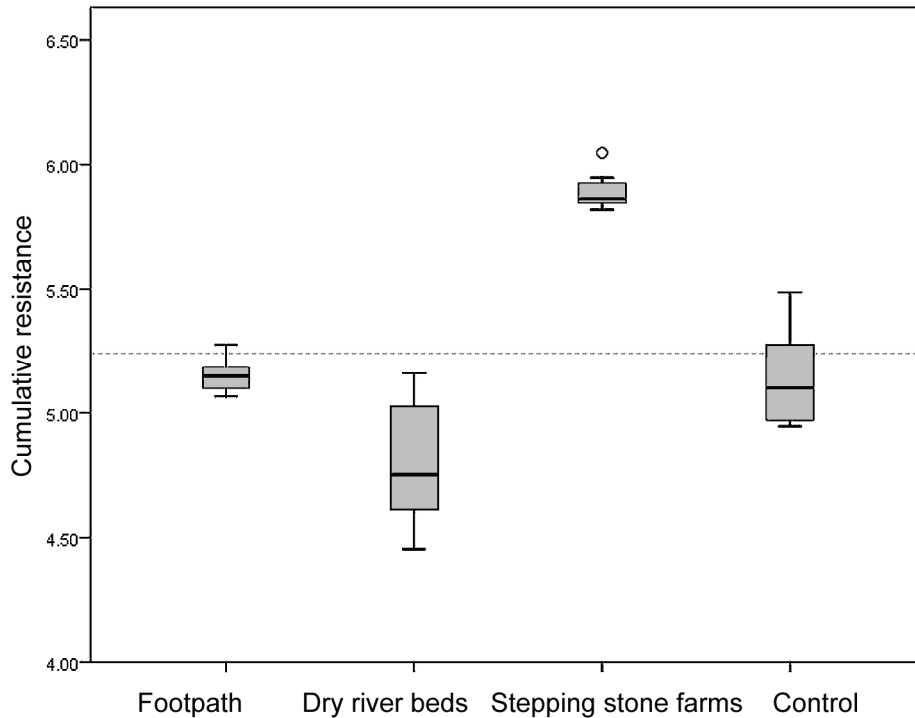


Fig. 5.6: Boxplot of the cumulative resistance for each corridor category. The dotted line represents the average cumulative resistance among all corridors.

## 5.4 Discussion

An important finding of the study is the concordance in patterns of crop raiding that were independently obtained from annual crop raiding monitoring and the household survey. This suggests that the data recorded by the monitoring was consistent and representative for the study area. The impact of crop raiding in the three villages does not appear to be consistently related to distance to the elephant refuges or to water sources, which is a different finding from other studies (Graham et al., 2010b; Naughton-Treves, 1998). Naitolya is close to the elephant refuges, relatively far away from water sources and heavily raided, whereas Loborsoit A is close to the refuges and water sources, but lightly raided; meanwhile in contrast, Lolkisale is further away from the refuges and water sources and is heavily raided. Contrary to the findings by Sitati et al. (2005), the protection methods of the farms do not appear to influence the levels of crop raiding in our study area.

The results support our 'daily refuge-to-crop raid' corridors hypothesis for crop raiding elephants. We found that scattered small farms surrounded by savanna enhance the landscape connectivity for elephants, increasing the accessibility of crop farms to elephants, and thus their vulnerability to raids. Stepping stone farms provide alternative desirable daily corridors for elephants across areas with high resistance. Since our study found that the dry river bed corridors have the lowest resistance for elephants, then these could be expected to be their corridors of choice, in line with the findings of Kikoti (2009). However, our analysis shows a pattern of crop raiding consistent with elephant corridors following the stepping stone farms. These results imply crop raiding elephants travel along corridors of highest resistance. We suggest that the high resistance of the stepping stone corridors, which is mostly due to their steeper slopes, is compensated by 'easy snacks'. In other words, scattered small farms of about 8 ha at less than 1000 m from each other form effective stepping stone corridors for crop raiding elephants.

A novelty of this study is the integration of a Bayesian expert system with a corridor network simulator to predict elephant crop raiding. The Bayesian expert system successfully predicts elephant occurrence in farming areas where daytime total counts fail to detect nocturnal crop raiding. The absence of spatial overlap between the refuges and the crop raiding zones is an interesting result. Although the total counts and crop raiding monitoring were not time coincident, it is reasonable to assume that elephant distribution remained stable during the study period, because the elephant population size did not change significantly over the last decade (Pittiglio et al., 2012; Stoner et al., 2007; TAWIRI, 2001). Outside protected areas, elephants are active mostly at night (Galanti et al., 2006; Ngene et al., 2009a), including for crop raiding (Graham et al., 2010b). Hence our results imply that daytime animal observations, such as total counts, are neither sufficient to predict crop raiding nor the corridors used at night. Nighttime elephant data can be obtained from radio- and satellite-collared elephants (Galanti et al., 2006; Graham et al., 2009). However, because in such studies only a few opportunistically selected animals are tracked, the data may not comprehensively represent the elephant distribution (Hebblewhite and Haydon, 2010), particularly in relation to crop raiding behavior. The Bayesian expert system successfully modeled the elephant activity during the entire 24 h period, by providing resistance raster maps for the corridor network simulator.

The 'direction' combined with the distance are important predictors of elephant movements, particularly for the stepping stone corridors. Similar findings are reported for birds (Fischer and Lindenmayer 2002). Therefore least-resistance path models based on distance (Chetkiewicz et al., 2006; Pinto and Keitt, 2009),

may become more accurate by including 'direction'. An additional complexity is that our study models one-way movements, not the reverse direction. That is, it does not take into consideration whether the nocturnal crop raiders use the same corridor in the morning when returning to their refuges and presumably have less motivation for 'snacking'.

The footpath corridors did not explain the spatial pattern of crop raiding in the study area. Contrary to the finding of Ngene et al. (2009a), elephants may not move along footpaths in TME due to the absence of regular ranger patrols outside the protected areas (Pittiglio et al., 2012). Finally, the control corridors were poor predictors of crop raiding due to their steepness (see Fig. 5.5(d)). Climbing is costly in terms of energetic consumption for heavyweight animals such the elephant and is therefore avoided (Wall et al., 2006).

While disruption of connectivity by habitat fragmentation is well established (Hanski, 1998; Newmark, 2008), our study demonstrates that fragmentation caused by small farms can enhance connectivity for elephants, providing alternative corridors and thereby increasing crop raiding in the villages further away from the elephant refuges. Our findings have conservation and management implications that may concern other crop raiding species. The spatial distribution and size of small farms between elephant refuges and farming blocks should be considered in land use planning. Small farms may act as stepping stones, large farms as barriers, and both influence the selection of corridors with potential negative consequences for farmers and elephants.

## **Acknowledgments**

This research was funded by the University of Twente, Faculty of Geo-Information Science and Earth Observation (ITC), the Netherlands, and the Global Environment Facility Project GCP/URT/124/WBG. The authors would like to thank the Food and Agriculture Organization of the United Nations (FAO), the Livestock, Environment and Development Initiative (LEAD), the African Wildlife Foundation (AWF) and the canvassers for their support to the crop raiding data collection. We also thank the GEF project for providing the GIS layers used in this analysis.

# 6

## **Landscape heterogeneity, fragmentation and human- wildlife conflicts: a synthesis**

## Synthesis

Landscape heterogeneity, namely how a landscape property varies across space and time (Li and Reynolds, 1995), influence biodiversity (Baldi, 2008; Cromsigt et al., 2009; Pianka, 1966), including herbivores distribution (Fryxell et al., 2005; Murwira and Skidmore, 2005) and abundance (Oliver et al., 2010; Wang et al., 2006). Fragmentation due to farming expansion modifies the level of heterogeneity, by reducing the size of natural vegetation patches and increasing the level of isolation between them (Fischer and Lindenmayer, 2007). In fragmenting landscapes, wildlife numbers and diversity decline, while simultaneously human-wildlife conflicts increases as a result of a longer interface between farms and wild lands. Yet, the critical level of heterogeneity for species response is not well understood (Fazey et al., 2005). Further, the way fragmentation intensifies human-wildlife conflicts has not yet been explicitly analyzed. The way spatial and temporal heterogeneity of vegetation cover in a savanna ecosystem influence elephant occurrence as well as elephant crop raiding patterns is determined by many factors and formed the main objective of this thesis. In this study the amount of vegetation cover was estimated from NDVI using remotely sensed data (Murwira and Skidmore, 2005). However, landscape heterogeneity and fragmentation as quantified from remote sensing imagery are scale-dependent phenomena i.e., what is heterogeneous or fragmented at a given scale (namely extent and resolution), may not be at another (Wiens, 2000). Animal perception of and response to spatial heterogeneity are also scale-dependent (Wiens, 2000), and differs among species in relation to their body size (Ritchie and Olff, 1999). Consequently, the study of a species-environment relationship require analysis at multiple spatial scales (Li and Wu, 2004) as well as accurate species distribution models (Guisan et al., 2006) that reflect species response to resource availability and stressors (Johnson et al., 1992). As such, in this synthesis I *first* discuss the robustness of the intensity–dominant scale method in quantifying landscape heterogeneity as in farming as well as semi-natural areas, including savanna. Some shortcoming of the method when dealing with a large dataset (and extent) is also highlighted. *Second*, I discuss the elephant’s response to savanna heterogeneity as modified by farming in relation to the theoretical framework proposed in chapter 4. The results obtained in the Tarangire–Manyara ecosystem are compared with those obtained by Murwira and Skidmore (2005) in a savanna landscape, in Zimbabwe. Further, the level of heterogeneity and fragmentation relevant to the elephant is studied. Thresholds for elephant persistence and decline in savanna ecosystems are proposed. *Third*, I discuss the applicability of the kernel density plus logistic regression approach based on total counts and SRF to predict seasonal elephant distribution as well as seasonal corridors. The effectiveness of these corridors in the Tarangire–Manyara ecosystem is discussed in the context of the scientific debate about

the role of corridors in providing connectivity to mitigate the effect of habitat fragmentation (Beier and Noss, 1998; Boitani et al., 2007; Haddad et al., 2003; Simberloff et al., 1992). *Fourth*, the role of elephant 'daily refuge-to-crop raid' corridors on raiding patterns and in particular, the effect of farm size and inter-farm distance on elephant movement behaviour is explained. The results presented in chapter 5 are further discussed in relation to the change in dominant scale observed between 2000 and 2006 (see chapter 4), which reflects an increasingly level of fragmentation and human-elephant interface. *Fifth*, a graphical overview of the main results obtained in this thesis is provided to highlight the link between farming, fragmentation, and crop raiding patterns in the Tarangire–Manyara ecosystem. *Sixth*, conservation and management implications and future research objectives are discussed.

## **6.1 The wavelet transform and the intensity–dominant scale method**

Tropical savannas are experiencing land use change rates higher than tropical forest (Lehmann, 2010). By 2050, an area of about  $10^9$  ha –as large as the United States of America– is expected to be converted to farmland (Tilman et al., 2001), mostly in Latin America and Sub-Saharan Africa (Sala et al., 2000). This conversion will affect species distribution, numbers and diversity as a result of increasingly fragmented landscapes (Sala et al., 2000). Yet, global fragmentation trends are unavailable, though more information is probably forthcoming (Butchart et al., 2010). The absence of information on fragmentation trends may reflect a lack of use of repeatable, accurate and reliable methods for quantification of heterogeneity and fragmentation. This makes spatiotemporal comparisons difficult (Bogaert, 2003; Tews et al., 2004). Fragmentation is mostly quantified using the patch mosaic approach (McGarigal et al., 2009). This approach relies on the identification of habitat patches and their matrix, based on a land cover classification (Gustafson, 1998). However, as shown in chapter 2 (Fig. 2.7(a) and (b)), patches and matrix may be hard to delineate in highly heterogeneous environments (McGarigal and Cushman, 2005; Pearson, 2002). In particular, a savanna often appears as a surface of continuous variation rather than a patchwork of contrasting cover classes (Pearson, 2002). Consequently, savanna shows the lowest mapping accuracies in the global cover datasets (Jung et al., 2006). The results presented in chapters 2 and 4 demonstrate that the intensity–dominant scale method based on the wavelet transform is accurate, repeatable, reliable, and general. Therefore this method forms a useful tool for monitoring vegetation heterogeneity at multiple spatial scales. Important properties of the method have been described in previous studies (Bradshaw and Spies, 1992; Murwira,

## Synthesis

2003; Strand et al., 2006; Torrence and Compo, 1998). Specifically, the wavelet transform does not require stationarity of the input data, and it is therefore suitable to analyze environmental data, which is aperiodic and non-uniform in patterns. It acts as a local filter and its dimension does not need to be defined a priori. The wavelet family can be chosen according to the form of the data and the objective of the study. Further, the method is parsimonious as only two metrics (the intensity and dominant scale) are needed to quantify spatial and temporal heterogeneity (Murwira and Skidmore, 2010). The results in chapter 2 and 4 also reveal characteristics that make this method successful. In particular:

1) The dominant scale matches real dominant landscape features that can be localized in the map both in agricultural and semi-natural landscapes (see Fig. 6.1). This implies that the method is applicable, general, and accurate in patchy as well as in gradient landscapes. Previous studies demonstrated the applicability of the method in mosaic landscapes, including an agriculture-dominated savanna.

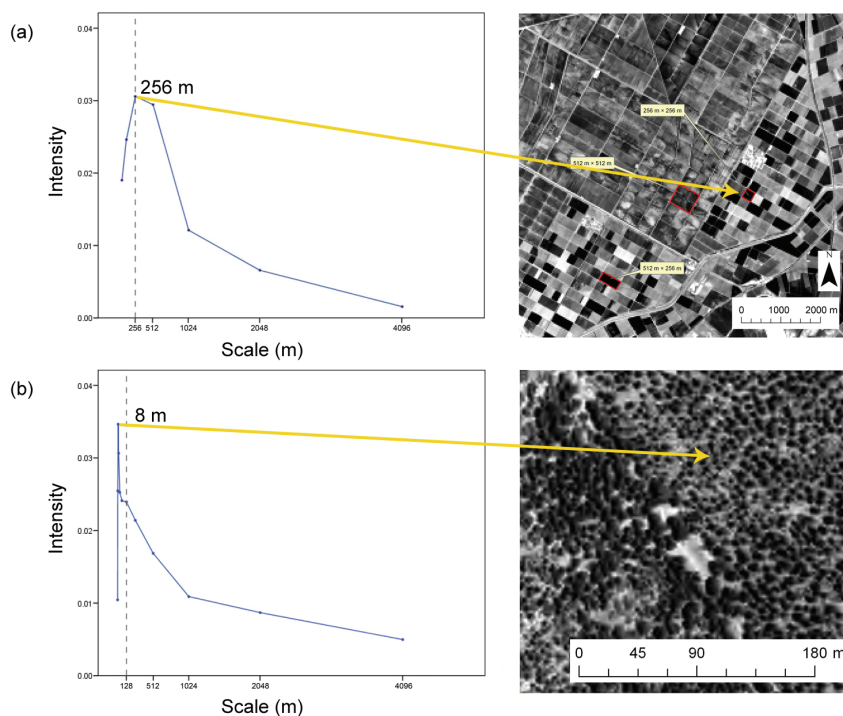


Fig. 6.1: The dominant scale of spatial heterogeneity in Andalucía, Spain, as measured by the intensity–dominant scale method based on the wavelet transform using Orthophoto (1 m resolution). The arrows indicate the match between the dominant scale and the landscape features both in agricultural (a) and semi-natural areas (b).

2) Dominant landscape features (equal or larger than the coarser image resolution) analyzed with the wavelet transform are resolution-independent from the original pixel size of the image both in patchy and gradient landscapes. In other words, the method is resolution- and sensor-robust irrespective of using Orthophoto (1 m), ASTER (15 m) or ETM+ (30 m) images. In contrast, other methods based on continuous environmental variation, such as variograms, may generate different dominant scales depending on the image characteristics (Tarnavsky et al., 2008). However, dominant landscape features smaller than the original image resolution cannot be detected by the wavelet transform (Strand et al., 2006). For example, the tree pattern captured by the Orthophoto in Andalucía, at the 8 m dominant scale, could not be captured by the ASTER and ETM+ images. A fine-grained pattern might be relevant for a small body-sized and sedentary animal, but not for a large body-sized and highly vagile animal (Laca et al., 2010; Prins and van Langevelde, 2008). Therefore high resolution images (e.g., Orthophoto, Quickbird) may be crucial to analyze the landscape heterogeneity relevant to a duiker, but not for elephant. Here I propose a theoretical framework of the relationship between the dominant landscape scale and the level of vegetation heterogeneity perceived by different body-sized species across spatial resolutions ( $s_1 < s_2 < s_3$ ) (Fig. 6.2).

3) Phenology and different atmospheric conditions influence the intensity of landscape heterogeneity but do not affect the dominant scale; hence no atmospheric correction is needed using this method (see chapter 2). Agricultural areas are characterized by regular patterns of crop fields. Crop type might vary within the fields, but plot size and boundaries hardly change between seasons. This can explain why the dominant scale of agricultural areas in Spain was constantly quantified at about 512 m, irrespective of the date of the images. However, this is a striking result for semi-natural areas, where the dominant scale of 54 images only varied between 64 and 128 m. As major land use changes (e.g., deforestation, fire, cultivation) could be excluded from the sampling units (i.e., quadrants) in the semi-natural areas during the study period, this result implies that phenology does not substantially affect the dominant scale of vegetation structure in European semi-natural environments. However, phenology may drastically change in semi-arid environments, particularly under very dry climatic conditions, such as during a drought. For this reason, in this thesis the spatial heterogeneity of the Tarangire–Manyara ecosystem and its change over time was quantified using images acquired during the wet season. Nevertheless, as shown in Box 6.1 and Fig. 6.3(a) and (b), no atmospheric correction is needed for quantifying the dominant scale using images acquired during the same season, even in savanna environments.

Synthesis

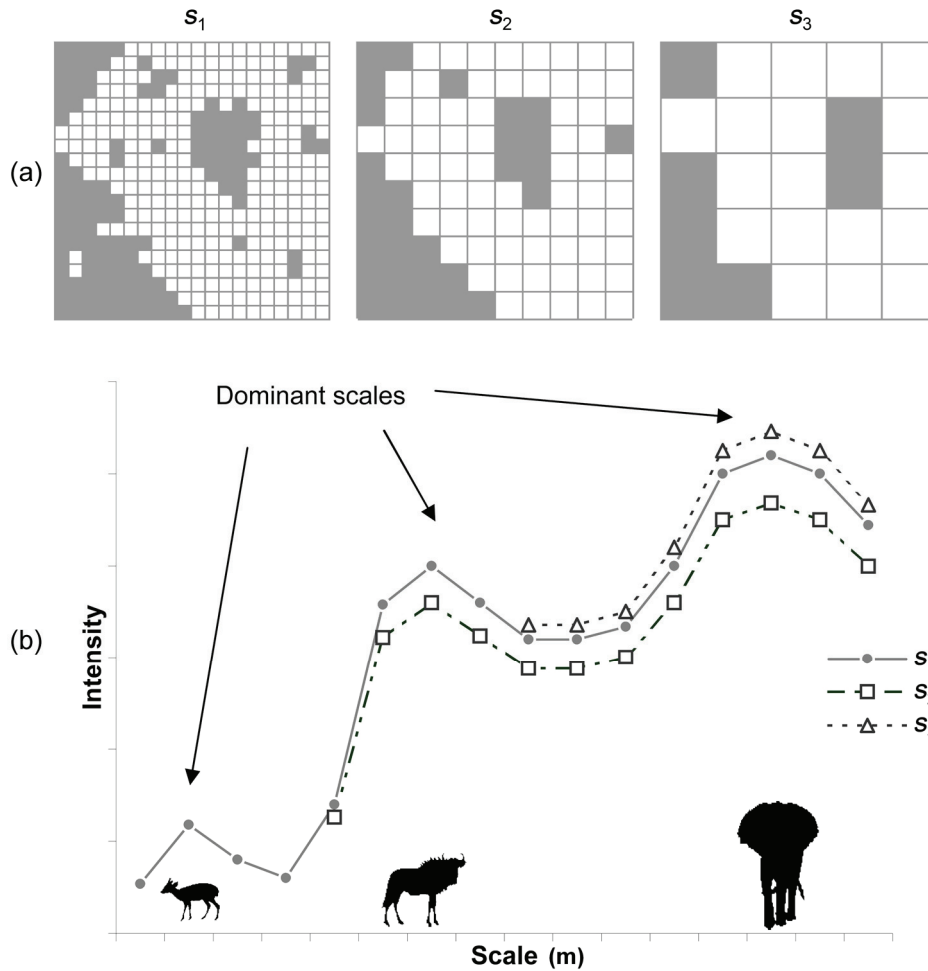


Fig. 6.2: The spatial resolution independence of the dominant landscape scale from the original pixel size of the satellite images and the 'perception scale' of heterogeneity by different body-sized animals. (a) Spatial patterns of features in images of different pixel size ( $s_1, s_2, s_3$ ); (b) wavelet energy curves of images with  $s_1, s_2, s_3$  pixel size and expected 'perception scale' by duiker, wildebeest and elephant.

4) As shown in chapter 2 and 4, the method is repeatable and the use of wavelet energy curves makes comparison across sites and studies easy (see Fig. 4.3 in chapter 4).

**Box 6.1**

To show the robustness of the intensity–dominant scale method against possible radiometric differences between images of different date, the dominant scale of NDVI-derived landscape heterogeneity of a TM image acquired on 17 February 1993 is compared with the dominant scale of an ETM+ acquired on 21 February 2000. The results are shown for three quadrants: Q001\_000, Q002\_000 and Q003\_000 in the TME (see Fig. 4.2 and Fig. 4.3 for reference). First, we applied a relative atmospheric correction on band 3 and 4 of the TM image using a regression method. The ETM+ image was used as reference (Song et al., 2001). Deep-water bodies and airstrips were used as pseudo variant objects for the regression analysis (Fig. 6.3(a)). Second, we calculated the NDVI for both the original and atmospherically corrected images and thus the dominant scale. As shown in Fig. 6.3(b) there is no difference in shape of NDVI-corrected and NDVI-original wavelet energy curves between the TM 1993 images. The same dominant scale emerges.

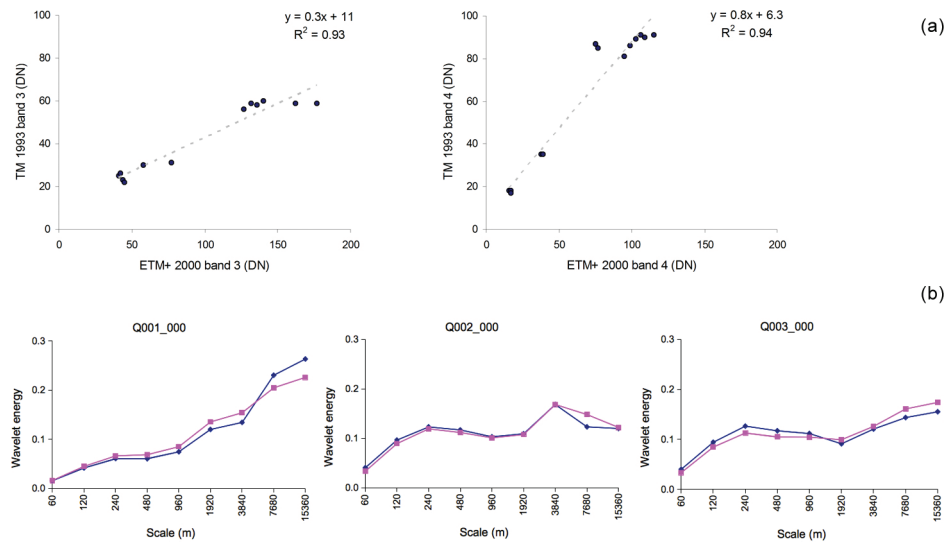


Fig. 6.3: (a) Relative atmospheric correction of band 3 and 4 of a TM image acquired on 17 February 1993 using a regression analysis and a reference ETM+ image acquired on 21 February 2000. (b) Wavelet energy curves of NDVI-original (pink line) and atmospherically corrected (blue line) spatial heterogeneity of TM in three quadrants.

## Synthesis

5) The results on the dominant scale of semi-natural savanna, confirm the theoretical framework presented in chapter 4 (see Fig. 6.4). The dominant scale reflects the change in spatial heterogeneity of vegetation cover due to farming expansion, and increases with increasing farming. At the beginning of the conversion process (Fig. 6.4,  $t_1$ ), the dominant scale is relatively large, representing large dominant patches of relatively homogeneous vegetation. Small scattered arable fields do not substantially modify the landscape structure (and therefore the dominant scale), as they are not clustered in large cultivated blocks. As farming expands in semi-natural savanna ecosystems, the natural vegetation patches become increasingly fragmented and smaller; consequently, the dominant scale is reduced (Fig. 6.4,  $t_2$ ). Eventually, the landscape becomes characterized by large blocks of farms and small patches of savanna vegetation and the dominant scale is large (Fig. 6.4,  $t_3$ ). In  $t_4$ , the dominant scale is greatest because the landscape is almost totally converted to agriculture.

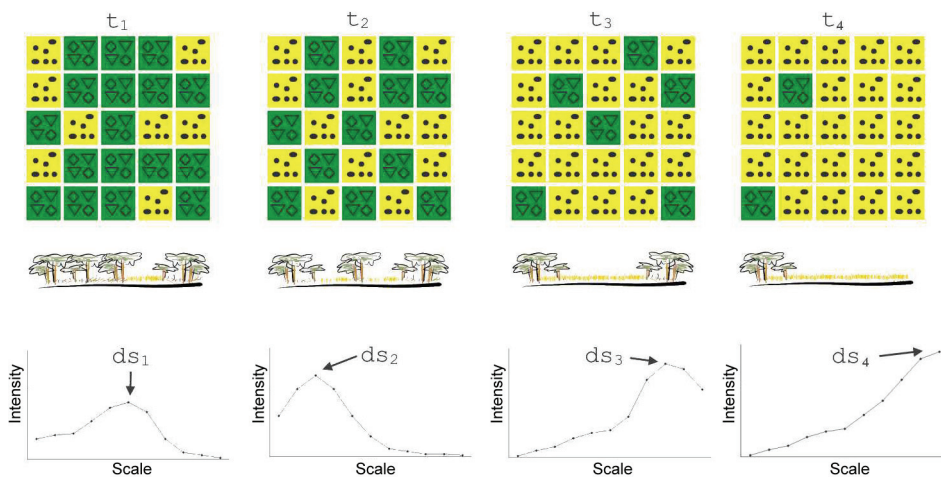


Fig. 6.4: The theoretical framework showing the fragmentation of a natural savanna (in green) in relation to farming expansion (in yellow). In  $t_1$  sparse and small arable fields do not affect the dominant scale of the landscape, which is relatively large; in  $t_2$  the dominant scale is reduced due to the expansion of farming; in  $t_3$  the dominant scale increases with cultivation; in  $t_4$  the dominant scale is greatest because the landscape is almost totally converted to agriculture.

This thesis also revealed a drawback with the method, particularly when performed over a very large extent. To overcome memory problems related to the large extent of the TME (even when using a supercomputer), we split the area in adjacent square quadrants of about 30 km x 30 km and performed the wavelet transform on these quadrants. This size was chosen in relation to the elephant home range in the study area (Galanti et al., 2000). Because the quadrant size or extent determines the number of the wavelet decompositions, dominant features larger than half quadrant (e.g., > 15 km in linear dimension) cannot be quantified by this method. In this thesis a quadrant of about 30 km x 30 km was adequate to quantify the largest dominant features in the landscape, including cultivation. However this size may not be appropriate for a farm-dominated savanna. This parameter should be chosen in relation to the environmental conditions, area of cultivation, and species home range.

## **6.2 The response of elephant to landscape heterogeneity and fragmentation using multiple resolution analysis**

The results presented in chapter 4 show that the dominant scale of NDVI-derived landscape heterogeneity did not substantially change in Tarangire–Manyara ecosystem during the wet season between 1988 and 2000. On average, the dominant scale was relatively large in both years, representing natural vegetation patches (e.g., in Q003\_002) as well as cultivated blocks (e.g., in Q003\_000) of about 8000–9000 m. We found that in the TME elephants respond to an intermediate patch size of about 7000–8000 m, which therefore reflects the scale of the dominant features in this landscape. This result is in line with the finding by Laca (2008) and Pretorius (2009) for large body-sized animals and conforms with the metabolic requirements of the species. Because of their low metabolic rates and large gut, elephants can satisfy their energetic needs by consuming large quantity of low quality food, which commonly occurs over large units (Prins and van Langevelde, 2008). As a result, resources distributed across coarse-grained landscapes like in TME, represent optimal habitat for the elephant and may explain the elephant population stability observed in TME. We found that elephant occurrence and density did not substantially change over the years in the TME. This finding is in line with the results by TAWIRI (2001). However, this level of heterogeneity may not be suitable for small body-sized and specialized herbivores like the duiker or impala. Because nutritional requirements and energy balance are allometrically scaled, these small herbivores (especially lactating females), are not able to fulfill their dietary needs across coarse-grained landscapes (Prins and van

## Synthesis

Langevelde, 2008). These animals need low quantity but high quality food (Olf and Ritchie, 2002), which commonly occur in small localized patches. In the Tarangire–Manyara ecosystem, observed declines in the population of antelopes, wildebeest and zebra in the wet season (TAWIRI, 2001) may therefore not only be related to overhunting and agricultural expansion in the Simanjiro plains (TNRF, 2005), but also to the coarse heterogeneity of the landscape.

As a consequence, fragmentation is also expected to impact species differently. Small and less mobile animals with a small home range, may be more impacted by fragmentation and patch isolation than large, mobile animals with a large home range, which are more sensitive to total habitat area (Davidson, 1998). As shown by the heterogeneity and fragmentation analysis conducted at multiple spatial scales, the TME is a relatively low human impacted and low fragmented savanna. This is particular evident when comparing the heterogeneity of the study area and its change over time with the finding of a previous similar study in a heavy human dominated savanna in Zimbabwe (Murwira and Skidmore, 2005). In the Zimbabwean study, the dominant scale of NDVI-derived landscape heterogeneity maximizing elephant occurrence was about 750 m in early 1980s, and reduced to 450 m in early 1990s, due to agricultural expansion. The Zimbabwean study further showed that elephant numbers not only declined between the 1980s and the 1990s, but disappeared from the ecosystem if the dominant scale decreased to less than 400 m (Murwira and Skidmore 2005). The scale of elephant-environment relationship is 10 times larger in TME (see point A in Fig. 6.5) and well within the critical threshold of elephant persistence (point B, Fig. 6.5).

A highly fragmented landscape, with a threshold of 30-40% of land being converted to agriculture, was earlier identified in Zimbabwe as the tipping point for elephant persistence (Hoare and Toit 1999). In the TME, farming covered 6% of the total study area in 1988 (about 750 km<sup>2</sup>) and 9% in 2000 (1140 km<sup>2</sup>). On the contrary, in the Zimbabwean study, cultivation increased from 8% of the total study area in 1884 (about 294 km<sup>2</sup>) to 44% in 1992 (1651 km<sup>2</sup>; Murwira et al. 2010), determining a significant change in the landscape structure, i.e., about a 58% annual increase against a 5% annual increase in TME. These results suggest that the dominant scale of NDVI-derived landscape heterogeneity not only reflects the amount of cultivation but also the resulting fragmentation level that may pose a risk to elephant persistence. In Sebungwe, Zimbabwe, the vegetation cover is a mosaic of natural patches and farms, which results in a highly fragmented landscape for the elephant. In the TME, Tanzania, cultivation is mostly clumped in large cultivated blocks in the western and northern parts of

the study area. Therefore, the level of fragmentation for the elephant is substantially lower in TME than in Zebungwe.

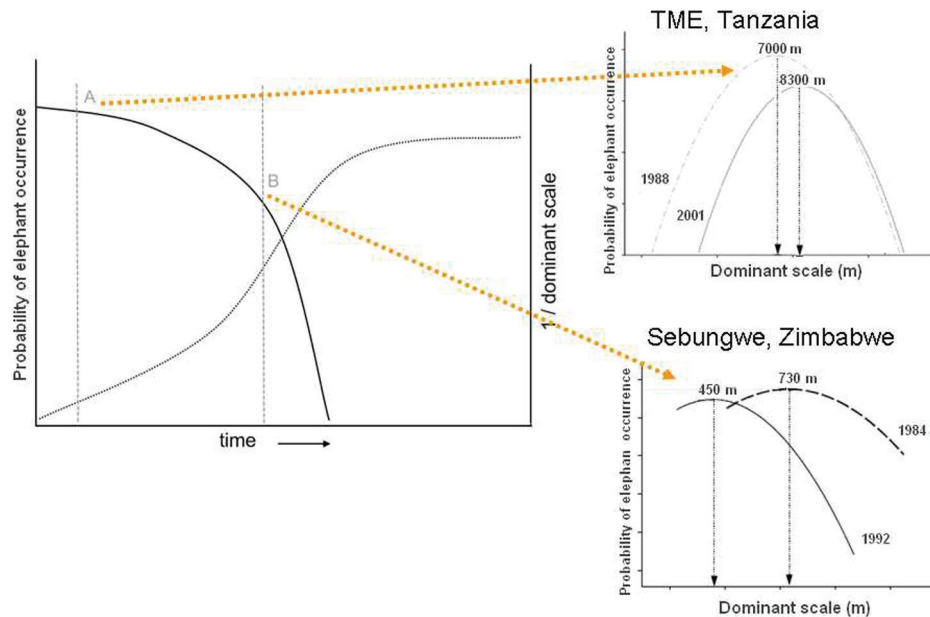


Fig. 6.5: The theoretical framework showing the response of elephant to changes in heterogeneity due to farming expansion. Point A and B indicate the case studies in Tanzania and Zimbabwe (TME, Tarangire–Manyara ecosystem).

### 6.3 New approaches to identify and predict seasonal and daily corridors as well as species distribution

The role of corridors in providing connectivity over time is controversial and highly debated (Boitani et al., 2007). This is partly due to the fact that the effect of fragmentation on species distribution can be positive or negative, depending on the way it is measured, the scale of analysis, the species under study as well as the ‘matrix’ surrounding the fragmented habitats (Collinge, 1996; Fahrig, 2003). Recent studies have highlighted the need of identifying corridors for keystone species using long-term datasets (Magurran et al., 2010) as well as species distribution models that account for detectability, ecological traits and environmental context, particularly for large body-sized and highly vagile animals (Mackenzie et al., 2002; McPherson and Jetz, 2007; Rota et al., 2011).

## Synthesis

In chapter 3 a new approach is proposed based on long-term aerial surveys. Repeated aerial surveys have been widely used for monitoring large terrestrial mammals, such as red kangaroo (Caughley, 1974), elk (Samuel et al., 1987), moose (Gasaway et al., 1985), caribou (Courtois et al., 2003), white-tailed deer (Pettoirelli et al., 2007; Potvin et al., 2004); saiga antelope (Singh and Milner-Gulland, 2011); elephant (Chamaillé-Jammes et al., 2008), wildebeest (Ottichilo et al., 2001), zebra (Kahurananga and Silkiluwasha, 1997), buffalo (Prins and Douglas-Hamilton, 1990) and antelopes (East, 1999; Stoner et al., 2007). The method described in chapter 3 is transparent, repeatable and potentially relevant for many wildlife species. These aerial surveys are snapshots in time and space. A kernel density function was therefore used to generate probabilities of elephant occupancy that account for the temporal and spatial discontinuity of the aerial surveys as well as the high vagility of elephant, and environmental context. These probabilities of elephant occupancy were used to define presence and absence data, which were further input in the logistic regression analysis. Logistic regression was then used to identify determinants of seasonal elephant distributions. This approach (kernel-based probability of occupancy plus logistic regression) produced high accurate seasonal distribution maps of elephant (AUC = 0.9) and successfully identified seasonal corridors for elephant. These corridors matched four traditional migration routes described in the 1960s based on field experience (Lamprey, 1964). The results presented in this thesis, in combination with those of Lamprey (1964), suggest that these corridors have been persistently used by elephant for more than 40 years, providing landscape connectivity in the Tarangire–Manyara ecosystem. Because the elephant is a keystone species of the savanna ecosystem (Hoare and Toit, 1999), other migratory herbivore species are expected to benefit from these corridors (Douglas-Hamilton et al., 2005).

This approach also identified environmental and anthropogenic determinants of elephant distribution in the TME. At the landscape scale, elephant occurrence decreases away from protected areas and permanent water sources all year round. These results are consistent with those of other studies (Douglas-Hamilton et al., 2005; Ngene et al., 2009b). However a detailed analysis of the data revealed that higher vegetation biomass and proximity to seasonal dams increases elephant occurrence seasonally, even close to infrastructures. These results suggest that elephant tracks water and green vegetation in both seasons (Loarie et al., 2009).

We recognize that the size of the kernel smoothing parameter  $h$  is of importance in this method, because large  $h$  values over-smooth the data, affecting the regression analysis. In our study however this potential drawback of the method

was minimized by using the likelihood cross validation method, which selects  $h$  based on statistical properties of the data. The probability volume contour is also of great importance in our method, because large thresholds may include sub-optimal areas (and thus over-predict suitable areas) while small thresholds may exclude sparse locations representing transit corridors (which were the scope of chapter 3). A 95% volume contour substantially minimized the inclusion of sub-optimal areas in the regression model, as shown in Fig. 6.6.

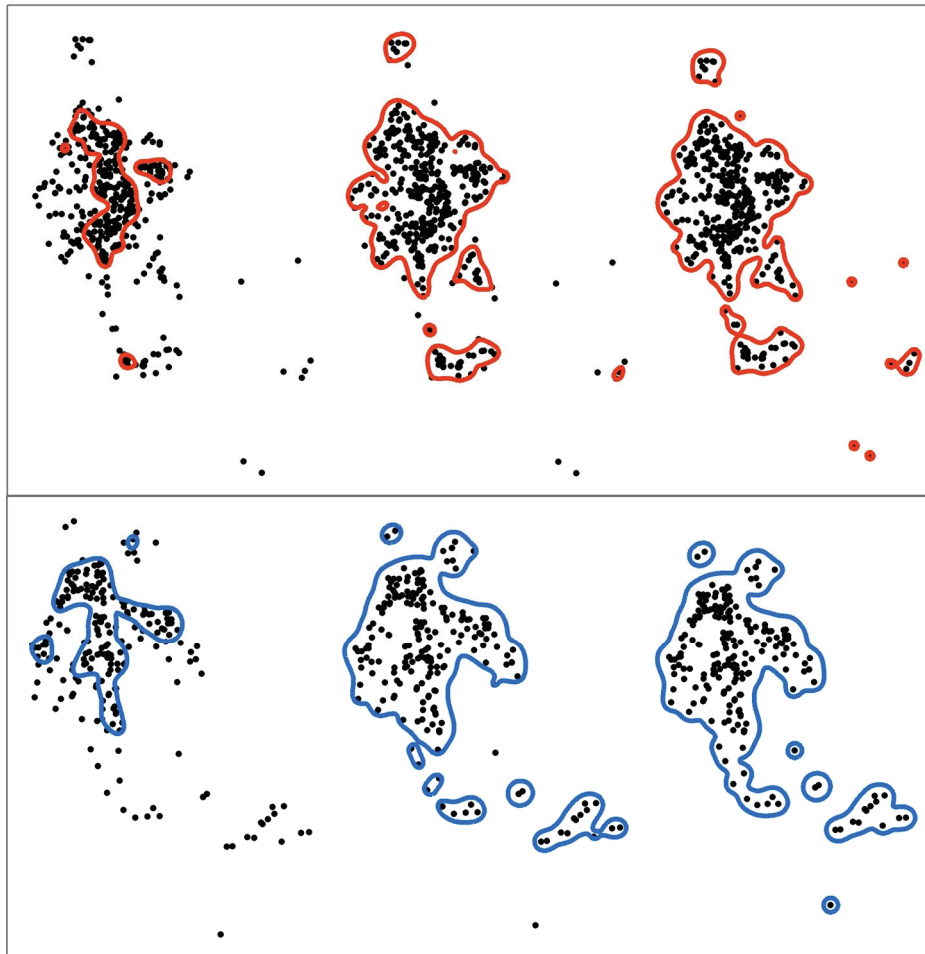


Fig. 6.6: From left to right, 50, 90 and 95% probability of volume contour for dry (in red) and wet (in blue) season. The points represent the elephant locations in the dry (up) and wet (bottom) season.

However, the results presented in this thesis also show that daytime animal observations, such as total counts, are neither sufficient to predict corridors nor resources used at night, including food crops. Nighttime elephant data can be obtained by radio- or satellite-collared elephants (Galanti et al., 2006; Graham et al., 2009). However because in such studies only a few opportunistically selected animals are tracked, the data may not comprehensively represent the elephant distribution (Hebblewhite and Haydon, 2010), particularly in relation to crop raiding behavior. The Bayesian expert system successfully modeled the elephant activity during the entire 24 h period, by providing resistance raster maps for the corridor network simulator (i.e., UNICOR; Landguth et al., 2012). The integration of the Bayesian expert system with UNICOR represents a novel approach to successfully predict crop raiding patterns. These results further confirm the usefulness of the expert systems in predicting wildlife distribution in absence of direct field observations (Murray et al., 2009; Niamir et al., 2011).

## **6.4 Fragmentation, corridors and human-elephant conflicts**

According to our analysis, no substantial changes occurred in the dominant scale of landscape heterogeneity along the elephant migration routes between 1988 and 2006, except for two quadrants. In quadrant Q004\_001 (including the Mkungunero Game Controlled Area) the dominant scale decreased from about 15,000 m in 1988 to about 8000 m in 2006. In quadrant Q001\_001 (including Lolkisale Game Controlled Area, Lolkisale, Loborsoit A and Naitolya villages see Fig. 4.2, in chapter 4), the dominant scale increased from about 2000 m in 1988 to about 8000 m in 2001, but then decreased to about 500 m in 2006 (after the period of the SRF surveys). This value is relatively close to the critical threshold of elephant persistence (about 400 m), as measured by a previous similar study in Zimbabwe (Murwira and Skidmore, 2005). In both quadrants the decline in dominant scale was related to an increase in agriculture. Continued agricultural expansion may obstruct the migration routes of elephant towards the dispersal areas outside the park, as already occurred in the western side of the Tarangire National Park (see chapter 3).

A detailed analysis of the fragmentation pattern in the north-eastern side of TME, and the crop raiding analysis revealed striking results. The dominant scale of about 500 m obtained for quadrant Q001\_001 in 2006 represents a landscape structure mostly dominated by small peasant farms (< 5 ha; see Table 5.3 and 5.4). Small farms are highly vulnerable to crop raiding due to insufficient protection (Sillero-Zubiri and Switzer, 2001; Sitati et al., 2005). The findings reported in chapter 5 shows that the distribution of small farms that are

surrounded by savanna influence the movement behaviour of crop raiding elephants, by enhancing connectivity for elephants, providing alternative corridors and thereby increasing crop raiding in the villages further away from the elephant refuges. Contrary to other studies (Graham et al., 2010b; Naughton-Treves, 1998), predictors such as distance to elephant refuges and drinking water did not consistently explain the crop raiding patterns in the TME. Disruption of connectivity by habitat fragmentation is well established (Hanski, 1998; Newmark, 2008), but the way different degrees of fragmentation influence daily movement is poorly understood. This thesis demonstrates that a dominant scale of about 500 m represents a level of fragmentation that may have positive effect on elephant distribution and connectivity. As ‘snacking points’, these farms compensate the energetic needs of the elephant to move along stepping stone corridors across higher resistance landscapes. These findings have conservation and management implications that may concern other crop raiding species. The spatial distribution and size of small farms between elephant refuges and cultivated blocks should be considered in land use planning. Small farms may act as stepping stones, large farms as barriers, and both influence the selection of corridors with potential negative consequences for farmers and elephants.

Our study also shows that large blocks of cultivated land (covering about 20-30% of the quadrants) in the western side of TME repel the elephant. This result is in line with the findings by Murwira and Skidmore (2005). However our results also suggest that agriculture has contributed to reshaping the distribution of elephants toward the less cultivated areas in the north-eastern and south-eastern part of the TME, without affecting the total population. In other words, in the TME the elephant is affected by the existence of large and clumped cultivated patches, which represent a loss of habitat area (see Davidson, 1998) rather than small and dispersed arable fields. A graphical overview of the main results in TME is presented in Fig. 6.7 to show the effect of a farming expansion on landscape heterogeneity, elephant occurrence and crop raiding patterns.

## **6.5 Filling the gaps: What is new? What is left? Future research objectives**

This study provided the following insights in the analysis of landscape patterns and ecological processes:

- 1) The intensity–dominant scale method based on the wavelet transform is an effective tool for monitoring environmental heterogeneity and its changes over time and space;

## Synthesis

- 2) Vegetation heterogeneity and fragmentation relevant to a species can be accurately and appropriately quantified using the intensity–dominant scale method;
- 3) Fragmentation driven by scattered small-scale farms surrounded by savanna is a predictor of crop raiding patterns;
- 4) Daytime total counts and SRF can be successfully used to predict seasonal species distribution and corridors, but cannot predict resources and corridors used at night;
- 5) The Bayesian expert system can successfully predict a 24 h species distribution from daytime animal observations.

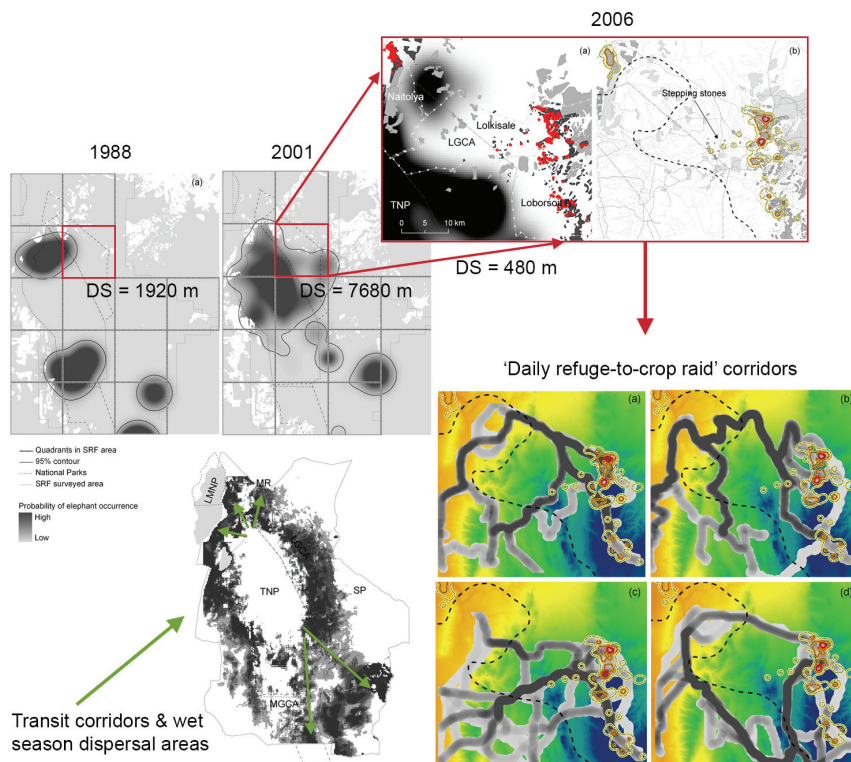


Fig. 6.7: An overview of the main results in the Tarangire–Manyara ecosystem (TME). See Fig. 3.4, Fig. 4.4, Fig. 5.3 and Fig. 5.5 for reference.

The findings presented in this thesis have conservation and management implications for elephant populations outside protected areas. In particular, the

dominant scale of NDVI-derived vegetation heterogeneity and its change over time due to farming expansion, as quantified by the intensity–dominant scale method, is a useful indicator of the level of heterogeneity relevant to the elephant in savanna ecosystems. A dominant scale of about 7000–8000 m represents optimal habitat for the elephant in the TME. In contrast, a dominant scale of about 15,000 m appears to repel the elephant as it is associated with large blocks of farms. In the TME a dominant scale of about 500 m appears to amplify the impact of crop raiding by enhancing habitat connectivity for elephants. Increasing conflicts between local farmers and elephants may undermine elephant conservation efforts (Nelson et al., 2003). In Sebungwe, Zimbabwe, a dominant scale less than 400 m represents a highly fragmented landscape, which may pose a risk to elephant persistence (Murwira and Skidmore, 2005). Future studies based on the intensity–dominant scale method are required for increasing our understanding of elephant–environment relationships and human–elephant conflicts for a larger geographical area, including different climatic and environmental conditions. However, because NDVI is known to saturate for high vegetation biomass values (Hobbs, 1995), other proxy of vegetation cover and biomass may be needed in forest ecosystems. Here other wavelets may also be explored to discriminate among patches of evergreen and deciduous forest, savanna and farming (see Ouma et al., 2008). This could be an appropriate area for future research. In this study we chose the Haar wavelet because we were interested in capturing edges between farming and natural vegetation in the TME (mainly dominated by open savanna) and because of its capability of handling large datasets. This thesis also shows that the intensity–dominant scale method based on the wavelet transform represents an effective tool for testing ecological hypotheses on determinants of species distribution and diversity. This study tested the landscape heterogeneity hypothesis on a single herbivore species, the elephant. An appropriate application of the method would be determining the dominant scale of vegetation heterogeneity for different herbivore species in order to test the body size/heterogeneity hypothesis, i.e., whether different body-sized herbivores respond to different levels of heterogeneity and fragmentation (Ritchie and Olff, 1999). The method can also be used to test the hypothesis that higher heterogeneous landscapes sustain higher levels of biodiversity (Fischer and Lindenmayer, 2007; Prins and Olff, 1998). In this regard repeated aerial surveys represent a broadly available source of daytime wildlife data. Because daytime data may not be sufficient to predict resources and corridors used at night, including crop raiding behaviour, expert systems or nighttime wildlife monitoring are recommended for modeling a 24 h species distribution.



# Appendix A

Table A.1: Statistical tests (B, logistic coefficient; s.e., standard error; Wald statistic and significance) for individual normalized predictors for dry and wet season distribution of elephant: 1 distance from dams; 2 distance from rivers; 3 distance from settlements; 4 distance index from protected areas; 5 distance index from semi-protected areas; 6 slope; 7 topographic position index (TPI); 8 distance from lakes; 9 distance from tarmac roads; 10 distance from minor roads; 11 monthly average NDVI; 12 closed trees; 13 closed shrubs; 14 cultivated areas; 15 herbaceous vegetation on flooded areas; 16 herbaceous vegetation or savanna; 17 open to very open shrubs; 18 open to very open trees; 19 river banks and bare areas; 20 trees or shrubs on flooded areas; 21 woody vegetation; 22 elevation; con, constant.

	Dry season					Wet season				
	B	s.e.	Wald	df	<i>p</i>	B	s.e.	Wald	df	<i>p</i>
1 <sup>a</sup>	-0.34	0.05	52.2	1	<0.001	-0.32	0.02	314	1	<0.001
2 <sup>a</sup>	-0.88	0.04	452.2	1	<0.001	-0.67	0.03	638.8	1	<0.001
3	0.44	0.04	113.4	1	<0.001	0.37	0.02	296.3	1	<0.001
4	-1.93	0.04	2120	1	<0.001	-0.94	0.02	1518	1	<0.001
5	-1.09	0.03	1515	1	<0.001	-0.29	0.02	306.8	1	<0.001
6	-0.48	0.03	342	1	<0.001	-0.27	0.02	162.9	1	<0.001
7	-0.08	0.02	14.8	1	<0.001	-0.03	0.02	4	1	0.05
8	-1.34	0.03	1553	1	<0.001	-1.21	0.02	3344	1	<0.001
9	0.45	0.06	50.8	1	<0.001	-	-	-	-	-
10	0.2	0.04	28.7	1	<0.001	0.12	0.02	32.3	1	<0.001
11 <sup>b</sup>	1.39	0.03	1629	1	<0.001	0.37	0.02	394	1	<0.001
12	-	-	866.1	9	<0.001	-	-	2121	9	<0.001
13	2.31	0.18	160.2	1	<0.001	0.22	0.12	3.1	1	0.08
14	0.82	0.2	16.7	1	<0.001	0.34	0.12	8	1	0.01
15	1.61	0.18	80.8	1	<0.001	0.25	0.12	4.6	1	0.03
16	1.9	0.17	119.8	1	<0.001	0.05	0.11	0.2	1	0.68
17	2.15	0.17	160.8	1	<0.001	0.79	0.11	50.9	1	<0.001
18	2.68	0.17	246.6	1	<0.001	0.89	0.11	63.4	1	<0.001
19	0.58	0.52	1.3	1	0.27	-2.92	0.39	57.3	1	<0.001
20	1.03	0.18	31.1	1	<0.001	-0.41	0.13	10.4	1	<0.001
21	4.42	0.21	440.5	1	<0.001	5.21	0.16	1101	1	<0.001
22	-	-	-	-	-	0.06	0.02	8.2	1	<0.001
con	-5.61	0.17	1066	1	<0.001	-2.05	0.11	361.8	1	<0.001

<sup>a</sup> only permanent in dry season.

<sup>b</sup> monthly average NDVI (March–April) in the wet season.

## Appendix B

Table B.1: Two-way ANOVA results of the crop raiding events obtained from the monitoring data. (VLG, village; Yr, year; VLG × Yr, interaction; Resid., residuals).

Source	df	Damaged area per farm ( $R^2_{adj} = 13\%$ )				Farm size ( $R^2_{adj} = 11\%$ )				Proportion of damaged area per farm ( $R^2_{adj} = 18\%$ )			
		Sum of Squares	Mean Square	F	<i>p</i>	Sum of Squares	Mean Square	F	<i>p</i>	Sum of Squares	Mean Square	F	<i>p</i>
VLG <sup>1</sup>	2	58014	29007	9.2	0.001	85774	42887	13	0.001	51701	25851	8.7	0.001
Yr	1	3167	3167	1	0.3	163	163	0.1	0.8	454	454	0.2	0.7
VLG x Yr	2	17226	8613	2.7	0.06	7213	3606	1.1	0.3	69741	34871	11.8	0.001
Resid.	202	639122	3164			654190	3239			597150	2956.2		

<sup>1</sup> Tamhane post hoc test,  $p < 0.05$

# Appendix C

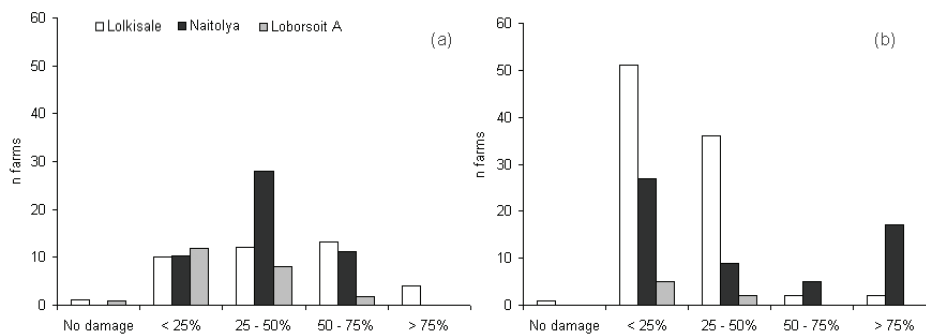


Fig. C.1 Number of farms by class of damaged area per farm in the three villages in 2006 (a) and 2008 (b). Results obtained from the household survey data



# Bibliography

- Acerbi-Junior, F.W., Clevers, J.G.P.W., Schaepman, M.E., 2006. The assessment of multi-sensor image fusion using wavelet transforms for mapping the Brazilian Savanna. *International Journal of Applied Earth Observation and Geoinformation*. 8, 278-288.
- Addison, P.S., 2002. *The illustrated wavelet transform handbook: introductory theory and applications in science, engineering, medicine and finance*, Institute of physics (IoP), Bristol.
- Allison, P.D., 1999. *Logistic Regression Using the SAS System: theory and applications*, SAS Institute Inc., Cary, NC.
- Amolins, K., Zhang, Y., Dare, P., 2007. Wavelet based image fusion techniques - An introduction, review and comparison. *ISPRS Journal of Photogrammetry and Remote Sensing*. 62 249-263.
- Aplin, P., 2006. On scales and dynamics in observing the environment. *International Journal of Remote Sensing*. 27, 2123 - 2140.
- Atkinson, P.M., 2004. Resolution manipulation and sub-pixel mapping, in: De Jong, S.M., van der Meer, F. (Eds.), *Remote sensing image analysis: including the spatial domain*. Kluwer Academic, Dordrecht, pp. 359.
- Atkinson, P.M., Aplin, P., 2004. Spatial variation in land cover and choice of spatial resolution for remote sensing. *International Journal of Remote Sensing*. 25, 3687-3702.
- Baldi, A., 2008. Habitat heterogeneity overrides the species–area relationship. *Journal of Biogeography*. 35, 675-681.
- Baldi, A., McCollin, D., 2003. Island ecology and contingent theory: the role of spatial scale and taxonomic bias. *Global Ecology & Biogeography*. 12, 1-3.
- Barbosa, A.M., Real, R., Vargas, J.M., 2009. Transferability of environmental favourability models in geographic space: The case of the Iberian desman (*Galemys pyrenaicus*) in Portugal and Spain. *Ecological Modelling*. 220, 747-754.
- Beier, P., Loe, S., 1992. In my experience: A checklist for evaluating impacts to wildlife movement corridors. *Wildlife Society Bulletin*. 20, 434-440.

## Bibliography

- Beier, P., Noss, R.F., 1998. Do Habitat Corridors Provide Connectivity? *Conservation Biology*. 12, 1241-1252.
- Beltran-Abuanza, J.M., 2009. Method development to process hyper-temporal remote sensing (RS) images for change mapping, MSc thesis. University of Twente, Enschede, The Netherlands.
- Bennett, A.F., 1999. Linkages in the landscape: the role of corridors and connectivity in wildlife conservation, World Conservation Union, Gland, Switzerland.
- Bennett, G., Mulongoy, K.J., 2006. Review of Experience with Ecological Networks, Corridors and Buffer Zones, Secretariat of the Convention on Biological Diversity, Montreal.
- Beyer, H.L., 2004. Hawth's Analysis Tools for ArcGIS. Available from <http://www.spatial ecology.com/htools>.
- Blanc, J.J., Barnes, R.F.W., Craig, G.C., Douglas-Hamilton, I., Dublin, H.T., Hart, J.A., Thouless, C.R., 2005. Changes in elephant numbers in major savanna populations in eastern and southern Africa. *Pachyderm*. 38, 19-28.
- Bogaert, J., 2003. Lack of agreement on fragmentation metrics blurs correspondence between fragmentation experiments and predicted effects. *Conservation Ecology*. 7, r6.
- Boitani, L., Falcucci, A., Maiorano, L., Rondinini, C., 2007. Ecological networks as conceptual frameworks or operational tools in conservation. *Conservation Biology*. 21, 1414-1422.
- Bolger, D.T., Newmark, W.D., Morrison, T.A., Doak, D.F., 2008. The need for integrative approaches to understand and conserve migratory ungulates. *Ecology Letters*. 11, 63-77.
- Borner, M., 1985. The increasing isolation of Tarangire National Park. *Oryx*. 19, 91-96.
- Bradshaw, G.A., Spies, T., 1992. Characterizing canopy gap structure in forests using wavelet analysis. *Journal of Ecological Society*. 80, 205-215.
- Brotans, L., Thuiller, W., Araujo, M.B., Hirzel, A., 2004. Presence-absence versus presence-only modelling methods for predicting bird habitat suitability. *Ecography*. 27, 437-448.
- Bruce, A., Gao, H.-Y., 1996. *Applied Wavelet Analysis with S-PLUS*, Springer, New York.

- Burn, R.W., Underwood, F.M., Blanc, J., 2011. Global Trends and Factors Associated with the Illegal Killing of Elephants: A Hierarchical Bayesian Analysis of Carcass Encounter Data. *PLoS ONE*. 6, e24165.
- Butchart, S.H.M., Walpole, M., Collen, B., van Strien, A., Scharlemann, J.P.W., Almond, R.E.A., Baillie, J.E.M., Bomhard, B., Brown, C., Bruno, J., Carpenter, K.E., Carr, G.M., Chanson, J., Chenery, A.M., Csirke, J., Davidson, N.C., Dentener, F., Foster, M., Galli, A., Galloway, J.N., Genovesi, P., Gregory, R.D., Hockings, M., Kapos, V., Lamarque, J.-F., Leverington, F., Loh, J., McGeoch, M.A., McRae, L., Minasyan, A., Morcillo, M.H., Oldfield, T.E.E., Pauly, D., Quader, S., Revenga, C., Sauer, J.R., Skolnik, B., Spear, D., Stanwell-Smith, D., Stuart, S.N., Symes, A., Tierney, M., Tyrrell, T.D., Vié, J.-C., Watson, R., 2010. Global Biodiversity: Indicators of Recent Declines. *Science*. 328, 1164-1168.
- Cairns, S.C., Grigg, G.C., 1993. Population dynamics of red kangaroos (*Macropus rufus*) in relation to rainfall in the South Australian pastoral zone. *Journal of Applied Ecology*. 30, 444-458.
- Castel, V., 2009. Socio Economic Baseline Survey. Descriptive analysis., Food and Agriculture Organization for the United Nations (FAO), Rome, Italy.
- Caughley, G., 1974. Bias in aerial survey. *Journal of Wildlife Management*. 38, 921-933.
- Chamaillé-Jammes, S., Fritz, H., Valeix, M., Murindagomo, F., Clobert, J., 2008. Resource variability, aggregation and direct density dependence in an open context: the local regulation of an African elephant population. *Journal of Animal Ecology*. 77, 135-144.
- Chamaillé-Jammes, S., Valeix, M., Fritz, H., 2007. Managing heterogeneity in elephant distribution: interactions between elephant population density and surface-water availability. *Journal of Applied Ecology*. 44, 625-633.
- Channell, R., Lomolino, M.V., 2000. Dynamic biogeography and conservation of endangered species. *Nature*. 403, 84-86.
- Chetkiewicz, C.L.B., Clair, C.C.S., Boyce, M.S., 2006. Corridors for Conservation: Integrating Pattern and Process. *Annual Review of Ecology, Evolution and Systematics*. 37, 317-342.
- Chiyo, P.I., Cochrane, E.P., Naughton, L., Basuta, G.I., 2005. Temporal patterns of crop raiding by elephants: a response to changes in forage quality or crop availability? *African Journal of Ecology*. 43, 48-55.

## Bibliography

- Collinge, S.K., 1996. Ecological consequences of habitat fragmentation: implications for landscape architecture and planning. *Landscape and Urban Planning*. 36, 59-77.
- Conover, W.J., Iman, R.L., 1981. Rank Transformations as a Bridge Between Parametric and Nonparametric Statistics *The American Statistician*. 35, 124-129
- Courtois, R., Gingras, A., Dussault, C., Breton, L., Ouellet, J.-P., 2003. An aerial survey technique for the forest-dwelling ecotype of Woodland Caribou, *Rangifer tarandus caribou*. *Canadian Field-Naturalist*. 117, 546-554.
- Couteron, P., 2002. Quantifying change in patterned semiarid vegetation by Fourier analysis of digitised aerial photographs. *International Journal of Remote Sensing*. 23, 3407-3425.
- Couteron, P., Barbier, N., Gautier, D., 2006. Textural Ordination Based on Fourier Spectral Decomposition: A Method to Analyze and Compare Landscape Patterns. *Landscape Ecology*. 21, 555-567.
- Cromsigt, J.P.G.M., Prins, H.H.T., Olf, H., 2009. Habitat heterogeneity as a driver of ungulate diversity and distribution patterns: interaction of body mass and digestive strategy. *Diversity and Distributions*. 15, 513-522.
- Dale, M.R.T., Mah, M., 1998. The use of wavelets for spatial pattern analysis in ecology. *Journal of Vegetation Science*. 9, 805–815.
- Damschen, E.I., Haddad, N.M., Orrock, J.L., Tewksbury, J.J., Levey, D.J., 2006. Corridors increase plant species richness at large scales. *Science*. 313, 1284-1286.
- Davidson, C., 1998. Issues in measuring landscape fragmentation. *Wildlife Society Bulletin*. 26, 32–37.
- de Beer, Y., van Aarde, R.J., 2008. Do landscape heterogeneity and water distribution explain aspects of elephant home range in southern Africa's arid savannas? *Journal of Arid Environments*. 72, 2017-2025
- de Knegt, H.J., 2010. Beyond the here and now. Herbivore ecology in a spatial-temporal context, PhD thesis. Wageningen University, Wageningen, The Netherlands.
- de Knegt, H.J., Van Langevelde, F., Skidmore, A.K., Delsink, A., Slotow, R., Henley, S., Bucini, G., De Boer, W.F., Coughenour, M.B., Grant, C.C., Heitkönig, I.M.A., Henley, M., Knox, N.M., Kohi, E.M., Mwakiwa, E., Page, B.R., Peel, M., Pretorius, Y., Van Wieren, S.E., Prins, H.H.T.,

2011. The spatial scaling of habitat selection by African elephants. *Journal of Animal Ecology*. 270-281.
- de Leeuw, J., Prins, H.H.T., Nguguna, E.C., Said, M.Y., De By, R., 1998. Interpretation of DRSRS Animal Counts (1977±1997) in the Rangeland Districts of Kenya, Ministry of Planning and National Development and Change, Nairobi, Kenya.
- Di Gregorio, A., Jansen, L.J.M., 2005. Land Cover Classification System. Classification concepts and user manual, Second edition. ed., Food and Agriculture Organization of the United Nations (FAO), Rome, Italy.
- Donoho, D.L., Johnstone, I.M., 1995. Adapting to unknown smoothness via wavelet shrinkage. *Journal of the American Statistical Association*. 90, 1200-1224.
- Douglas-Hamilton, I., Krink, T., Vollrath, F., 2005. Movements and corridors of African elephants in relation to protected areas. *Naturwissenschaften*. 92, 158-163.
- Drent, R.H., Prins, H.H.T., 1987. The herbivore as prisoner of its food supply, in: van Andel, J., Bakker, J., Snaydon, R.W. (Eds.), *Disturbance in grasslands; species and population responses*. Dr. W. Junk Publishing Company, Dordrecht, pp. 133-149.
- Dublin, H.T., Hoare, R.E., 2004. Searching for Solutions: The Evolution of an Integrated Approach to Understanding and Mitigating Human–Elephant Conflict in Africa. *Human Dimensions of Wildlife*. 9, 271-278.
- Dungan, J.L., Perry, J.N., Dale, M.R.T., Legendre, P., Citron-Pousty, S., Fortin, M.J., Jakomulska, A., Miriti, M., Rosenberg, M.S., 2002. A balanced view of scale in spatial statistical analysis. *Ecography*. 25, 626-640.
- East, R., 1999 African antelope database 1998, in: Group, I.S.A.S. (Ed.), IUCN, Gland, Switzerland and Cambridge, UK.
- Edkins, M.T., Kruger, L.M., Harris, K., Midgley, J.J., 2008. Baobabs and elephants in Kruger National Park: nowhere to hide. *African Journal of Ecology*. 46, 119-125.
- Elith, J., Graham, C.H., 2009. Do they? How do they? Why do they differ? On finding reasons for differing performances of species distribution models. *Ecography*. 32, 66-77.
- Elith, J., Graham, C.H., Anderson, R.P., Dudi'k, M., Ferrier, S., Guisan, A., Hijmans, R.J., Huettmann, F., Leathwick, J.R., Lehmann, A., Li, J., Lohmann, L.G., Loiselle, B.A., Manion, G., Moritz, C., Nakamura, M.,

## Bibliography

- Nakazawa, Y., Overton, J.M., Peterson, A.T., Phillips, S.J., Richardson, K.S., Scachetti-Pereira, R., Schapire, R.E., Soberón, J., Williams, S., Wisz, M.S., Zimmermann, N.E., 2006. Novel methods improve prediction of species' distributions from occurrence data. *Ecography*. 29, 129-151.
- Fahrig, L., 2003. Effects of habitat fragmentation on biodiversity. *Annual Review of Ecology, Evolution, and Systematics*. 34, 487-515.
- FAO-Africover, 2002. Tanzania - Multipurpose Landcover database (Africover), Food and Agriculture Organization of United Nations (FAO), <http://www.africover.org> (accessed 28 December 2009).
- Fazey, I., Fischer, J., Lindenmayer, D.B., 2005. What do conservation biologists publish? *Biological Conservation*. 124, 63-73.
- Fischer, J., Lindenmayer, D.B., 2002. The conservation value of paddock trees for birds in a variegated landscape in southern New South Wales. 2. Paddock trees as stepping stones. *Biodiversity and Conservation*. 11, 833-849.
- Fischer, J., Lindenmayer, D.B., 2007. Landscape modification and habitat fragmentation: a synthesis. *Global Ecology and Biogeography*. 16, 265-280.
- Fischer, J., Lindenmayer, D.B., Fazey, I., 2004. Appreciating Ecological Complexity: Habitat Contours as a Conceptual Landscape Model. *Conservation Biology*. 18, 1245-1253.
- Fisher, P., 1997. The pixel: a snare and a delusion. *International Journal of Remote Sensing*. 18, 679 - 685.
- Forman, R.T.T., 1995. *Land mosaics: the ecology of landscapes and regions*, Cambridge University Press, Cambridge.
- Forshaw, M.R.B., Haskell, A., Miller, P.F., Stanley, D.J., Townshend, J.R.G., 1983. Spatial resolution of remotely sensed imagery A review paper. *International Journal of Remote Sensing*. 4, 497 - 520.
- Franklin, A.B., Noon, B.R., George, T.L., 2002. What is habitat fragmentation? *Studies in Avian Biology*. 25, 20-29.
- Fryxell, J.M., Wilshurst, J.F., Sinclair, A.R.E., Haydon, D.T., Holt, R.D., Abrams, P.A., 2005. Landscape scale, heterogeneity, and the viability of Serengeti grazers. *Ecology Letters*. 8, 328- 335.

- Galanti, V., Preatoni, D., Martinoli, A., Wauters, L.A., Tosi, G., 2006. Space and habitat use of the African elephant in the Tarangire–Manyara ecosystem, Tanzania: Implications for conservation. *Mammalian Biology*. 71, 99-114.
- Galanti, V., Tosi, G., Rossi, R., Foley, C., 2000. The use of gps radio-collars To track elephants (*loxodonta africana*) in the Tarangire National Park (Tanzania). *Hystrix*. 11, 27-37.
- Gasaway, W.C., Dubois, S.D., Harbo, S.J., 1985. Biases in Aerial Transect Surveys for Moose during May and June. *The Journal of Wildlife Management*. 49, 777-784.
- Gereta, E., Ole Meing'ataki, G.E., Mduma, S., Wolanski, E., 2004. The role of wetlands in wildlife migration in the Tarangire ecosystem, Tanzania. *Wetlands Ecology and Management*. 12, 285-299.
- Gilbert-Norton, L., Wilson, R., Stevens, J.R., Beard, K.H., 2010. A Meta-Analytic Review of Corridor Effectiveness. *Conservation Biology*. 24, 660-668.
- Glenn, E.P., Huete, A.R., Nagler, P.L., Nelson, S.G., 2008. Relationship Between Remotely-sensed Vegetation Indices, Canopy Attributes and Plant Physiological Processes: What Vegetation Indices Can and Cannot Tell Us About the Landscape. *Sensor*. 8, 2136-2160.
- Gonthier, D.J., 2007. Notes on seeds deposited in elephant dung at Tarangire National Park, Tanzania. *African Journal of Ecology*. 47, 252-256.
- Gonzalez-Audicana, M., Otazu, X., Fors, O., Seco, A., 2005. Comparison between Mallat's and the 'a trous' discrete wavelet transform based algorithms for the fusion of multispectral and panchromatic images. *International Journal of Remote Sensing*. 26, 595 - 614.
- Goodchild, M.F., Quattrochi, D.A., 1997. Scale, Multiscaling, Remote Sensing and GIS, in: Quattrochi, D.A., Goodchild, M.F. (Eds.), *Scale in Remote Sensing and GIS*. CRC Press, Boca Raton, pp. 1-11.
- Gorte, B., 1999. Description in the data used in this book, in: Stein, A., van der Meer, F., Gorte, B. (Eds.), *Spatial statistics for remote sensing*. Kluwer Academic Publishers, Dordrecht, pp. 3-8.
- Goward, S.N., Dye, D.G., 1987. Evaluating North American net primary productivity with satellite observations. *Advances in Space Research*. 7, 165-174.

## Bibliography

- Graham, C.H., VanDerWal, J., Phillips, S.J., Moritz, C., Williams, S.E., 2010a. Dynamic refugia and species persistence: tracking spatial shifts in habitat through time. *Ecography*. 33, 1062-1069.
- Graham, M.D., Douglas-Hamilton, I., Adams, W.M., Lee, P.C., 2009. The movement of African elephants in a human-dominated land-use mosaic. *Animal Conservation*. 12 445-455.
- Graham, M.D., Notter, B., Adams, W.M., Lee, P.C., Ochieng, T.N., 2010b. Patterns of crop-raiding by elephants, *Loxodonta africana*, in Laikipia, Kenya, and the management of human–elephant conflict. *Systematics and Biodiversity*. 8, 435-445.
- Guisan, A., Lehmann, A., Ferrier, S., Austin, M., Overton, J.M.C., Aspinall, R., Hastie, T., 2006. Making better biogeographical predictions of species' distributions. *Journal of Applied Ecology*. 43, 386-392.
- Guisan, A., Thuiller, W., 2005. Predicting species distribution: offering more than simple habitat models. *Ecology Letters*. 8, 993-1009.
- Gustafson, E.J., 1998. Quantifying Landscape Spatial Pattern: What Is the State of the Art? *Ecosystems*. 1, 143-156.
- Haddad, N., 2000. Corridor length and patch colonization by a butterfly, *Junonia coenia*. *Conservation Biology*. 14, 738-745.
- Haddad, N.M., 2008. Finding the corridor more traveled. *Proceedings of the National Academy of Sciences, USA*. 105, 19569–19570.
- Haddad, N.M., Bowne, D.R., Cunningham, A., Danielson, B.J., Levey, D.J., Sargent, S., Spira, T., 2003. Corridor use by diverse taxa. *Ecology*. 84, 609–615.
- Hanski, I., 1998. Metapopulation dynamics. *Nature*. 396, 41-49.
- Harris, G.M., Russell, G.J., van Aarde, R.I., Pimm, S.L., 2008. Rules of habitat use by elephants *Loxodonta africana* in southern Africa: insights for regional management. *Oryx*. 42 66-75.
- He, Z., Zhao, W., Chang, X., 2007. The modifiable areal unit problem of spatial heterogeneity of plant community in the transitional zone between oasis and desert using semivariance analysis. *Landscape Ecology*. 22, 95-104.
- Hebblewhite, M., Haydon, D.T., 2010. Distinguishing technology from biology: a critical review of the use of GPS telemetry data in ecology.

## PHILOSOPHICAL TRANSACTIONS OF THE ROYAL SOCIETY B-BIOLOGICAL SCIENCES. 365 2303-2312

- Hill, M.J., Donald, G.E., 2003. Estimating spatio-temporal patterns of agricultural productivity in fragmented landscapes using AVHRR NDVI time series. *Remote Sensing of Environment*. 84, 367-384.
- Hoare, R., 2000. African elephants and humans in conflict: the outlook for co-existence. *Oryx*. 34, 34-38.
- Hoare, R.E., 1999a Data collection and analysis protocol for human-elephant conflict situations in Africa. A document prepared for the IUCN African Specialist Group's Human-Elephant Conflict Working Group., in, International Union for Conservation of Nature (IUCN), Arusha, pp. 30.
- Hoare, R.E., 1999b. Determinants of human-elephant conflict in a land-use mosaic. *Journal of Applied Ecology*. 36, 689-700.
- Hoare, R.E., Toit, J.T.D., 1999. Coexistence between People and Elephants in African Savannas. *Conservation Biology*. 13, 633-639.
- Hobbs, R.J., 1992. The role of corridors in conservation: Solution or bandwagon? *Trends in Ecology & Evolution*. 7, 389-392.
- Hobbs, T.J., 1995. The use of NOAA-AVHRR NDVI data to assess herbage production in the arid rangelands of Central Australia. *Int J Remote Sens*. 16, 1289-1302.
- Holland, J.D., Bert, D.G., Fahrig, L., 2004. Determining the Spatial Scale of Species' Response to Habitat. *Bioscience*. 54, 227-233.
- Horne, J.S., Garton, E.O., 2006. Likelihood Cross-Validation Versus Least Squares Cross-Validation for Choosing the Smoothing Parameter in Kernel Home-Range Analysis. *The Journal of Wildlife Management*. 70, 641-648.
- Horne, J.S., Garton, E.O., 2009. *Animal Space Use* 1.3.
- Illian, J., Penttinen, A., Stoyan, H., Stoyan, D., 2008. *Statistical analysis and modelling of spatial point patterns*, John Wiley & Sons Ltd.
- IUCN, 2010. 2010 IUCN Red List of Threatened Species. Version 2010.1, IUCN, Gland, Switzerland.
- Johnson, A.R., Wiens, J.A., Milne, B.T., Crist, T.O., 1992. Animal movements and population dynamics in heterogeneous landscapes. *Landscape Ecology*. 7, 63-75.

## Bibliography

- Jönsson, P., Eklundh, L., 2004. TIMESAT--a program for analyzing time-series of satellite sensor data. *Computers & Geosciences*. 30, 833-845.
- Jung, M., Henkel, K., Herold, M., Churkina, G., 2006. Exploiting synergies of global land cover products for carbon cycle modeling. *Remote Sensing of Environment*. 101, 534-553.
- Kahurananga, J., 1979. The vegetation of the Simanjiro Plains, Northern Tanzania. *African Journal of Ecology*. 17, 65-83.
- Kahurananga, J., Silkiluwasha, F., 1997. The migration of zebra and wildebeest between Tarangire National Park and Simanjiro Plains, northern Tanzania, in 1972 and recent trends. *African Journal of Ecology*. 35, 179-185.
- Kaswamila, A., 2009. Human-wildlife conflicts in Monduli District, Tanzania. *International Journal of Biodiversity Science & Management*. 5, 199-207.
- Keitt, T.H., Urban, D.L., 2005. Scale-specific inference using wavelets. *Ecology*. 86, 2497-2504.
- Kernohan, B.J., Gitzen, R.A., Millsbaugh, J.J., 2001. Analysis of animal space use and movements, in: Millsbaugh, J.J., Marzluff, J.M. (Eds.), *Radio Tracking Animal Populations*. Academic Press, New York, pp. 125-166.
- Kibebe, J.D.N., 2005. Socio-economic and ecological impacts of safari hunting and commercial farming on key stakeholders; Simanjiro District - Tanzania, in: Department of International Environment and Development Studies, Noragric, Norwegian University of Life Sciences, Oslo, pp. 134.
- Kikoti, A.P., 2009. Seasonal home range sizes, transboundary movements and conservation of elephants in northern tanzania. *Open Access Dissertations*. Paper 108.
- Kleiber, M., 1932. Body mass and metabolism. *Hilgardia*. 6, 315-349.
- Ko, C.-Y., Root, T.L., Lee, P.-F., 2011. Movement distances enhance validity of predictive models. *Ecological Modelling*. 222, 947-954.
- Kramer-Schadt, S., Kaiser, T.S., Frank, K., Wiegand, T., 2011. Analyzing the effect of stepping stones on target patch colonisation in structured landscapes for Eurasian lynx. *Landscape Ecology*. 26, 501-513.
- Laca, E.A., 2008. Foraging in a heterogeneous environment: intake and diet choice, in: Prins, H.H.T., van Langevelde, F. (Eds.), *Resource Ecology*:

- Spatial and Temporal Dynamics of Foraging. Springer, Dordrecht, pp. 81-100.
- Laca, E.A., Sokolow, S., Galli, J.R., Cangiano, C.A., 2010. Allometry and spatial scales of foraging in mammalian herbivores. *Ecology Letters*. 13, 311-320.
- Lamprey, H.F., 1963. Ecological separation of the large mammal species in the Tarangire Reserve, Tanganyika. *East African Wildlife Journal*. 1, 63-92.
- Lamprey, H.F., 1964. Estimation of the large mammal densities, biomass and energy exchange in the Tarangire Game Reserve and the Masai Steppe in Tanganyika. *African Journal of Ecology*. 2, 1-46.
- Landguth, E.L., Hand, B.K., Glassy, J., Cushman, S.A., Sawaya, M.A., 2012. UNICOR: a species connectivity and corridor network simulator. *Ecography*. 35, 9-14.
- Lehmann, C.E.R., 2010. Savannas Need Protection. *Science*. 327, 642-643.
- Levey, D.J., Bolker, B.M., Tewksbury, J.J., Sargent, S., Haddad, N.M., 2005. Effects of Landscape Corridors on Seed Dispersal by Birds. *Science*. 309, 146-148.
- Levin, S.A., 1992. The Problem of Pattern and Scale in Ecology: The Robert H. MacArthur Award Lecture. *Ecology*. 73, 1943-1967.
- Li, H., Reynolds, J.F., 1995. On definition and quantification of heterogeneity. In: *Oikos*, 73(1995)2, pp. 280-284.
- Li, H., Wu, J., 2004. Use and misuse of landscape indices. *Landscape Ecology*. 19, 389-399.
- Lloyd, C.D., Atkinson, P.M., Aplin, P., 2005. Characterising local spatial variation in land cover imagery using geostatistical functions and the discrete wavelet transform, in: Renard, P., Demougeot-Renard, H., Froidevaux, R. (Eds.), *Geostatistics for Environmental Applications: Proceedings of the Fifth European Conference on Geostatistics for Environmental Applications*. Springer, Berlin, pp. 391-402.
- Loarie, S.R., van Aarde, R.J., Pimm, S.L., 2009. Elephant seasonal vegetation preferences across dry and wet savannas. *Biological Conservation*. 142, 3099-3107.
- Loth, P.E., Prins, H.H.T., 1986. Spatial patterns of the landscape and vegetation of Lake Manyara National Park. *ITC journal*. 2, 115-130.

## Bibliography

- Luck, G.W., Daily, G.C., 2003. Tropical countryside bird assemblages: richness, composition, and foraging differ by landscape context. *Ecological Applications*. 13, 235-247.
- Ludwig, F., De Kroon, H., Prins, H.H.T., 2008. Impacts of savanna trees on forage quality for a large African herbivore. *Oecologia*. 155, 487-496.
- MacArthur, R.H., Wilson, E.O., 1967. *The theory of island biogeography*, Princeton University Press, New Jersey.
- Mackenzie, D.I., Nichols, J.D., Lachman, G.B., Droege, S., Royle, J.A., Langtimm, C.A., 2002. Estimating site occupancy rates when detection probabilities are less than one. *Ecology*. 83, 2248-2255.
- Magurran, A.E., Baillie, S.R., Buckland, S.T., Dick, J.M., Elston, D.A., Scott, E.M., Smith, R.I., Somerfield, P.J., Watt, A.D., 2010. Long-term datasets in biodiversity research and monitoring: assessing change in ecological communities through time. *Trends in Ecology & Evolution*. 25, 574-582.
- Mallat, S.G., 1989. A theory for multiresolution signal decomposition: the wavelet representation. *IEEE Transactions on pattern analysis and machine intelligence*. 11, 674-693.
- Mann, C.C., Plummer, M.L., 1995. Are wildlife corridors the right path? *Science*. 270, 1428-1430.
- Mather, P.M., 1999. *Computer processing of remotely - sensed images : an introduction*, Second edition ed., Wiley & Sons, Chichester etc.
- McGarigal, K., Cushman, S.A., 2005. The gradient concept of landscape structure., in: Wiens, J.A., Moss, M.R. (Eds.), *Issues and Perspectives in Landscape Ecology*. Cambridge University Press, Cambridge, pp. 112-119.
- McGarigal, K., Tagil, S., Cushman, S., 2009. Surface metrics: an alternative to patch metrics for the quantification of landscape pattern. *Landscape Ecology*. 24, 443-450.
- McPherson, J.M., Jetz, J., 2007. Effects of species' ecology on the accuracy of distribution models. *Ecography*. 30, 135-151.
- Meyers, S.D., Kelly, B.G., O'Brien, J.J., 1993. An introduction to wavelet analysis in oceanography and meteorology: With application to the dispersion of Yanai waves. *Monthly Weather Review*. 121, 2858-2866.

- MNRT, 1998. The wildlife policy of Tanzania, Ministry of Natural Resources and Tourism. Government Printer, Dar Es Salaam, Tanzania.
- Murray, J.V., Goldizen, A.W., O'Leary, R.A., McAlpine, C.A., Possingham, H.P., Choy, S.L., 2009. How useful is expert opinion for predicting the distribution of a species within and beyond the region of expertise? A case study using brush-tailed rock-wallabies *Petrogale penicillata*. *Journal of Applied Ecology*. 46, 842-851.
- Murwira, A., 2003. Scale Matters!: A New Approach to Quantify Spatial Heterogeneity for Predicting the Distribution of Wildlife Wageningen University, Wageningen.
- Murwira, A., Skidmore, A.K., 2005. The response of elephants to the spatial heterogeneity of vegetation in a Southern African agricultural landscape. *Landscape Ecology*. 20, 217-234.
- Murwira, A., Skidmore, A.K., 2006. Monitoring change in the spatial heterogeneity of vegetation cover in an African savanna. *International Journal of Remote Sensing*. 29, 3417-3456.
- Murwira, A., Skidmore, A.K., 2010. Comparing direct image and wavelet transform-based approaches to analysing remote sensing imagery for predicting wildlife distribution. *International Journal of Remote Sensing*. 31, 6425-6440.
- Murwira, A., Skidmore, A.K., Huizing, H.J.G., Prins, H.H.T., 2010. Remote sensing of the link between arable field and elephant (*Loxodonta africana*) distribution change along a tsetse eradication gradient in the Zambezi valley, Zimbabwe. *International Journal of Applied Earth Observation and Geoinformation*. 12, S123-S130.
- Mwalyosi, R.B.B., 1991. Ecological evaluation for wildlife corridors and buffer zones for Lake Manyara National Park and its immediate environment. *Biological Conservation*. 57, 171-186.
- National Bureau of Statistics Tanzania, 2006 2002 Population and Housing Census report, in, Dar Es Salaam.
- Naughton-Treves, L., 1998. Predicting Patterns of Crop Damage by Wildlife around Kibale National Park, Uganda. *Conservation Biology*. 12, 156-168.
- Naughton, L., Rose, R., Treves, T., 1999. The social dimensions of human-elephant conflict in Africa: A literature review and case studies from Uganda and Cameroon. Human-Elephant Conflict Task Force, IUCN, Gland, Switzerland.

## Bibliography

- Nelson, A., Bidwell, P., Sillero-Zubiri, C., 2003. A review of human-elephant conflict management strategies. People and Wildlife Initiative. Wildlife Conservation Research Unit, Oxford University, Oxford.
- Newmark, W.D., 2008. Isolation of African protected areas. *Frontiers in Ecology and the Environment*. 6, doi:10.1890/070003.
- Newmark, W.D., Manyaza, D.N., Gamassa, D.-G.M., Sariko, H.I., 1994. The Conflict between Wildlife and Local People Living Adjacent to Protected Areas in Tanzania: Human Density as a Predictor. *Conservation Biology*. 8, 249-255.
- Ngene, S.M., Gils, H.V., Wieren, S.E.V., Rasmussen, H., Skidmore, A.K., Prins, H.H.T., Toxopeus, A.G., Omondi, P., Douglas-Hamilton, I., 2009a. The ranging patterns of elephants in Marsabit protected area, Kenya: the use of satellite-linked GPS collars. *African Journal of Ecology*. 48, 386-400.
- Ngene, S.M., Skidmore, A.K., Gils, H.V., Douglas-Hamilton, I., Omondi, P., 2009b. Elephant distribution around a volcanic shield dominated by a mosaic of forest and savanna (Marsabit, Kenya). *African Journal of Ecology*. 47, 234-245.
- Niamir, A., Skidmore, A.K., Toxopeus, A.G., Muñoz, A.R., Real, R., 2011. Finessing atlas data for species distribution models. *Diversity and Distributions*. 17, 1173-1185.
- Norton-Griffiths, M., 1978. Counting Animals. A series of handbooks on techniques in African wildlife ecology, Grimsdell, J.J.R. ed., African Wildlife Foundation, Nairobi, Kenya.
- Nunez, J., Fors, O., Otazu, X., Pala, V., Arbiol, R., Merino, M.T., 2006. A Wavelet-Based Method for the Determination of the Relative Resolution Between Remotely Sensed Images. *IEEE Transactions on Geoscience and Remote Sensing*. 44, 2539-2548.
- Nunez, J., Otazu, X., Fors, O., Prades, A., Pala, V., Arbiol, R., 1999. Multiresolution-Based Image Fusion with Additive Wavelet Decomposition. *IEEE Transactions on Geoscience and Remote Sensing*. 37, 1204-1211.
- Ogden, R.T., 1997. Essential wavelets for statistical applications and data analysis, Birkhauser, Boston.
- OIKOS, 2002. Tarangire Manyara Conservation Project. Final Report, Arusha, Tanzania.

- Olf, H., Ritchie, M.E., 2002. Fragmented nature: consequences for biodiversity. *Landscape and Urban Planning*. 58, 83-92.
- Oliver, T., Roy, D.B., Hill, J.K., Brereton, T., Thomas, C.D., 2010. Heterogeneous landscapes promote population stability. *Ecology Letters*. 13, 473-484.
- Osborn, F.V., 2004. The concept of home range in relation to elephants in Africa. *Pachyderm*. 37, 37-44.
- Osborn, F.V., Parker, G.E., 2002. Community-based methods to reduce crop loss to elephants: experiments in the communal lands of Zimbabwe. *Pachyderm*. 33, 32-38.
- Osborn, F.V., Parker, G.E., 2003a. Linking two elephant refuges with a corridor in the communal lands of Zimbabwe. *African Journal of Ecology*. 41, 68-74.
- Osborn, F.V., Parker, G.E., 2003b. Towards an integrated approach for reducing the conflict between elephants and people: a review of current research. *Oryx*. 37, 80-84.
- Ottichilo, W.K., de Leeuw, J., Prins, H.H.T., 2001. Population trends of resident wildebeest [*Connochaetes taurinus hecki* (Neumann)] and factors influencing them in the Masai Mara ecosystem, Kenya. *Biological Conservation*. 97, 271-282.
- Ottichilo, W.K., Leeuw, J.d., Prins, H.H.T., 2000. Population trends of resident wildebeest [*Connochaetes taurinus hecki* (Neumann)] and factors influencing them in Masai Mara ecosystem, Kenya. *Biological Conservation Restoration and Sustainability*. 97, 271-282.
- Ouma, Y.O., Tetuko, J., Tateishi, R., 2008. Analysis of co-occurrence and discrete wavelet transform textures for differentiation of forest and non-forest vegetation in very-high-resolution optical-sensor imagery. *International Journal of Remote Sensing*. 29, 3417-3456.
- Pearce, J., Ferrier, S., 2000. An evaluation of alternative algorithms for fitting species distribution models using logistic regression. *Ecological Modelling*. 128, 127-147.
- Pearson, D.M., 2002. The application of local measures of spatial autocorrelation for describing pattern in north Australian landscapes. *Journal of Environmental Management*. 64, 85-95.
- Perry, J.N., Liebhold, A.M., Rosenberg, M.S., Dungan, J., Miriti, M., Jakomulska, A., Citron-Pousty, S., 2002. Illustrations and guidelines for

## Bibliography

- selecting statistical methods for quantifying spatial pattern in ecological data. *Ecography*. 25, 578–600.
- Pettorelli, N., Cote', S.D., Gingras, A., Potvin, F., Huot, J., 2007. Aerial surveys vs hunting statistics to monitor deer density: the example of Anticosti Island, Quebec, Canada. *Wildlife Biology*. 13, 321-327.
- Pettorelli, N., Vik, J.O., Mysterud, A., Gaillard, J.-M., Tucker, C.J., Stenseth, N.C., 2005. Using the satellite-derived NDVI to assess ecological responses to environmental change. *Trends in Ecology & Evolution*. 20, 503-510.
- Phillips, S., Anderson, R., Schapire, R., 2006. Maximum entropy modeling of species geographic distributions. *Ecological Modelling*. 190 231-259.
- Pianka, E.R., 1966. Latitudinal Gradients in Species Diversity: A Review of Concepts. *The American Naturalist*. 100, 33-46.
- Pinto, N., Keitt, T., 2009. Beyond the least-cost path: evaluating corridor redundancy using a graph-theoretic approach. *Landscape Ecology*. 24, 253-266.
- Pittiglio, C., 2009. Analysis of crop damage in Lolkisale, Naitolia and Loborsoit A villages (Monduli and Simanjiro Districts - Tanzania), Food and Agriculture Organization of the United Nations (FAO), Rome, Italy.
- Pittiglio, C., Skidmore, A.K., de Bie, C.A.J.M., Murwira, A., 2011. A common dominant scale emerges from images of diverse satellite platforms using the wavelet transform. *International Journal of Remote Sensing*. 32, 3665-3687.
- Pittiglio, C., Skidmore, A.K., van Gils, H.A.M.J., Prins, H.H.T., 2012. Identifying transit corridors for elephant using a long time-series. *International Journal of Applied Earth Observation and Geoinformation*. 14, 61-72.
- Potvin, F., Breton, L., Rivest, L.-P., 2004. Aerial surveys for white-tailed deer with the double-count technique in Quebec: two 5-year plans completed. *Wildlife Society Bulletin*. 3, 1099-1107.
- Press, W.H., Teukolsky, S.A., Vetterling, W.T., Flannery, B.P., 1992. *Numerical recipes in C (2nd ed.): the art of scientific computing*, Cambridge University Press, Cambridge.
- Pretorius, Y., 2009. Satisfying giant appetites. Mechanisms of small scale foraging by large African herbivores. PhD thesis, Wageningen University, Wageningen.

- Prins, H.H.T., 1987. Nature Conservation as an Integral Part of Optimal Land Use in East Africa: The Case of the Masai Ecosystem of Northern Tanzania. *Biological Conservation*. 40, 141-161.
- Prins, H.H.T., 1988. Plant phenology in Lake Manyara National Park, Tanzania. *Journal of Biogeography*. 15, 465-480.
- Prins, H.H.T., Douglas-Hamilton, I., 1990. Stability in a multi-species assemblage of large herbivores in East Africa. *Oecologia*. 83, 392-400.
- Prins, H.H.T., Loth, P.E., 1988. Rainfall patterns as background to plant phenology in northern Tanzania. *Journal of Biogeography*. 15, 451-463.
- Prins, H.H.T., Olff, H., 1998. Species-richness of African grazer assemblages: towards a functional explanation., in: Newbery, D., Prins, H.H.T., Brown, G. (Eds.), *Dynamics of Tropical Communities*. Blackwell Science, Oxford, pp. 449-489.
- Prins, H.H.T., van der Jeugd, H.P., Beekman, J.H., 1994. Elephant decline in Lake Manyara National Park, Tanzania. *Journal of African Ecology*. 32, 185 - 191.
- Prins, H.H.T., van Langevelde, F., 2008. Assembling a diet from different places, in: Prins, H.H.T., van Langevelde, F. (Eds.), *Resource Ecology: Spatial and Temporal Dynamics of Foraging*. Springer, Dordrecht, pp. 129 -158.
- Quinn, G.P., Keough, M.J., 2002. *Experimental design and data analysis for biologists*, Cambridge University Press, Cambridge.
- R Development Core Team, 2010 *R: A Language and Environment for Statistical Computing*, reference index version 2.11.1. R Foundation for Statistical Computing, in, Vienna, Austria.
- Redding, T.E., Hope, G.D., Fortin, M.J., Schmidt, M.G., Bailey, W.G., 2003. Spatial patterns of soil temperature and moisture across subalpine forest-clearcut edges in the southern interior of British Columbia *Canadian Journal of Soil Science*. 83, 121-130.
- Reid, R.S., Kruska, R.L., Muthui, N., Taye, A., Wotton, S., Wilson, C.J., Mulatu, W., 2000. Land-use and land-cover dynamics in response to changes in climatic, biological and socio-political forces: the case of southwestern Ethiopia. *Landscape Ecology*. 15, 339-355.
- Richards, J.A., Jia, X., 2006. *Remote sensing digital image analysis: an introduction*, Fourth edition ed., Springer-Verlag, Berlin.

## Bibliography

- Ricketts, T.H., 2001. The matrix matters: effective isolation in fragmented landscapes. *The American Naturalist*. 158, 87-99.
- Ritchie, M.E., Olf, H., 1999. Spatial scaling laws yield a synthetic theory of biodiversity. *Nature*. 400, 557-560.
- Roderick, M.L., Noble, I.R., Cridland, S.W., 1999. Estimating woody and herbaceous vegetation cover from time series satellite observations. *Global Ecology and Biogeography*. 8, 501-508.
- Rodríguez, E., Morris, C.S., Belz, J.E., 2006. A Global Assessment of the SRTM Performance. *Photogrammetric Engineering and Remote Sensing*. 72, 249-260.
- Rogers, K.H., 2003. Adopting a Heterogeneity Paradigm : Implications for Management of Protected Savannas, in: Du Toit, J.T., Biggs, H., Rogers, K.H. (Eds.), *The Kruger Experience: Ecology And Management Of Savanna Heterogeneity*. Island Press, Washington, pp. 41-58.
- Rota, C.T., Fletcher, R.J., Evans, J.M., Hutto, R.L., 2011. Does accounting for imperfect detection improve species distribution models? *Ecography*. 34, 659-670.
- Sala, O.E., Stuart Chapin , F.I., Armesto, J.J., Berlow, E., Bloomfield, J., Dirzo, R., Huber-Sanwald, E., Huenneke, L.F., Jackson, R.B., Kinzig, A., Leemans, R., Lodge, D.M., Mooney, H.A., Oesterheld, M.n., Poff, N.L., Sykes, M.T., Walker, B.H., Walker, M., Wall, D.H., 2000. Global Biodiversity Scenarios for the Year 2100. *Science*. 287, 1770-1774.
- Samuel, M.D., Garton, E.O., Schlegel, M.W., Carson, R.G., 1987. Visibility Bias during Aerial Surveys of Elk in Northcentral Idaho. *The Journal of Wildlife Management*. 51, 622-630.
- Sankaran, M., Ratnam, J., Hanan, N.P., 2004. Tree-grass coexistence in savannas revisited : insights from an examination of assumptions and mechanisms invoked in existing models. *Ecology Letters*. 7, 480-490.
- Saunders, S.C., Chen, J., Drummer, T.D., Crow, T.R., Brosofske, K.D., Gustafson, E.J., 2002. The patch mosaic and ecological decomposition across spatial scales in a managed landscape of northern Wisconsin, USA. *Basic and Applied Ecology*. 3, 49-64.
- Saunders, S.C., Chen, J., Drummer, T.D., Gustafson, E.J., Brosofske, K.D., 2005. Identifying scales of pattern in ecological data: a comparison of lacunarity, spectral and wavelet analyses. *Ecological Complexity*. 2 87-105.

- Schooley, R.L., 2006. Spatial Heterogeneity and Characteristic Scales of Species–Habitat Relationships. *Bioscience*. 56, 533-537.
- Serneels, S., Lambin, E.F., 2001. Impact of land-use changes on the wildebeest migration in the northern part of the Serengeti-Mara ecosystem. *Journal of Biogeography*. 28, 391-407.
- Shrader, A., Pimm, S., van Aarde, R., 2010. Elephant survival, rainfall and the confounding effects of water provision and fences. *Biodiversity and Conservation*. 19, 2235-2245.
- Sillero-Zubiri, C., Switzer, D., 2001. Crop raiding primates: Searching for alternative, humane ways to resolve conflict with farmers in Africa. *People and Wildlife Initiative*. , in, *Wildlife Conservation Research Unit*, Oxford University, Oxford.
- Silverman, B.W., 1986. *Density Estimation for Statistics and Data Analysis*, Chapman and Hall, London.
- Simberloff, D., 1998. Flagships, umbrellas, and keystones: Is single-species management passé in the landscape era? *Biological Conservation*. 83, 247-257.
- Simberloff, D., Cox, J., 1987. Consequences and costs of conservation corridors. *Conservation Biology*. 1, 63-71.
- Simberloff, D., Farr, J.A., Cox, J., Mehlman, D.W., 1992. Movement Corridors: Conservation Bargains or Poor Investments? *Conservation Biology*. 6, 493-504.
- Singh, N.J., Milner-Gulland, E.J., 2011. Conserving a moving target: planning protection for a migratory species as its distribution changes. *Journal of Applied Ecology*. 48, 35–46.
- Sitati, N.W., Walpole, M.J., 2006. Assessing farm-based measures for mitigating human-elephant conflict in Transmara District, Kenya. *Oryx*. 40 279-286.
- Sitati, N.W., Walpole, M.J., Leader-Williams, N., 2005. Factors affecting susceptibility of farms to crop raiding by African elephants: using a predictive model to mitigate conflict. *Journal of Applied Ecology*. 42, 1175-1182.
- Sitati, N.W., Walpole, M.J., Smith, R.J., Leader-Williams, N., 2003. Predicting spatial aspects of human–elephant conflict. *Journal of Applied Ecology*. 40, 667-677.

## Bibliography

- Skidmore, A.K., 1989. An expert system classifies Eucalypt forest types using thematic mapper data and digital terrain model. *Photogrammetric Engineering and Remote Sensing*. 55, 1449-1464.
- Skidmore, A.K., 1990. Terrain position as mapped from a gridded digital elevation model. *International Journal of Geographical Information Systems*. 4, 33-49.
- Smith, R.J., Kasiki, S.M., 2000. A spatial analysis of human–elephant conflict in the Tsavo ecosystem, Kenya., African Elephant Specialist Group, Human–Elephant Conflict Task Force, Gland.
- Song, C., Woodcock, C.E., Seto, K.C., Lenney, M.P., Macomber, S.A., 2001. Classification and Change Detection Using Landsat TM Data: When and How to Correct Atmospheric Effects? *Remote Sensing of Environment*. 75, 230-244.
- Southwell, C., 1996. Bias in aerial survey of feral goats in the rangeland of Western Australia. *Rangeland Journal*. 18, 99-103.
- Stoner, C., Caro, T., Mduma, S., Mlingwa, C., Sabuni, G., Borner, M., Schelten, C., 2007. Changes in large herbivore populations across large areas of Tanzania. *African Journal of Ecology*. 45, 202-215.
- Strand, E.K., Robinson, A.P., Bunting, S.C., 2007. Spatial patterns on the sagebrush steppe/Western juniper ecotone. *Plant Ecology*. 190, 159-173.
- Strand, E.K., Smith, A.M.S., Bunting, S.C., Vierling, L.A., Hann, D.B., Gessler, P.E., 2006. Wavelet estimation of plant spatial patterns in multitemporal aerial photography. *International Journal of Remote Sensing*. 27, 2049-2054.
- Tarnavsky, E., Garrigues, S., Brown, M.E., 2008. Multiscale geostatistical analysis of AVHRR, SPOT-VGT, and MODIS global NDVI products. *Remote Sensing of Environment*. 112, 535-549.
- TAWIRI, 2001. Aerial census in Tarangire ecosystem. Wet season, May 2001. Wildlife Survey Report, TAWIRI, FZS, Arusha, Tanzania.
- TAWIRI, 2004. Total counts of elephants and buffalo in the Tarangire ecosystem. Dry season 2004. Wildlife Survey Report, TAWIRI & FZS, Arusha, Tanzania.
- TCP, 1998. Analysis of migratory movements of large mammals and their interactions with human activities in the Tarangire area in Tanzania as a

- contribution and sustainable development strategy. Final report, University of Milan & Istituto OIKOS, Arusha, Tanzania.
- Tews, J., Brose, U., Grimm, V., Tielbörger, K., Wichmann, M.C., Schwager, M., Jeltsch, F., 2004. Animal species diversity driven by habitat heterogeneity/diversity: the importance of keystone structures. *Journal of Biogeography*. 31, 79-92.
- Tilman, D., Fargione, J., Wolff, B., D'Antonio, C., Dobson, A., Howarth, R., Schindler, D., Schlesinger, W.H., Simberloff, D., Swackhamer, D., 2001. Forecasting Agriculturally Driven Global Environmental Change. *Science*. 292, 281-284.
- TNRF, 2005 Social, Ecological Dynamics and Complexity in the Simanjiro Plains: A Round Table Discussion. 1-31.
- Torrence, C., Compo, G.P., 1998. A practical guide to wavelet analysis. *Bulletin of the American Meteorological Society*. 79, 61-78.
- Tucker, C.J., Sellers, P.J., 1986. Satellite remote sensing and primary production. *International Journal of Remote Sensing*. 7, 1395-1416.
- Turner, D.P., Cohen, W.B., Kennedy, R.E., Fassnacht, K.S., Briggs, J.M., 1999. Relationships between Leaf Area Index and Landsat TM Spectral Vegetation Indices across Three Temperate Zone Sites. *Remote Sensing of Environment*. 70, 52-68.
- Turner, M.G., 1989. Landscape ecology : the effect of pattern on process. *Annual Review of Ecological Systems*. 20, 171-197.
- TWCM, 2000. Total Count of Elephant and Buffalo in the Tarangire Ecosystem (including Lake Manyara National Park), March 2000. Wildlife Survey Report, TWCM & FZS, Arusha, Tanzania.
- Uezu, A., Beyer, D.D., Metzger, J.P., 2008. Can agroforest woodlots work as stepping stones for birds in the Atlantic forest region? *Biodiversity and Conservation*. 17, 1907-1922.
- Varotsos, P.A., Sarlis, N.V., Skordas, E.S., 2003. Attempt to distinguish electric signals of a dichotomous nature. *Physical Review E*. 68, 031106.031101-031106.031107.
- Vos, C.C., 1999. A frog's-eye view of the landscape. PhD thesis, Wageningen University, Wageningen
- Wall, J., Douglas-Hamilton, I., Vollrath, F., 2006. Elephants avoid costly mountaineering. *Current biology : CB*. 16, R527-R529.

## Bibliography

- Walsh, S.J., Moody, A., Allen, T.R., Brown, D.G., 1997. Scale dependence of NDVI and its Relationship to Mountainous Terrain, in: Quattrochi, D.A., Goodchild, M.F. (Eds.), *Scale in Remote Sensing and GIS*. CRC Press, Boca Raton, pp. 27-55.
- Wang, G., Hobbs, N.T., Boone, R.B., Illius, A.W., Gordon, I.J., Gross, J.E., Hamlin, K.L., 2006. Spatial and Temporal Variability Modify Density Dependence in Populations of Large Herbivores. *Ecology*. 87, 95-102.
- Wasser, S., Poole, J., Lee, P., Lindsay, K., Dobson, A., Hart, J., Douglas-Hamilton, I., Wittemyer, G., Granli, P., Morgan, B., Gunn, J., Alberts, S., Beyers, R., Chiyo, P., Croze, H., Estes, R., Gobush, K., Joram, P., Kikoti, A., Kingdon, J., King, L., Macdonald, D., Moss, C., Mutayoba, B., Njumbi, S., Omondi, P., Nowak, K., 2010. Elephants, Ivory, and Trade. *Science*. 327, 1331-1332.
- Western, D., 1975. Water availability and its influence on the structure and dynamics of a savannah large mammal community. *African Journal of Ecology*. 13, 265-286.
- Wheatley, M., Johnson, C., 2009. Factors limiting our understanding of ecological scale. *Ecological Complexity*. 6, 150-159.
- Whitcher, B., 2010. Basic wavelet routines for one-, two- and three-dimensional signal processing. R package version 1.6.4.
- Wiens, J.A., 1989. Spatial scaling in ecology. *Functional Ecology*. 3, 385-397.
- Wiens, J.A., 2000. Ecological heterogeneity: an ontogeny of concepts and approaches, in: Hutchings, M.J., John, E.A., Stewart, A.J.A. (Eds.), *The ecological consequences of environmental heterogeneity*. Blackwell Science, Oxford, pp. 9-31.
- Wintle, B.A., Elith, J., Potts, J.M., 2005. Fauna habitat modelling and mapping: A review and case study in the Lower Hunter Central Coast region of NSW. *Austral Ecology*. 30, 719-738.
- Wisz, M.S., Hijmans, R.J., Li, J., Peterson, A.T., Graham, C.H., Guisan, A., Group, N.P.S.D.W., 2008. Effects of sample size on the performance of species distribution models. *Diversity and Distributions*. 14, 763-773.
- Wu, J., 2004. Effects of changing scale on landscape pattern analysis: scaling relations. *Landscape Ecology*. 19, 125-138.
- Young, K.D., Ferreira, S.M., van Aarde, R.J., 2009a. Elephant spatial use in wet and dry savannas of southern Africa. *Journal of Zoology*. 278, 189-205.

## Bibliography

- Young, K.D., Ferreira, S.M., Van Aarde, R.J., 2009b. The influence of increasing population size and vegetation productivity on elephant distribution in the Kruger National Park. *Austral Ecology*. 34, 329-342.



# Summary

Species distribution at the landscape level reflects the way organisms respond to resource availability, such as forage and refuge, and stressors, such as farming. Resources and stressors may vary spatially and temporally, determining the level of heterogeneity of a landscape. Savanna fragmentation due to farming expansion modifies the level of vegetation heterogeneity relevant to a given wildlife species, by reducing the size of and the connectivity among savanna patches. In fragmenting landscapes, wildlife numbers and diversity decline, while simultaneously the interface between farms and wild lands increases with potential negative consequences for people and wildlife. Yet, the critical level for a response by wildlife to vegetation heterogeneity is not well understood. Further, the way savanna fragmentation intensifies human-wildlife conflicts has not yet been explicitly analyzed. In this context, remote sensing provides a potential source of spatiotemporal consistent data for the analysis of a wildlife-environment relationship. However, such analysis requires accurate species distribution data as well as multiresolution methods as both vegetation heterogeneity and savanna fragmentation are resolution-dependent phenomena.

The way spatial and temporal heterogeneity of vegetation cover in a savanna ecosystem influence elephant occurrence and their crop raiding pattern formed the main objective of this thesis. The amount of vegetation cover was estimated from the Normalized Difference Vegetation Index (NDVI) using the intensity-dominant scale method based on the wavelet transform. For the intensity-dominant scale method, the intensity refers to the maximum contrast or variance in vegetation cover (e.g., in NDVI) measured at successively increasing window sizes or scales. The dominant scale represents the window size or scale at which this maximum variance in vegetation cover (i.e., maximum intensity) occurs. The dominant scale metric explained 80% of the variance in elephant occurrence in a farming-dominated savanna landscape in Zimbabwe and outperformed two NDVI-based direct image methods of estimating landscape heterogeneity. Therefore, the intensity-dominant scale method appears a useful tool for monitoring vegetation heterogeneity. However, its applicability in semi-natural, gradient environments such as low human impacted and low fragmented savanna as well as its robustness to scaling has not yet been explored.

## Summary

This study first tested the robustness of the intensity–dominant scale method in farmland and semi-natural systems against the pixel size of satellite imagery in Andalucía, Spain. Next, the method was applied to quantify the level of heterogeneity of vegetation cover relevant to the elephant for a low human impacted savanna in the Tarangire–Manyara ecosystem (TME), northern Tanzania. The results were compared with those obtained from a previous study in a farming-dominated savanna landscape in Zimbabwe. Then the level of fragmentation, as measured by the size and distribution of farms in the savanna was used to predict ‘daily refuge-to-crop raid’ corridors for elephant and resulting crop raiding patterns in the TME.

The results presented in this thesis demonstrate that the intensity–dominant scale is an invaluable method for monitoring vegetation heterogeneity both in agricultural and natural landscapes including savanna. The dominant scale metric is resolution-robust, accurate, and reliable. The level of heterogeneity relevant to elephant can be accurately and appropriately quantified with the intensity–dominant scale method. In particular, spatial and temporal heterogeneity of the vegetation cover was found to control elephant occurrence in the TME. For small changes of the dominant scale due to sparse and small arable fields, the probability of elephant occurrence remains stable and associated with relatively large patches of natural vegetation (linear dimension of about 7000–8000 m). Then as cultivation increases, the dominant scale is reduced first. Subsequently, it increases in proportion to the amount of cultivation. The elephant presence decreases in relation to smaller and larger dominant scales. Large dominant scales (of about 15,000–16,000 m) determined by large blocks of farms reshape the distribution of elephant towards less cultivated areas, without affecting the total population. Further, fragmentation driven by scattered small farms surrounded by savanna is a predictor of elephant crop raiding patterns. These farms act as ‘stepping-stone corridors’ for elephant providing ‘snacking points’ during their nighttime movement. Our findings have conservation and management implications for other wildlife species. In particular, this thesis provides insights on the role of scale in understanding ecological patterns, (i.e., species distribution, level of heterogeneity relevant to a species) and processes (i.e., functional connectivity, wildlife movement and human-wildlife conflicts). It may contribute to improve our understanding of crop raiding patterns.

# Samenvatting

De verspreiding van diersoorten over het landschap reflecteert de manier waarop de soort reageert op de aanwezigheid van enerzijds zijn levensvoorwaarden zoals voedsel en schuilplaatsen en anderzijds op stressfactoren zoals landbouwactiviteiten. Levensvoorwaarden en stressfactoren variëren beide in ruimte en tijd en bepalen daardoor de heterogeniteit van het landschap. Versnippering van de savanne door landbouwuitbreiding leidt tot een patroon van kleine, geïsoleerde savanne fragmenten met gevolgen voor bepaalde diersoorten. Het aantal diersoorten en het aantal individuen per soort daalt in versnipperde landschappen terwijl tegelijkertijd de grens tussen cultuur- en natuurlandschappen langer wordt waaruit potentieel negatieve gevolgen voor mens en dier voortvloeien. Toch is de kritische responsdrempel van diersoorten voor de heterogeniteit van vegetatiepatronen in het landschap nauwelijks onderzocht. Verder is de wijze waarop versnippering van de savanne de conflicten tussen mens en dier intensiveert nergens expliciet geanalyseerd. In deze context is remote sensing een potentiële bron van tijdreeksen van vergelijkbare geografische gegevens voor een analyse van relaties tussen diersoorten en hun milieu. Een dergelijke analyse vereist verder betrouwbare gegevens van de verspreiding van de soort, evenals methoden geschikt voor een reeks van ruimtelijke resoluties omdat de heterogeniteit en versnippering van de savanne afhangt van de waarnemingsschaal. Een beter begrip van de manier waarop de geografische en historische heterogeniteit van de savanne vegetatie het voorkomen van de olifant en de veroorzaakte oogstschade door de olifant bepaalt vormt de belangrijkste doelstelling van dit proefschrift.

De vegetatiebedekking werd geschat met behulp van een Genormaliseerde Vegetatie-Index (beter bekend als NDVI) met gebruikmaking van de intensiteit-dominante-schaal methode gebaseerd op wavelet-transformatie. De intensiteit is de maximale variantie in de vegetatiebedekking (NDVI) gemeten met toenemende venstergrootte, met andere woorden over verschillende schalen. The dominante schaal is de venstergrootte met de grootste variantie in vegetatiebedekking. De dominante schaal verklaarde 80% van de variantie in het voorkomen van de olifant in een savanne landschap gedomineerd door landbouw in Zimbabwe en overtrof hiermee twee andere NDVI-beeldverwerkingsmethoden ter inschatting van de heterogeniteit in het landschap. Daarmee lijkt de intensiteit-dominante-schaal methode bruikbaar om

## Samenvatting

de heterogeniteit van de vegetatie te monitoren. Maar de toepasbaarheid in half-natuurlijke gradiëntmilieus zoals savanne met weinig versnippering door menselijke invloed en de schaalgevoeligheid van de intensiteit-dominant-schaal methode zijn niet onderzocht. Deze studie testte eerst de resolutie-gevoeligheid van the intensiteit-dominante-schaal methode in een cultuurlandschap en een half-natuurlijk landschap in Andalusië, Spanje. Vervolgens werd de methode toegepast om de het heterogeniteitsniveau van het landschap te kwantificeren voor zover relevant voor de olifant in de licht beïnvloede savanne van het Tarangire-Manyara ecosysteem (TME) in het noorden van Tanzania. De resultaten werden vergeleken met die verkregen in een voorafgaand onderzoek in een landschap gedomineerd door de landbouw in Zimbabwe. Daarna werd de mate van versnippering, gemeten aan de omvang en verspreiding van de akkers in de savanne, gebruikt ter voorspelling van de corridors gebruikt voor nachtelijke strooptochten door de olifant naar de akkers vanuit hun schuilplaatsen gedurende de dag. De gepresenteerde resultaten demonstreren dat de intensiteits-dominante-schaal methode goed bruikbaar is voor de monitoring van heterogeniteit in vegetatiepatronen in zowel half-natuurlijke als cultuurlandschappen. De dominante schaal maat blijkt resolutie-ongevoelig, accuraat en betrouwbaar en daardoor geschikt voor het meten van heterogeniteit in het landschap zoals van belang voor de olifant. Meer in het bijzonder bleek dat de aanwezigheid van de olifant in het onderzoeksgebied verklaard kon worden door de ruimtelijke en temporele heterogeniteit in de vegetatie. Kleine ruimtelijke verschillen in de dominante schaal door verspreide, kleine akkers hebben geen invloed op de aanwezigheid van de olifant geassocieerd met grotere oppervlakten savanne (7000–8000 m lang). Als de akkerbouw zich uitbreidt daalt de dominante schaal eerst om vervolgens evenredig toe te nemen met de oppervlakte van de velden. De aanwezigheid van de olifant neemt af bij zowel de kleinere en de grotere dominante schaal. De grotere dominante schaal (15,000–16,000 m) als gevolg van grote gebieden met aaneengesloten landbouwbedrijven leidt tot een herverdeling van de olifant over minder intensief gecultiveerde gebieden zonder verandering in het aantal olifanten. Verder blijkt versnippering van de savanne door kleine landbouwbedrijven een goede voorspeller voor nachtelijk strooptochten van de olifant naar de velden. Onze bevindingen hebben implicaties voor natuurbescherming en natuurbeheer voor andere diersoorten.

In deze thesis is vooral inzicht ontwikkeld in de rol van de schaal van het landschap voor het begrijpen van verspreidingspatronen (van diersoorten en het niveau van heterogeniteit van belang voor de soort) en van ecologische processen (gebruik van corridors en mens-dier conflicten). Hopelijk dragen deze

inzichten bij aan een effectievere preventie van gewasschade door de olifant en andere beschermende soorten.



# Publications

**Pittiglio**, C., Skidmore, A.K., van Gils, H.A.M.J., Prins, H.H.T., 2012. Identifying transit corridors for elephant using a long time-series. *International Journal of Applied Earth Observation and Geoinformation*. 14, 61-72.

**Pittiglio**, C., Skidmore, A.K., de Bie, C.A.J.M., Murwira, A., 2011. A common dominant scale emerges from images of diverse satellite platforms using the wavelet transform. *International journal of remote sensing*. 32, 3665-3687.

**Pittiglio**, C., Skidmore, A.K., van Gils, H.A.M.J., Prins, H.H.T. Elephant response to spatial heterogeneity in a savanna landscape of northern Tanzania. In press, *Ecography*.

**Pittiglio**, C., Skidmore, A.K., van Gils, H.A.M.J., McCall, M.K., Prins, H.H.T. Farms as stepping stones for crop raiding elephants in northern Tanzania. Under review.

Clements, A.C.A., Pfeiffer, D.U., Martin, V., **Pittiglio**, C., Best, N., Thiongane, Y., 2007. Spatial Risk Assessment of Rift Valley Fever in Senegal. *Vector-Borne Zoonotic Dis.* Volume 7, Number 2, 2007.



# Biography

Claudia Pittiglio was born on June 22, 1970 in Rome, Italy. She obtained her high school diploma in scientific studies in 1989 with distinction. She earned a laureate with honours in Biology (Bachelor and MSc) in 1996 at the University of Rome 'La Sapienza', defending the thesis 'Ecological niche overlap of sympatric Stone martens (*Martes foina* Erxleben) and Pine martens (*Martes martes* L.) in Tuscany. This research included 18 months of fieldwork concerning trapping and monitoring of radio-collared martens, and vegetation mapping. During the study period she obtained two fellowships of the University of Rome La Sapienza as part time assistant for lectures and laboratory activities to the undergraduates in the Department of Animal and Human Biology.

From 1996 to 2001 Claudia Pittiglio worked as researcher and GIS expert for the University of Rome La Sapienza, the Institute of Applied Ecology (IEA), and various NGOs within several research projects on the ecology and conservation of vulnerable species (e.g., wolf and otter) as well as the management of pest species (e.g., wild boar, coypu, porcupine and red deer) and resulting human-wildlife conflicts. These researches, which required extended period of fieldwork, were conducted in various conservation areas of Italy. In 2002-2003 she was awarded by the University of Rome 'La Sapienza' with a yearly scholarship for advanced courses for graduates abroad. She chose the International Institute for Geo-Information Science and Earth Observation (ITC), in the Netherlands, for improving her skills in vegetation mapping, spatial ecology, statistics and remote sensing. From 2001 to 2010, Claudia Pittiglio provided consulting services in GIS, ecological and epidemiological modelling to FAO, in Rome, Dakar, Arusha, Dar es Salaam and Nairobi. In December 2005 she registered as PhD candidate at the NRS Department of ITC (currently ITC Faculty of University of Twente) with a sandwich construction between ITC and FAO. She spent the first eight months of her PhD in Tanzania as a FAO consultant within the Global Environment Facility project (GCP-URT-124-WBG), titled "Novel forms of livestock and wildlife integration adjacent to protected areas in Africa – Tanzania". During this period, she passed the qualifier and collected part of the data that were analyzed in this thesis. The data analysis was granted by the ITC scholarship and was conducted at ITC. During this period she continued to collaborate with FAO in the framework of the GEF project.



# ITC Dissertation List

[http://www.itc.nl/Pub/research/Graduate-programme/Graduate-programme-PhD\\_Graduates.html](http://www.itc.nl/Pub/research/Graduate-programme/Graduate-programme-PhD_Graduates.html)

